Università degli Studi di Catania
International PhD
in
Energy
XXVI cycle

A NEW DYNAMIC RESPONSE FACTOR FOR THE ASSESSMENT OF THE THERMAL PERFORMANCE OF BUILDINGS BASED ON THE HARMONIC ANALYSIS

Maria Giuga

Coordinator of Phd
Prof. Luigi Marletta

Tutor
Prof. Luigi Marletta

a.a. 2010/2014

Contens

Introduction

The reliable estimation of buildings energy needs for cooling is a crucial issue in the implementation ofthe EPB Directive 2010/31/EU (formerly 2002/91/EC), especially in central and southern Europe climates.

On this purpose one of the main topics is to predict the behavior of the opaque envelope subjected to variable boundary conditions.

1 The reasons for Energy evaluation

Buildings are designed to create an isolated space from the surrounding environment and provide the desired interior environmental conditions for the occupants. In addition to fulfilling the function of creating favourable indoor environmental conditions, buildings are expected to be durable and energy efficient.

In Italy, the legislator takes the above mentioned aspects into great consideration, with particular attention to the last one,which is typically addressed as the energy saving issue. Because of the increasing uncertainty on the energy scene, the energy saving issue becomes really important in all those countries which are not able to produce energy on their own.

In recent years, a significant effort in the direction of energy efficient buildings has been promoted by governments and scientific communities, who are discussing strategies to implement energy regulations and reduce building energy consumption.

The EU, where the civil sector covers 40% of entire energy consumption, is trying to pursue this target in many ways. One of them is the introduction of mandatory energy certifications for the majority of buildings.

Energy certification is a procedure to assess energy performance and to produce an energy certificate by an authorized institute or person. A certification programme generally includes an “energy rating” process to quantify the energy use and an authorized “energy labelling” scale to classify the corresponding performance, as well as a minimum requirement to eliminate unacceptable performances.

For new buildings, as well as for existing ones, energy performance certificates have to be made available to the owners or to the tenants when buildings are constructed, sold or rented out.

A basic aspect of most regulations is the thermal performance of the building envelope, usually with a certificate containing information about the impact of the envelope on the building energy performance.

The success of building energy regulation relies on three decisive points: to achieve a certificate which produces expected results for the amount of resources invested; the accuracy of the certification process (i.e. its capability to accurately quantify real energy savings); and the commitment to reduce greenhouse gases in order to prevent impact on global warming.

In many countries, the certification process relies on different levels of computational building performance simulation.

2 Legislation and tecnical standards

The European Union is currently the major catalyst driving energy efficiency policies in the building sector.

Building energy performance assessment became compulsory in Europe after the issue of the European Directive on the “Energy performance of buildings” (EPBD, European Union 2003).

2.1 Directive 2002

The Directive presses member States to provide the Normative and Legislative tools aimed at promoting “the improvement of energy efficiency of the buildings in the European Community", in accordance with the national specific environmental and climatic conditions, and the preexisting norms.

To such intention it traces four principal action lines:

- the implementation of a common calculation method for building energy efficiency, based on an integrated approach applied to both the building envelope and the installed systems for winter-summer air-conditioning,ventilation, lighting; the incentive to the use of renewable energy sources;
- the respect for energy efficiency lower limits for new/existingbuildings;
- the inspection of the boilers and the heating and cooling systems;
- the introduction of an energy certification system, which allows the evaluation of the buildings energy performance and the possible

improvement interventions: the energy certification is finalized to reflect the energy quality of a building into its commercial value and to encourage the investments for energy savings.

2.2 Legislative Decree 19/08/2005 n. 192, Legislative Decree29/12/2006 n. 311 and DPR 25/06/2009 n.59

The legislative Decree 19/08/2005 n. 192, "Realization of the Directive 2002/91/CE related to the energy efficiency in the house-building", has been replaced by the 29/12/2006 legislative Decree, whose title is: "Corrective and integrative dispositions to the Legislative Decree 19 August 2005, n. 192, as realization of the directive 2002/91/CE, related to energy efficiency in house-building".

This Decree wants to establish "criterions, conditions and methods to improve the building energy performance, to promote the development, the exploitation and the integration of renewable sources and energy diversification,to contribute to realize the national duties derived from Kyoto Protocol, to promote the competitiveness of the most advanced compartments through technological development".

Application fields include:

- the "planning and realization of new buildings and installed systems, of new installed systems in existing buildings, and the restructuring of buildings and existing systems";

- the control, maintenance and inspection of the thermal systems of buildings;
- the energy certification of buildings, i.e. the document that describes the building energy performance through the calculation of specific energy parameters.

The energy performance is determined through the "quantity of annual energy consumed or necessary to satisfy the different needs related to a building standard use, such as winter and summer air conditioning, preparation of domestic hot water, ventilation and lighting", while the reference parameter for a possible classification of the building, or for a comparison between different buildings, is the energy performance index.

To such purposes, the Decree provides the following instruments:

- the methodology for the calculation of the integrated energy performance of the buildings, in accordance with UNI and EN technical rules;
- the application of least requirements regarding the building energy performance: appendix C presents some threshold values for the energy performance index (in $kWhm^2$/year) for heating, for the thermal transmittance of opaque and transparent building components, for the seasonal mean global efficiency of the thermal systems.
- the general criterions for the energy certification of buildings: appendix E provides the list of technical documents to be produced for the this certification;
- the promotion of energy rational use through the information and user awareness, the formation and the updating of the operators (art.1);

As regards the summer performance of buildings, the only reference regards the check that the surface mass for all kind of walls (vertical, horizontal,tilted) has to be more than 230 kg/m^2, for all climatic zones, except for the F one (in which the mean monthly value of solar irradiance on the horizontal surface is equal or more than 290 W/m^2), or the use of alternative structures, which assure the same positive effects on thermal comfort.

This means that the dynamic characteristics (decrement factor and timeshift) of the alternative solutions must be better than those for structures which respect the surface mass threshold value.

The method for the calculation of the dynamic thermal characteristics, under sinusoidal boundary conditions, is reported in the UNI EN ISO 13786:2001(later updated in 2008).

A simplified method of calculation for flat components is provided in this standard consisting of flat layers of homogeneous or substantially homogeneous building materials[1].

The recent DPR 59/09 introduces threshold values for the dynamic characteristics for the use of the alternative solutions as mentioned above.

It also focuses on building summer performance, but since the relative technical rule for the calculation of the need of primary energy for summer conditioning was not yet available when the DPR was issued, it establishes threshold values for envelope performance, depending on the climatic zone and recommends the use

[1]The thermal dynamics of the building components thus obtained can also be used in the calculation of the internal temperature of a room, the daily output of peak energy, energy demands for heating and cooling and to study the effects of intermittent heating and cooling. The calculation method, the subject of this thesis, has been developed from these characteristics, which will be presented in detail in the next chapter.

of solar shadings, the thermal inertia of the opaque envelope and natural ventilation as instruments to contain summer overheating.

2.3 2.3 Legislative Decree 26/06/2009 amended by the Decree of the Ministry of Economic Development 22.11.2012 and Technical rules UNI TS 11300

In the Legislative Decree 26/06/2009, which contains the drive-lines for energy certification of buildings, the total energy performance of a building is expressed by a global energy performance index, called EPgl (in kWh/m2year, forresidential buildings):

$$EP_{gl} = EP_i + EP_{acs} + EP_e + EP_{ill}$$

where:

EP_i is the energy performance index for winter conditioning

EP_{acs} is the energy performance index for the domestic hot water production

EP_e is the energy performance index for summer conditioning

EP_{ill} is the energy performance index for artificial lighting

While the EP_i and EP_{acs} indexes are related to the energy certification, for summer conditioning only a qualitative evaluation of the envelope characteristics to contain summer energy need is provided.

All these indexes must be calculated applying the technical rules UNI/TS11300, in particular:

- UNI/TS 11300-1: Energy performance of buildings - Part 1:Evaluation of energy needs for space heating and cooling; it defines the calculation method of the envelope energy performance for heating and cooling.
- UNI/TS 11300-2: Energy performance of buildings - Part 2:Evaluation of primary energy needs and system efficiencies for space heating and domestic hot water production; it permits the calculation of the building performance for the specific installed heating system, starting from the known envelope performance.

These rules permit the calculation of the energy needs for heating and domestic hot water production, but not yet that of the energy needed for cooling.

In order to make a qualitative evaluation of building performance in summer conditions, the Decree presents two possible methods:

a) Calculation of the building thermal performance for cooling ($EP_{e,invol}$): This index is given by the ratio between the need of thermal energy forcooling (energy required by the envelope to keep indoor comfort conditions, it is not primary energy because the system efficiency is not included) and thesurface of the conditioned volume. For the classification of the envelope qualityfive classes are considered (Table 2.1):

$EP_{e,invol}$ (kWh/m^{2}year)	Performance	Quality class
$EP_{e,invol}$<10	Very good	I
10≤$EP_{e,invol}$<20	Good	II
20≤$EP_{e,invol}$<30	Medium	III
30≤$EP_{e,invol}$<40	Sufficient	IV
$EP_{e,invol}$≥40	Poor	V

Table 2.1: Classification of the envelope quality for summer according to the I method

b) Calculation of quality parameters: the decrement factor f_a (non-dimensional) and time shift τ (h), calculated according to the UNI EN ISO 13786.

The decrement factor is given by the ratio between the dynamic thermal transmittance and the steady-state thermal transmittance;

The time shift is the time occurring between the highest outdoortemperature and the peak of the thermal flux getting into the room.

The classification of the envelope quality is done according to the following Table 2.1:

Decrement factor	Time shift (h)	Performance	Quality class
f_a<0.15	τ >12	Very good	I
0.15≤ f_a <0.30	12≥ τ >10	Good	II
0.30≤ f_a <0.40	10≥ τ >8	Medium	III
0.40≤ f_a <0.60	8≥ τ >6	Sufficient	IV
f_a ≥0.60	6 ≥ τ	Poor	V

Table 2.2: Classification of the envelope quality for summer according to the II method

The technical rule UNI TS 11300-1 is based on the UNI EN ISO 13790:2008 monthly method for the calculation of the thermal energy need for heating and cooling space.

In particular, in summer conditions, the cooling load (in MJ) is given by:

$$Q_{C,nd} = Q_{C,gn} - \eta_{C,ls} \cdot Q_{C,ht} = (Q_{int} + Q_{sol}) - \eta_{C,ls} \cdot (Q_{C,tr} + Q_{C,ve})$$

Where $Q_{C,gn}$ represents the internal load, including solar energy throughopenings, $Q_{C,ht}$ represents the heat transfer for transmission and ventilation, $\eta_{C,ls}$is the loss utilization factor for cooling (non-dimensional), defined as a functionof τ and γ_C:

$$\eta_{C,ls} = f(\tau, \gamma_C)$$

where

$$\tau = \frac{\mathrm{C}}{\mathrm{H}}$$

And

$$\gamma_C = \frac{Q_{C,gn}}{Q_{C,ht}}$$

τ is the building time constant (h) which characterizes the inside thermalinertia of the heated space, given by the ratio between C, that is the real insidethermal capacity (J/K) and H, that it is the coefficient of thermal loss of thebuilding (W/K) (the average thermal transmittance of the building), while γ_C(non-dimensional) is the ratio between the free contributions by solar andinternal sources $Q_{C,gn}$ and the total heat transfer $Q_{C,ht}$.

The rule presents the correlation in graphical form, too (Figure 2. 1).

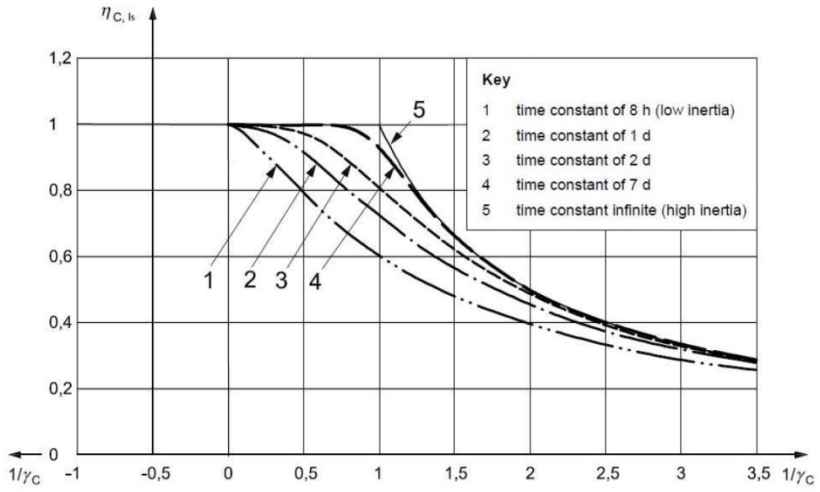

Figure 2.1 Correlation between the loss utilization factor for cooling and the gain-loss ratio

2.4 EPB Directive 2010/31/EU

In May 2010, the European Parliament approved a new legislation based on the recast of the European Directive on the energy performance of Buildings (200/91/EC). This directive aims at reducing energy consumption and greenhouse gas emissions by 20%, as well as increasing the share of renewables by 2020, in order to confront climate change, high energy prices, the growing import energy dependency and its possible geopolitical impacts (1). In fact, reduced energy consumption and an increased use of energy from renewable sources also have an important part to play in promoting security of energy supply, technological developments and in creating opportunities for employment and regional development, in particular in rural areas.

One of the key topics of the EPB Directive 2010/31/EU (formerly2002/91/EC) is the increase of the buildings energy performances insummer. A reliable assessment of the cooling consumptions (io: and interior temperature) may

beconsidered as a first useful step to understand how to improve building thermal behaviour, which depends basically on complexcorrelations between gains, losses and storage of heat.

The envelope components (i.e., walls, roofs and windows) havenot only to meet the minimum law requirements on thermalinsulation, but also have to provide a suitable thermal response tothe external heat fluxes, so that it is possible to decrease the temperaturepeaks and ensure adequate internal comfort conditions insummer. From this point of view, the estimate of the dynamic thermal propertiesof the opaque envelope components is of great importance in the thermal analysis of buildings.

As regards building performance, the impact of windows, fenestration and glazed structure is becoming more and more important, given the fact that thermal protection of opaque building elements isgradually strengthened. These structures combine many vital functions of the building (aesthetics, provision of view to the exterior, daylight thermal comfort, protection against noise, sun, cold and wind, safety, etc.) which are usually conflicting and time variant, both diurnal and seasonal. Heat transfer through windows accounts for a significant portion of the energy used in the building sector for covering both heating and cooling needs, since the optical characteristics of conventional fenestration products renders them more “vulnerable” to energy flows compared with opaque building elements.

Another international standard to take into consideration for the development of a method for calculating internal temperate in summer conditions is thestandard

UNI EN ISO 13972: 201213 792, which will be discussed later on, in the section on validation procedures.

3 The Admittance Method: a new dynamic simulation code for building energy performance analysis.

The energy performance concerns the amount of energy consumed or estimated to satisfy all the needs of the building. As a consequence, extensive research activities, both at national and international levels, have been carried out to create a general framework for a calculation methodology of the building energy performance. Many problems have arisen, concerning the definition of energy rating, the accuracy of the calculation methodology, the discrepancies between an application to new or to existing buildings, the layout of the energy performance certificate.

In this work we have chosen to investigate and further develop the potentialities offered by Harmonic Analysis though an extension of the Admittance method. Applied to energy saving studies for buildings, the traditional method (the Admittance method proposed by the standard UNI EN ISO 13786) offers the possibility of characterizing different building components through synthetic parameters of clear physical meaning and minor computational effort. Our work aims at enhancing the traditional methodproposing a complete mathematical calculation method for the building energy evaluation.

The proposed method could serve as a sort of link between the need for simplification by the technicians (supported and endorsed by national legislation and the EU and by many international standards).

The extension of the Admittance method described by the rules and its IT development (creating user-friendly interface), would balance the needs of the technicians, focused on simplifying procedures for calculation (needs supported and endorsed by national legislation and the EU and many international standards, which allow the use of algorithms that describe the steady-state), with the need to make calculations in dynamic regime that describe the real state in much more detail, both in terms of thermal load and the evaluation of the thermal inertia and both the individual building components and inside of the building.

3.1 Decrement factor and thermal admittance

Let us consider an homogeneous slab of finite thickness, excited by sinusoidal temperature variations θ_{si} and θ_{so} on its internal and external surface, respectively. In particular, let $\bar{\theta}_{si}$ and $\bar{\theta}_{so}$ be the mean values, whereas $\tilde{\theta}_{si}$ and $\tilde{\theta}_{so}$ are the respective cyclic fluctuations about the mean value.

Under the hypothesis of unidirectional conductive heat transfer through the slab in the direction normal to its surfaces, the cyclic heat fluxes $\tilde{q}_i$ and $\tilde{q}_o$ occurring on the two surfaces of the slab can be written as a function of the surface temperatures in the following form:

$$\begin{bmatrix} \tilde{q}_{si} \\ \tilde{q}_{so} \end{bmatrix} = \begin{bmatrix} Y_{11} & Y_{12} \\ Y_{21} & Y_{22} \end{bmatrix} \begin{bmatrix} \tilde{\theta}_{si} \\ \tilde{\theta}_{so} \end{bmatrix} \qquad (1)$$

In equation (1), the heat flux q_i is positive when it enters the slab surface. The elements of the transfer matrix are calculated as follows (Davies, 1994):

$$z_{11} = z_{22} = \cosh\left(t + it\right) \tag{2}$$

$$z_{12} = \frac{\sinh\left(t + it\right)}{\xi \cdot \left(1 + i\right)} \tag{3}$$

$$z_{21} = \xi \cdot \left(1 + i\right) \cdot \sinh\left(t + it\right) \tag{4}$$

In equations (2) to (4), i is the imaginary unit ($i^2 = -1$). Only two parameters appear in the definition of the transmission matrix, namely the cyclic thickness t and the thermal effusivityξ, defined in equations (5) and (6), that collect all the data concerning the thermal properties of the material, the slab thickness L and the period P of the cyclic heat transfer:

$$t = \left[\frac{\omega}{2 \cdot \lambda/(\rho c)}\right]^{1/2} \cdot L = \left[\frac{\pi}{P \cdot 3600} \cdot \frac{\rho c}{\lambda} \cdot L^2\right]^{1/2} \tag{5}$$

$$\xi = \left[\frac{2\pi \cdot \lambda \cdot \rho \cdot c}{P \cdot 3600}\right]^{1/2} \tag{6}$$

However, in practical applications it is more useful to provide an equation that involves the air temperatures $\tilde{\theta}_i$ and $\tilde{\iota}_o$ instead of the temperature on the wall surfaces; this leads to the introduction of the surface thermal resistances R_{si} and R_{so}.

Furthermore, it seems more suitable to consider explicitly in equation (1) the heat flux released from the wall to the indoor environment, and to hold it positive; this implies to put a minus sign before the term $\tilde{\iota}$ appearing in equation (1). The final

expression for a multi-layered construction made up of *n* different homogenous layers becomes:

$$\begin{bmatrix} \tilde{q}_i \\ -\tilde{q}_o \end{bmatrix} = \underbrace{\begin{bmatrix} 1 & R_{si} \\ 0 & 1 \end{bmatrix} \begin{bmatrix} Z_{11} & Z_{12} \\ Y_{11} & Y_{12} \end{bmatrix} \cdots \begin{bmatrix} Z_{11} & Z_{12} \\ Y_{11} & Y_{12} \end{bmatrix} \begin{bmatrix} 1 & R_{so} \\ 0 & 1 \end{bmatrix}}_{\text{TRANSFER MATRIX}} \begin{bmatrix} \tilde{\theta}_o \\ \tilde{\theta}_i \end{bmatrix} = \begin{bmatrix} Z_{11} & Z_{12} \\ Y_{11} & Y_{12} \end{bmatrix} \begin{bmatrix} \tilde{\theta}_o \\ \tilde{\theta}_i \end{bmatrix} \quad (7)$$

The transfer matrix of the multi-layered wall is obtained through the product of the matrices related to each layer, also including the matrix associated to the surface thermal resistances. In equation (7), the sol-air temperature can be used in place of the outdoor temperature when the effect of the solar radiation absorbed on the outer surface of the wall has to be taken into account.

Now, starting from equation (7), with a little algebra and taking into account the property reported in equation (8), one can calculate the heat flux released from the inner surface to the indoor environment according to equation (9):

$$\det[Z] = [Z_{11} \cdot Z_{22} - Z_{12} \cdot Z_{21}] = 1 \quad (8)$$

$$\tilde{q}_i = \frac{1}{Z_{12}} \tilde{\theta}_o - \frac{Z_{11}}{Z_{12}} \tilde{\theta}_i \quad (9)$$

It is now possible to introduce the so-called *periodic thermal transmittanceX*, defined as the cyclic heat flux released from the inner surface of the wall per unit cyclic temperature variation imposed on the other side of the wall, while holding a constant indoor temperature ($\tilde{\theta}_{i,\,-}$):

$$X = \frac{\tilde{q}_{i,\,-}}{\tilde{\theta}_{o,\,-}} = -\frac{1}{Z_{12}} \quad (10)$$

Note that the periodic thermal transmittance resulting from equation (10) is a complex number. The *decrement factorf* is the amplitude of X, normalized with respect to the steady thermal transmittance U; on the other hand, the time lag φ_X is the phase of X, measured in hours and referred to an excitation having a period P:

$$f = \left|\frac{X}{U}\right| \quad \varphi_X = \frac{P}{2\pi} \cdot \arctan\left(\frac{\mathrm{Im}(X)}{\mathrm{Re}(X)}\right) \tag{11}$$

Furthermore, starting from equation (9) the *thermal admittanceY*can also be introduced. This is defined as the cyclic heat flux entering the inner surface of the wall per unit cyclic temperature variation imposed on the same side, while holding a constant outer temperature ($\tilde{\iota}_o$):

$$Y = -\frac{\tilde{\iota}}{\tilde{\iota}} - \frac{Z_{22}}{Z_{12}} \tag{12}$$

However, when dealing with internal partitions separating two spaces with identical thermal conditions ($\tilde{\iota}_i$ $\tilde{\iota}_o$), from equation (9) we get:

$$\tilde{\iota} \quad \frac{Z \quad -1}{Z_{12}} \cdot \tilde{\iota}_i \tag{13}$$

The term $(Z_{22} - 1)/Z_{12}$ occurring in equation (13) is called by some authors *modified thermal admittance* (Millbank and Harrington-Lynn, 1974), and is also referred to in the standard ISO 13792:2012.

Now, the dynamic thermal properties defined so far are usually calculated with reference to sinusoidal forcing conditions with a period $P = P_1 = 24$ h. However,

all the relations previously introduced can also be applied to any harmonic of order n, i.e. having a period $P_n = P_1/n$.

3.2 The surface factor

Despite the interest shown in the scientific literature towards the dynamic transfer properties, little reference is made to the thermal response of the opaque components to the radiant heat fluxes occurring on their internal surface, such as those associated to solar heat gains through the windows or to internal radiant loads.

Some attempts were done in the past in this sense. For instance, the thermal storage factor defined in the Carrier method (Carrier, 1962) is worth mentioning as the ratio of the rate of instantaneous cooling load to the rate of solar heat gain. This factor has to be determined through appropriate tables depending on the weight per unit floor area of the opaque components and the running time. Therefore, its use requires interpolation among table data, it is rather rough because it doesn't account for the actual sequence of the wall layers, and it lacks of any theoretical basis, as it comes out from numerical simulations.

A substantially different approach can be found in the framework of the Admittance Procedure, laid down in the early Seventies (Millbank et al, 1974), where these contributions are taken into account by means of the so called surface factor. Nonetheless, the surface factor has been paid little attention: to the authors' knowledge, little reference is made to this parameter in the whole scientific literature (Beattie and Ward, 1999) (Rees et al., 2000), while its definition has

only recently been recovered in the CIBSE guide (CIBSE, 2006) and in international Standard ISO 13792:2012.

According to the definition provided by Millbank and Harrington-Lynn (1974), the surface factor F quantifies the thermal flux released by a wall to the environmental point per unit heat gain impinging on its internal surface, when the air temperatures on both sides of the wall are held equal.

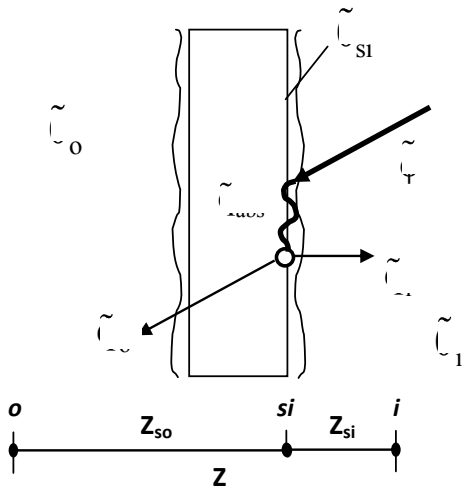

Figure 3.1 - Energy balance on the internal surface for the definition of the surface factor

With reference to Figure 3.1, let $\tilde{\phi}$ be the cyclic radiant heat flux acting on the inner surface of the wall, as a result of the radiant energy released by internal sources or transmitted through the glazing. The following definition holds:

$$F = \frac{\tilde{\quad}}{\tilde{\quad}} = \frac{\tilde{\quad}}{\tilde{\quad}} \tag{14}$$

In order to provide an operational formulation to *F*, one can consider that the amount of thermal energy absorbed by the wall ($\alpha \cdot \tilde{\varphi}$) is re-emitted to the internal and to the external environment, according to the following balance equation:

$$\alpha \cdot \tilde{\phi} \quad \tilde{q}_i \quad \tilde{q}_o \tag{15}$$

The cyclic heat fluxes $\tilde{q}_i$ and $\tilde{\varphi}$ can be written as a function of the thermal impedances Z_{si} and Z_{so} represented in Figure 3.1:

$$\tilde{q}_i \quad \frac{\tilde{\theta}_{si} \quad \tilde{\theta}_i}{Z_{si}} \tag{16}$$

$$\tilde{q}_o \quad \frac{\tilde{\theta}_{si} \quad \tilde{\theta}_o}{Z_{so}} = \frac{\tilde{\theta}_{si} \quad \tilde{\theta}_o}{Z - Z_{si}} \tag{17}$$

In equation (16) and (17), $\tilde{\theta}_{si}$ is the temperature fluctuation measured on the inner surface of the wall. Under the hypothesis subtended in the definition of the surface factor, i.e. $\tilde{\theta}_i \quad \tilde{\theta}_o$, it is possible to eliminate $\tilde{\theta}_{si}$ by combining equation (16) and (17):

$$\frac{\tilde{\varphi}}{\tilde{\varphi}} = \frac{Z - Z_{si}}{Z_{si}} \tag{18}$$

Equation (18) suggests that the ratio of the heat fluxes released by the internal surface respectively to the indoor and the outdoor environment equals the inverse ratio of the corresponding thermal impedances. Now, by combining equation (18) and equation (15), one obtains:

(19)

At this stage, one must considerthat the thermalimpedanceZsibetween the surface of the wall and the indoor air is purely resistive, thus $Z_{si} = R_{si}$. Moreover, the inverse of the wall thermal impedance Z corresponds to its thermal admittance Y. Such positions imply the following expression for the surface factor F :

$$F = \frac{\tilde{}}{\alpha \cdot} \quad -1 - Y \cdot R_{si} \tag{20}$$

For internal partitions separating two spaces with identical thermal conditions, in equation (20) the admittance Y should be replaced by the *modified thermal admittance* introduced in equation (13) (Millbank and Harrington-Lynn, 1974).

The value calculated according to equation (20) is a complex number, characterized in terms of amplitude |F| and phase φ_F. The latter can be assessed through equation (21), and will always result negative, denoting a delay of the wall response to the radiant heat flux acting on it.

$$\varphi_F = \frac{P}{2\pi} \cdot \arctan\left(\frac{\mathrm{Im}(F)}{\mathrm{Re}(F)}\right) \tag{21}$$

Hence, the surface factor depends not only on the geometrical and thermo-physical properties of the wall, but also on the period P of the cyclic radiant flux. Since in a real building any energy input linked to weather conditions can be considered periodic with a 24-hour frequency, the surface factor is conventionally calculated for $P = 24$ h.

Moreover, the definition of surface factor provided in equation (20) can also be applied to a steady radiant flux. In this case, the admittance Y has to be replaced by the stationary thermal transmittance U of the wall:

$$\bar{F} = \frac{\bar{q}_i}{\bar{q}_{abs}}\bigg|_{\tilde{t}_i \; \tilde{t}_o} = 1 - U \cdot R_{si} \tag{22}$$

As to the internal surface resistance R_{si}, important remarks will be given later.

3.3 The Surface Factor for monolayer walls

A first analysis concerning the behaviour of walls as a result of incident radiative fluxes can be conducted by determining the module and the phase of surface factor Z for homogeneous walls consisting of a single layer of various construction materials, to vary the layer thickness. Table 3.1 shows the thermo-physical properties of the most common building materials; in Figure 3.2 the module and the Z phase are plotted as a function of wall thickness[2]. For the calculation of Z, the internal and external threshold resistance have respectively been assigned the following values:

$R_i = 0.22$ [m²·K¹·W⁻¹] $\qquad\qquad$ $R_e = 0.075$ [m²·K¹·W⁻¹]

These values are in fact found to be more suitable for a calculation scheme in summer rather than the standard values reported in [18] ($R_i = 0.13$ m²·K¹·W⁻¹, R_e

[2] The phase of this parameter is always negative, since thermal energy is returned from the wall with a delay in respect to the action of the solar radiation on it; here we prefer to represent it as positive, defining it as "delay".

= 0.04 $m^2 \cdot K^1 \cdot W^{-1}$), used for the calculation of the transmittance of the walls in winter conditions during the project.

From the diagrams in Figure 3.2 it can be firstly noted that the curves are spaced apart in proportion to the *generalized thermal effusivity*, defined by:

$$\zeta = \sqrt{\frac{2\pi}{P} \cdot \rho \lambda c} \tag{9}$$

For all the materials taken into consideration, a thickness of about 15 cm marks the maximum delay, more than 2.5 hours for high values of ζ (heavy and not very insulating material), about 1.5 hours for the average values of ζ (light material) and less than half an hour for the insulation. In light of the results, the insulating materials appear more capable of "reflecting" the heat wave, the other vice versa in inverse relationship to the effusivity.

It is observed that, whereas the delay is reduced to zero when the thickness tends to zero, the admittance Y formally reduces to a constant value that only depends on the surface resistance, for which we have:

$$Z = 1 - \frac{R_i}{R_i + R_e} = 0.254 \tag{10}$$

	Material	*Conductivity* λ ($W \cdot m^{-1} \cdot K^{-1}$)	*Density* ρ ($kg \cdot m^{-3}$)	*Specific heat* c ($J \cdot kg^{-1} \cdot K^{-1}$)	*Effusivity* ζ ($W \cdot m^{-2} \cdot K^{-1}$)
A	***Concrete with closed structure with natural aggregates***	1.16	2000	880	12.18
B	***Concrete with closed structure of expanded clays***	0.5	1400	880	6.69
C	***Autoclaved concrete***	0.19	600	1010	2.89
D	***Hollowbrick***	0.35	750	840	4.00
E	***Porousbrick***	0.17	630	840	2.56
F	***Perforatedbrick***	0.43	1200	840	5.61
G	***Solid brick***	0.72	1800	840	8.90
H	***Blocks of tufa***	0.7	1600	840	8.27
I	***Lava***	2.9	2200	840	19.74
L	***Blocks of limestone***	1.5	1900	840	13.20
M	***Polystyrene***	0.036	30	1400	0.34
N	***Polyurethane***	0.032	40	1450	0.37
O	***Fiberglass***	0.04	35	1030	0.32
P	***Cork***	0.045	115	1800	0.82
Q	***Plaster of lime and gypsum***	0.7	1400	840	7.74
R	***Mortar of lime and cement***	0.9	1800	840	9.95
S	***Granite***	3.2	2500	840	22.11
T	***Marble***	3	2700	840	22.24
U	***Timber(fir)***	0.12	450	2700	3.26
V	***TImber (oak)***	0.22	850	2700	6.06

Table 3.1 Characteristics of the most common building materials

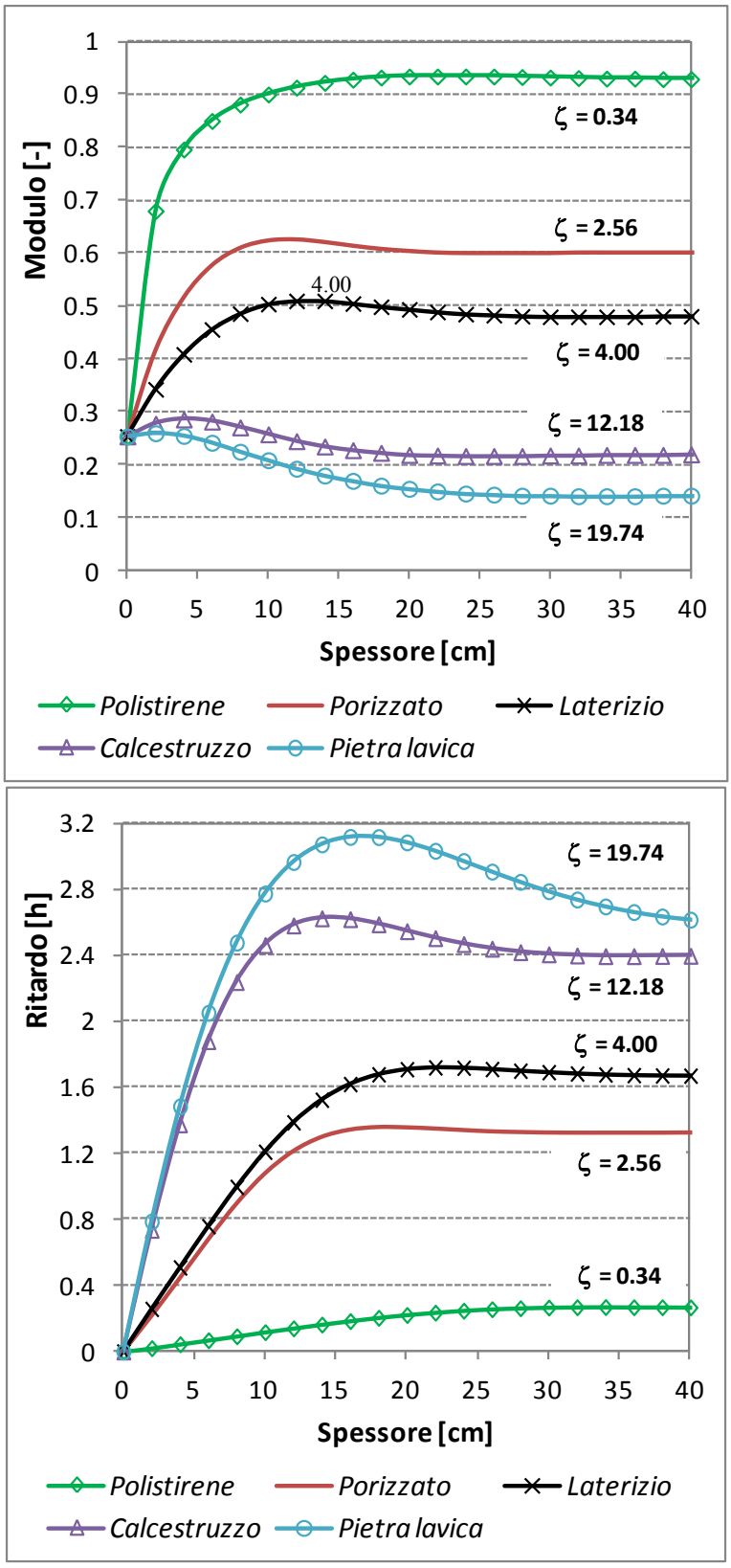

Figure3.2 - module and delay of Z for walls monolayer according to the thickness

The conductive thermal resistance Rλ and air thermal capacity C, are respectively defined as:

$$R_\lambda = \frac{s}{\lambda} \qquad [m^2 \cdot K \cdot W^{-1}] \qquad C = \rho \cdot c_p \cdot s \qquad [J \cdot m^{-2} \cdot K^{-1}] \qquad (11)$$

Plotting the values of Z for every recurrent given material in Table 3.1 as a function of the previously given characteristic quantities, it is possible to construct the maps shown in Figure 3.3, valid for single-layer walls of s = 10 cm thickness. The properties of the same materials in thicknesses more usual in practice are shown in Figure 3.4.

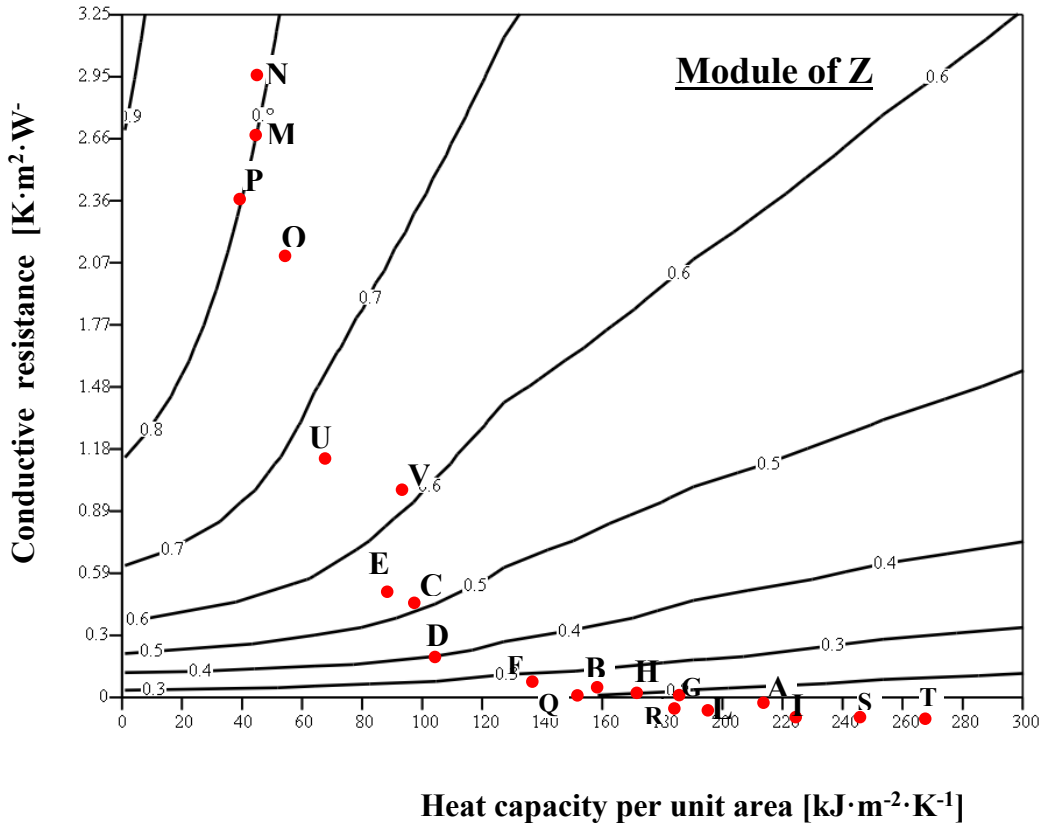

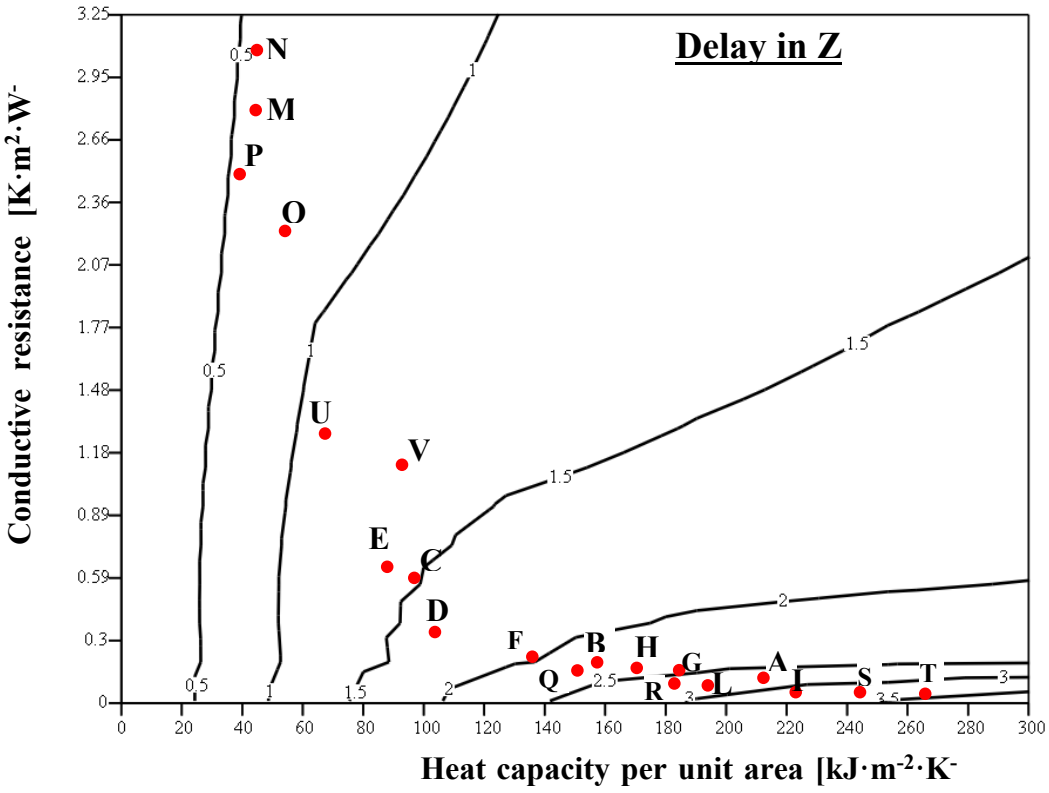

Figure3.1 - module and delay of Z for monolayer walls - thicness s=10 cm.

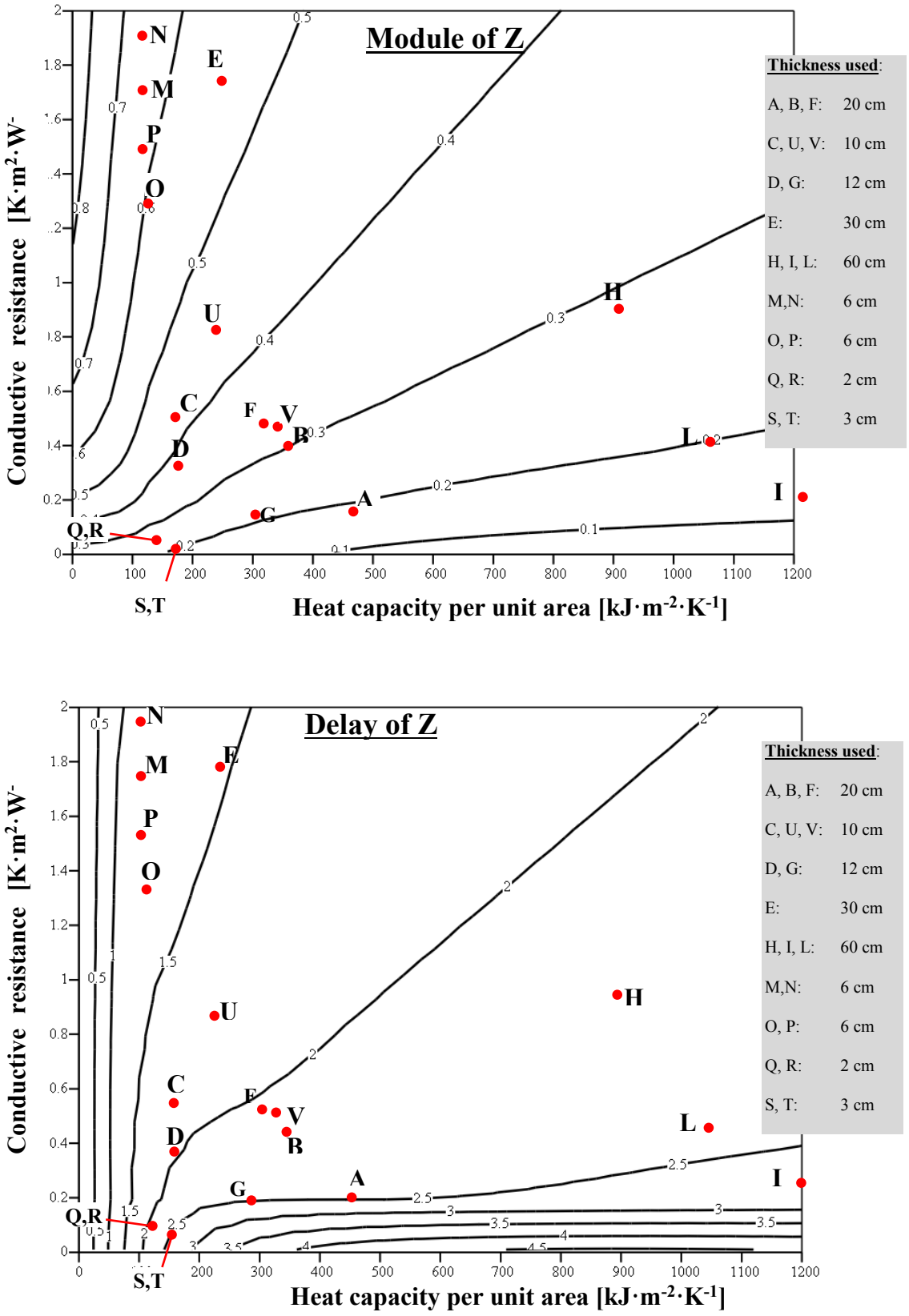

Figure3.2 - module and delay of Z for monolayer walls - thickness given in table.

3.4 The role of harmonics in the determination of Z

As mentioned above, the factor of the surface of a wall, as a dynamic parameter, depends on the pulsation of the forcing function. Solar radiation I_{sol} can be considered, for the purpose of dynamic analysis of buildings, forcing a periodic of period P = 24 h; as such, it is possible to approximate it with an endless series of simple sinusoidal functions (Fourier series) called "harmonics". The first, frequency $f_1=2\pi / P$, is called the "fundamental harmonic"; successive harmonics have frequencies equal to an integer multiple of the fundamental frequency $f_n=2\pi/(P/n)$. We therefore have:

$$I_{sol}(\tau) = I_m + \sum_{n=1}^{\infty} \gamma_n(\tau) \tag{12}$$

$$\gamma_n(\tau) = A_n \cdot \cos\left(\frac{2\pi \cdot n}{P} \cdot \tau\right) + B_n \cdot \sin\left(\frac{2\pi \cdot n}{P} \cdot \tau\right) \tag{13}$$

Here the term I_m expresses the average value of the function $I_{sol}(\tau)$:

$$I_m = \frac{1}{P} \cdot \int_0^P I_{sol}(\tau) d\tau \tag{14}$$

A_n e $B_n$are the coefficients of the n-ma harmonic, given by:

$$A_n = \frac{2}{P} \cdot \int_0^P I_{sol}(\tau) \cdot \cos\left(\frac{2\pi \cdot n}{P} \cdot \tau\right) d\tau \qquad B_n = \frac{2}{P} \cdot \int_0^P I_{sol}(\tau) \cdot \sin\left(\frac{2\pi \cdot n}{P} \cdot \tau\right) d\tau \tag{15}$$

In practice, the function Isol (τ) can be approximated by a series expansion that only includes an appropriate number N of harmonics, that is:

$$I_{sol}(\tau) \cong I_m + \sum_{n=1}^{N} A_n \cdot \cos\left(\frac{2\pi \cdot n}{P} \cdot \tau\right) + \sum_{n=1}^{N} B_n \cdot \sin\left(\frac{2\pi \cdot n}{P} \cdot \tau\right) \quad (16)$$

The accuracy in the approximation of the original function obviously depends on the number N of harmonics considered.

The surface factor Z, calculated according to Eq. (8) as provided by the standard UNI EN ISO 13792: 2005, refers to a period P = 24 h, and is therefore representative of the response of a wall solely to the first harmonic of the forcing function. In the following we will therefore try to show how this parameter is really able to describe the behaviour of the wall in respect to the periodic forcing function considered in its entirety.

First, it is interesting to highlight the extent of the contribution of each harmonic in the development in series in equation (16). The forcing function, considered here as an example, is the intensity of solar radiation that penetrates the environment through a glazed surface free of obstructions and exposed to the west; its time course is shown in Figure 3.5, together with the curves obtained using Eq. (16) to vary the number of harmonics included in the summation.

The diagram shows that by restricting ourselves to the first 5 harmonics, it is possible to reconstruct the time profile of the force in question in an extremely precise way. This result can also be understood in the light of the right-hand diagram; here the effective value of V_n of each harmonic means is shown - defined as in equation (17) and representative of its energy content - normalized in respect to the effective value V_1 of the first harmonic. It is clear that the weight of the harmonics decreases rapidly, becoming negligible for n>5; in any case, the

first harmonic is not sufficient to fully characterize the forcing function that acts on the wall.

$$V_n = \sqrt{\frac{1}{P(n)} \cdot \int_0^{P(n)} \gamma_n^2(\tau)\, d\tau} \qquad \text{where:} \qquad P(n) = \frac{24}{n} \qquad (17)$$

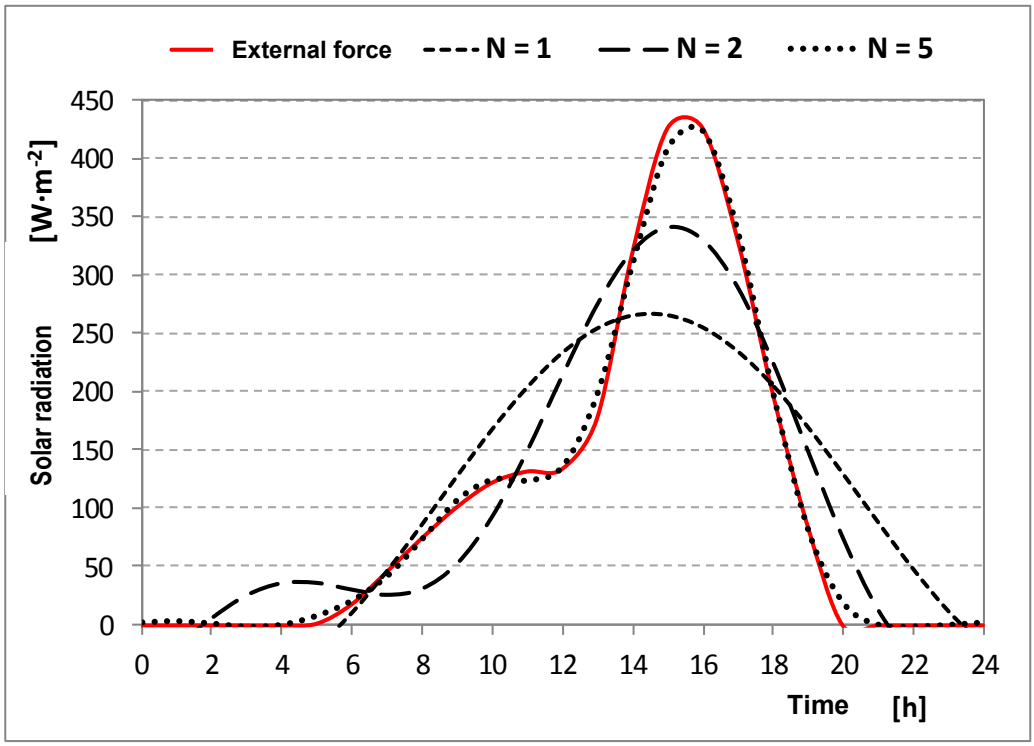

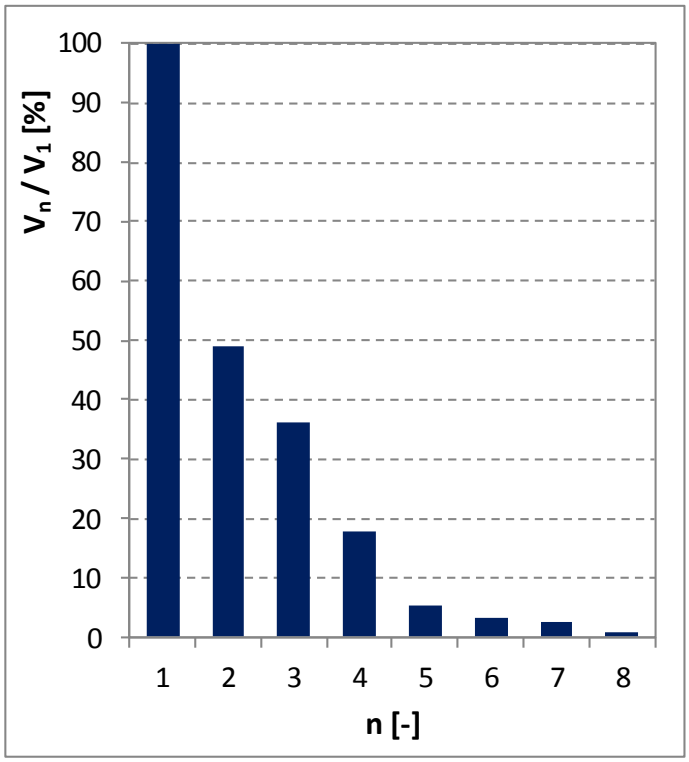

Figure3.3 – harmonic contribution to the construction of the periodic forcing.

In the light of what we have seen so far, it is possible to write the heat flux q (τ) emitted by a wall in response to the incident solar radiation in the following form:

$$q(\tau) = \bar{Z} \cdot I_m + \sum_{n=1}^{N} |Z_n| \cdot \gamma_n \left(\tau - \phi_{Z,n}\right) \tag{18}$$

Figure 3.5 shows the trend of module and the Z phase to vary the index of the harmonic n, for monolayer walls in different materials but of constant thickness (s = 10 cm). As can be seen, apart from polystyrene, for which the Z module is almost unitary, for all the other materials Z decreases significantly with n: the materials namely allow themselves to be more easily permeated by the thermal wave the higher the frequency, thereby reducing the rate of energy returned to the environment. The phase shift - especially for heavier materials - also shows a significant reduction in the growth of the index n of the harmonic.

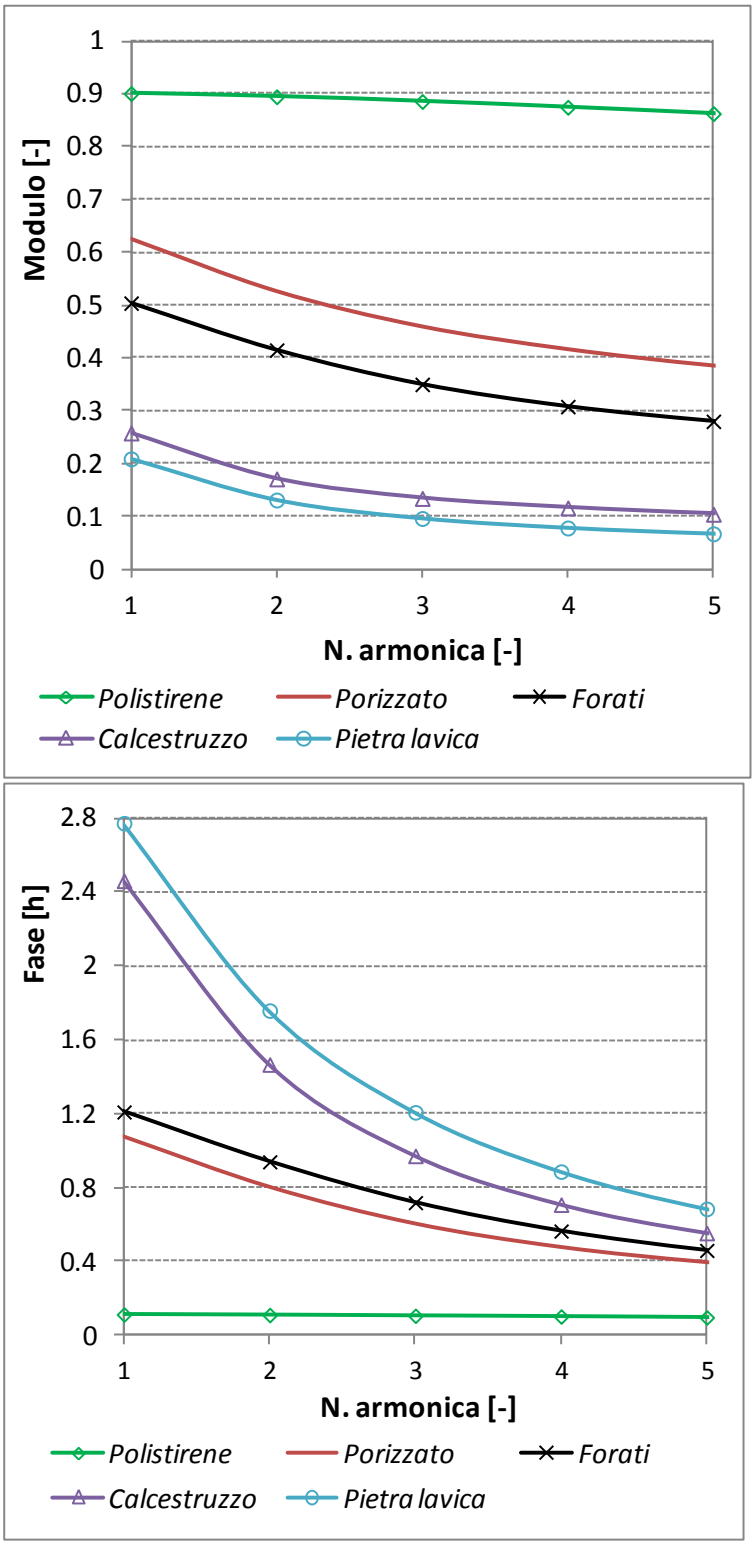

Figure 3.6 – Dependence of Z index of the harmonic (s = 10 cm)

Whereas Figure 3.6 shows the response of the walls to the solar forcing function (force) calculated according to (18), that is, by summing up the responses due to individual harmonics in which the forcing function has been decomposed. From an analysis of the curves in the figure, you can determine the actual values of attenuation and phase shift θ of the response in respect to the forcing function; in particular, the attenuation may be defined as the ratio between the peak value of the response (q_{max}) and the peak value of the driving force (I_{sol_max}) and phase shift as the temporal distance between the two peaks (delay).

At this point, it is useful to compare the values of attenuation and phase shift so defined, with the module and the phase of the surface factor Z of the fundamental harmonic (N = 1), Table 3.2.

Note that the data of "attenuation" is very close to the “Z module”, and consequently it is only in the first harmonic that it is possible to realistically estimate the breakdown that the peak of radiation undergoes when it re-emerges from the wall as a response stream. However, the time lag between forcing function and response calculated with only the first harmonic ("Z phase") overestimates the real delay with which the absorbed solar radiation is re-emitted into the environment, and expressed in the data of "phase displacement".

The advantage of comparison comes from the fact that the regulations usually only refer to only the first harmonic. UNI EN ISO 13792: 2005, for example, in defining the surface factor, requires us to work solely with P = 24 hours, neglecting the consideration of harmonics after the first.

As shown here, therefore, makes it clear that to realistically assess the response of the system (and, by construction materials, especially the phase shift), it is not

sufficient to refer to the fundamental harmonic, but it is necessary to consider the contribution of a suitably large number of harmonics.

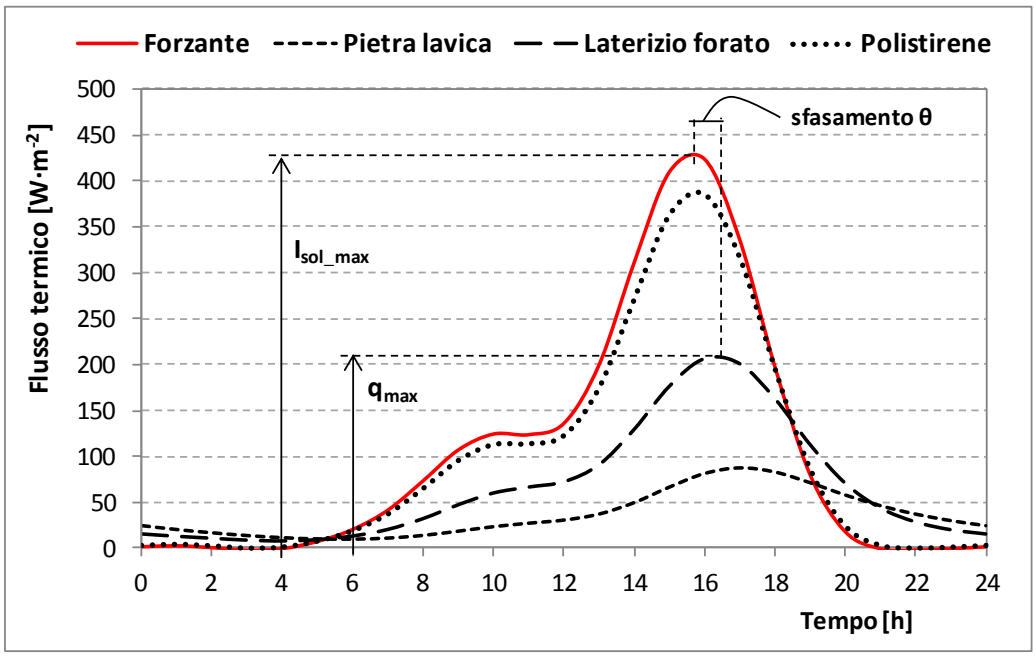

Figure 3.8 – Response of single-layer walls to solar forcing rebuilt with N=5 harmonics.

	*Module of Z** [-]	*Attenuation*** [-]	*Phase of Z** [h]	*phase sghift θ*** [h]
Lava	0.209	0.201	2.7	1.1
Concrete	0.258	0.257	2.5	1.2
Hollowbrick	0.504	0.482	1.2	0.8
Porousbrick	0.625	0.602	1.1	0.7
Polystyrene	0.901	0.902	0.1	0.1

* : calculated for the fundamental harmonic (N = 1)

** :calculated for N=5 harmonic

Table 3.2 - Evaluation of phase shift and attenuation of the response (10 cm thick).

3.5 The wall energy balance

According to the definition of the previously mentioned dynamic thermal properties, it is possible to state right away the energy balance for an opaque component subject to periodic forcing conditions, while the analytical procedure for the calculation of the time-dependent internal air temperature in an enclosed spacewill be presented in the followingsection.

First of all, it is necessary to consider that the heat flux q_i reported in equation (19) is the overall heat flux released by a wall per unit radiant heat flux impinging on its inner surface, where the convective and radiant terms are still combined together. However, it is important to extract the convective component of this overall heat flux, since it is the one involved in the energy balance equation of the whole enclosure.

In order to single out the convective component, one can observe that the convective and the overall heat flux are inversely proportional to the respective surface thermal resistance. Hence, equation (23) can be stated:

$$\tilde{q}_{c,i,n} = \frac{h_c}{h_c + h_r} \cdot F \cdot (\alpha \cdot \tilde{\varphi}_{...} - h_c \cdot (\tilde{\theta}_{si,n} - \tilde{\theta}_{o,n})) \tag{23}$$

Here, h_c and h_r are the surface heat transfer coefficients by convection and radiation, respectively. Their sum is the combined heat transfer coefficient, whose reciprocal is the surface thermal resistance, $R_{si} = 1/(h_c + h_r)$.

Now, equation (24) can be stated. It represents the overall density of heat flux released by a wall to the indoor environment as a response to the n-th harmonic component of the whole set of forcing conditions. Here, θ_o is the air temperature

on the outer side of the wall; however, it can also be interpreted as the sol-air temperature when one wants to account for both the outdoor temperature and the solar irradiation absorbed on the outer surface. On the other hand, equation (25) is the stationary term, obtained by considering the average value of each forcing condition.

Finally, the time-dependent response of the wall is obtained by recombining such contributions as in equation (26); the summation of the harmonics is truncated to the harmonic of order N_H.

$$\tilde{q}_{i,n} = \tilde{\theta}_{o,n} - \tilde{\theta}_{i,n} \cdot h_c - R_{si} \cdot (\alpha \cdot \tilde{\phi}_n) \tag{24}$$

$$\bar{q}_i = U \cdot \left(\bar{\theta}_o - \bar{\theta}_i\right) + h_c \cdot R_{si} \cdot \bar{F} \cdot (\alpha \cdot \bar{\phi}) \tag{25}$$

$$q_i(\tau) = \bar{q}_i + \sum_{n=1}^{N_H} \tilde{q}_{i,n} \tag{26}$$

The following point to address is the determination of the radiant heat flux ϕ circulating into the enclosure and acting on the inner surface of a wall. This term appears in equation (25) (mean value) and equation (24) (cyclic variation around the mean value), and is basically due to the solar radiation transmitted through the glazing and to the radiant component of other internal sources (lighting, appliances, people). However, its evaluation is not easy, as it implies the knowledge of the radiation distribution within the indoor environment.

In this study, the authors adopted a simplified approach, based on the Ulbricht sphere model, i.e. the hypothesis of uniform distribution of the radiant heat gains

all over the surfaces of the enclosed space. According to this model, the radiant heat flux acting on the generic surface can be calculated as:

$$\phi = \frac{1}{A_{tot}} \cdot \left[\frac{\psi_{lw}}{1 - r_{m,lw}} + \frac{\psi_{sw}}{1 - r_{m,sw}} \right] \tag{27}$$

Here, r_m is the weighted mean reflectivity of the enclosing surface, defined as:

$$r_m = \left(\sum_k^{surf} r_k \cdot A_k \right) \Big/ \sum_k^{surf} A_k \tag{28}$$

Moreover, a distinction is made between short-wave (sw) and long-wave (lw) radiant heat gains, as the reflectivity of walls and glazing to such contributions is not the same. In equation (27) ψ_{sw} relates to the solar radiation transmitted through the glazing, whereas ψ_{lw} accounts for internal radiant sources and for the fraction of solar energy absorbed by the glazing and re-emitted towards the indoor environment. All of the data needed in equation (27) are usually known.

3.6 The room energy balance

Finally, the energy balance on the indoor environment can be written as in equation (29). Here, one can recognize the contributions due to:

(1) convective heat flux released by the opaque components, calculated according to equation (24) to (26);

(2) heat transfer through the window, that is proportional to the thermal transmittance U_w;

(3) infiltration of outdoor air, measured by the air changes per hour n_a ;

(4) convective fraction of the internal loads, Q_{int} (people, lighting, appliances);

(5) convective thermal power released by heating or cooling plants.

$$\sum_{k=1}^{surf} q_{i,k}(\tau) + \left(U_w \cdot A_w + 0.34 \cdot n_a \cdot V\right)\left[\theta_o(\tau) - \theta_i(\tau)\right] + x_c \cdot \dot{\zeta}_{int}(\tau) + \dot{\zeta}_{sys}(\tau) = 0 \qquad (29)$$

Due to the negligible heat capacity of the indoor air, the thermal balance assumes the same form as for steady state conditions. If one needs to solve equation (29) in relation to a free-running space, $Q_{sys}(\tau) = 0$.

Now, under the assumption of periodic driving forces, in equation (29) every time-dependent variable can be written as the sum of its mean value plus a series of harmonic components. Thus, the following relationship holds for the indoor air temperature $\theta_i(\tau)$:

$$\theta_i(\tau) = \bar{\theta}_i + \sum_{n=1}^{N_H} \tilde{\theta}_{i,n}(\tau) \qquad (30)$$

Finally, it is useful to remind that every harmonic function should comply the condition expressed in equation (31):

$$\sum_{\tau=1}^{24/n} \tilde{\theta}_{i,n}(\tau) = 0 \qquad \text{for } n = 1,2 \ldots N_H \qquad (31)$$

According to these specifications, if one aims to determine the indoor temperature profile $\theta_i(\tau)$ for a free running space, equation (29) has to be solved in search for the following data:

- the mean value, $\overline{\theta}_i$;
- the harmonic components $\tilde{\iota}_{i,n}$, for n ranging from 1 to N_H;

Thus, for every time step τ, a number (N_H + 1) of unknown variables should be determined. This can be done since an equivalent number of equations is available.

On the other hand, for rooms under thermostat constraint, the temperature profile $\theta_i(\tau)$ is known a priori. In this case, equation (29) provides the dynamic thermal load Q_{sys} (τ).

It is to be reminded that, despite the calculation of the dynamic thermal properties is well established in the literature, a general model based on them and aimed at finding the room thermal response, is not yet covered in the literature. Moreover, some peculiar features are introduced in the present study:

- the calculation of the surface factor with more appropriate values of the surface thermal resistance R_{si};
- the adoption of the Ulbricht hypothesis for evaluating the distribution of the radiant heat gains in the enclosed space.

Finally, it is necessary to remark that the proposed methodology, in its present form, is not suitable in case of variable parameters, e.g. with a variable ventilation rate. Indeed, in this case the variable parameter should also undergo the Fourier analysis in order to be decomposed in harmonic components, which would considerably complicate the solution of equation (29). However, an improved and more general version of the methodology is being developed at the moment.

In the following, the validation of the formulation presented so far is discussed. It is based on the procedure reported in the ISO Standard 13792, devoted to the calculation of the internal temperature of a room in summer without mechanical cooling. Furthermore, the approximation introduced by considering only the first harmonic (P = 24 h), as suggested by the simplified approach proposed in the ISO Standard 13792:2012, will be discussed.

4 The validation procedure

The validation of new mathematical codes for the dynamic thermal simulation of buildings can be performed by comparison with appropriate reference values, obtained through experimental measurements or by means of well established codes.

In particular, the international Standard ISO 13792 proposes a procedure that allows the validation of mathematical models for the calculation of the summer internal temperature in enclosures without mechanical cooling. The procedure consists in the calculation of the hourly profile of the operative temperature for a test room in different conditions; for every test case, the minimum, average and maximum values of the operative temperature shall then be compared to the reference values reported in the Standard. As far as its reliability is concerned, the computer code under examination will belong to class I, II or III based on the difference Δ between the calculated values and the reference values; the model is classified according to the worst result:

- Class I: $-1°C < \Delta < 1°C$
- Class II: $-1°C < \Delta < 2°C$
- Class III: $-1°C < \Delta < 3°C$

Figure 4.1 reports the geometry of the test room. Two different cases are considered: in Case A the surface of the window is $A_w = 3.5$ m^2, whereas $A_w = 7.0$ m^2 in case B. The climatic conditions are also different (see Figure 4.2): case A

applies to warm climates (latitude 40°N), whereas case B applies to temperate climates (latitude 52°N).

For each room geometry, different sub-cases are considered, distinguished by a test number (from 1 to 3, according to the type of floor/ceiling) and by a second letter, associated to the ventilation rate (case *a*: 1 h^{-1}, case *c*: 10 h^{-1}). There is also a sub-case *b*, that applies to a variable ventilation rate, but this is not considered in the framework of this study, since the proposed model only allows constant parameters.

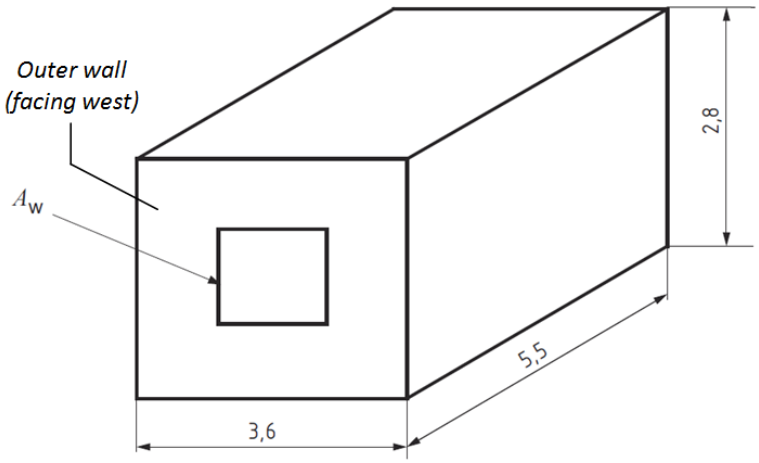

Figure 4.1 - Geometry of the sample room proposed in the ISO Standard 13792:2012

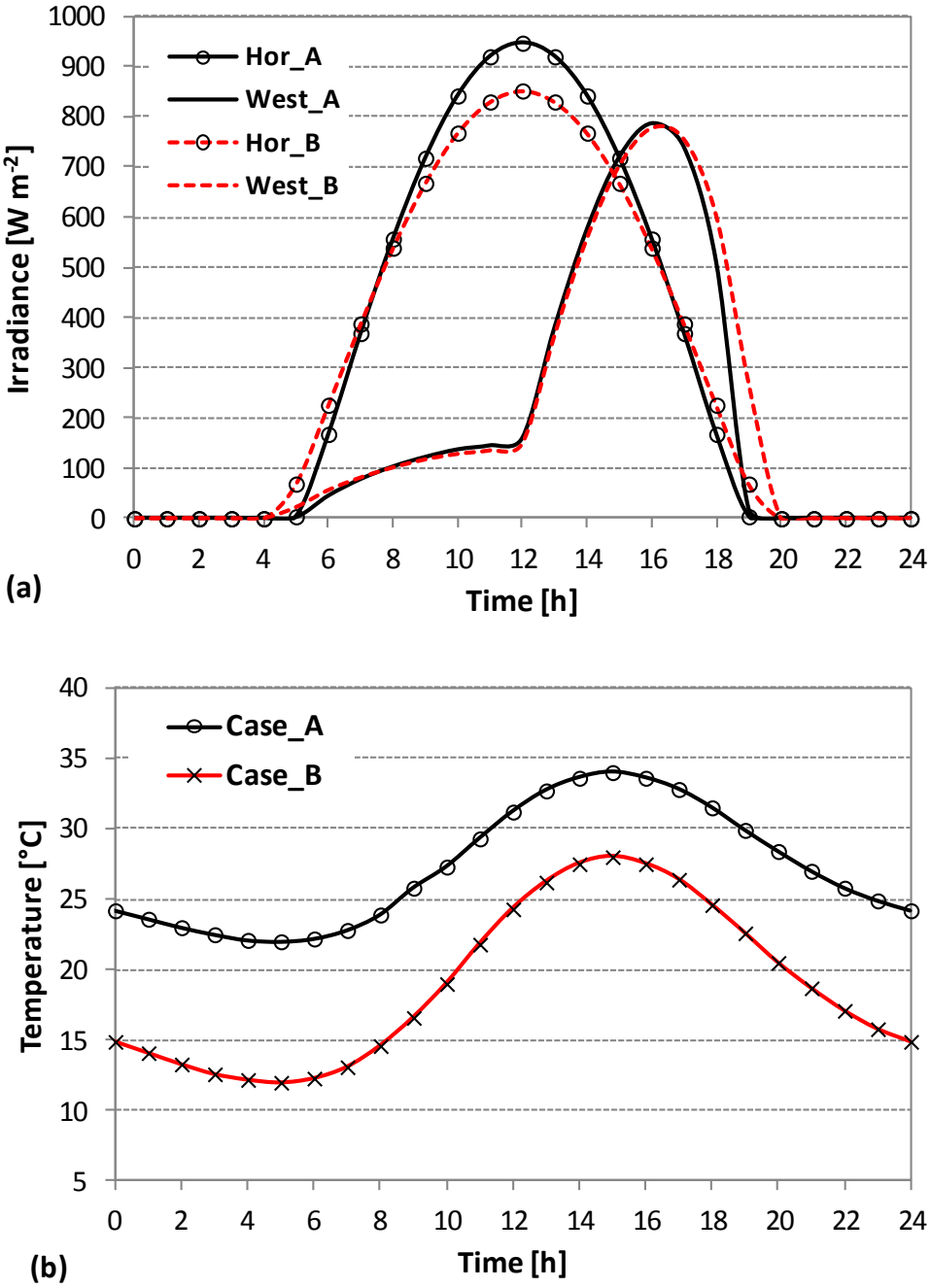

Figure 4.2 - Climatic data for the validation. (a) Solar irradiance, (b) Outdoor temperature

As concerns the composition of the opaque components, the external wall is made up of a double layer of masonry (115 mm plus 175 mm) with an intermediate insulation layer (60 mm) and an internal plastering (15 mm). The partition walls consist of two gypsum wallboards (12 mm each) with an intermediate layer of

mineral wool (100 mm). Ceilings and floors are basically composed of a concrete slab (200 mm) covered with an insulation layer (40 mm) plus a concrete screed (60 mm). In the test number 1, a further insulation layer (100 mm) is added to the bottom of the concrete slab. All the surfaces, except the outer wall and the roof in the test number 3, are bounded by similar rooms. The short-wave surface absorptance is $\alpha = 0.6$.

Now, in the calculation of the dynamic thermal properties (X, Y and F), the ISO Standard 13792 prescribes to use R_{si} = 0.22 m^2 K W^{-1} for any surface. However, in this study such recommended value has been used only for the calculation of X and Y. Instead, the surface factor F is calculated through more appropriate values, introduced in Evola and Marletta (2013) and reported in Table 4.1, together with the recommended values for the convective heat transfer coefficient h_c to be used in equation (23).

		Walls	Ceiling	Floor
R_{si}	[m^2 K W^{-1}]	0.6	0.85	0.7
h_c	[W m^{-2} K^{-1}]	1.4	1.0	1.2

Tabella 4.1 Values retained for Rsi and hc in the calculation of the surface factor

Table 4.2 collects the dynamic thermal properties for the vertical and horizontal envelope components, calculated for the fundamental harmonic (P = 24 h) with the relations introduced in the previous sections.

From Table 4.2 one can learn that the opaque components that contain an insulation layer very close to the internal surface, i.e. the partitions and the ceiling

in test case 1, show a surface factor F quite high and a low time shift φ_F. This means that these envelope components tend to give back a very high portion of the radiant heat flux absorbed on their inner surface, and this happens within around one hour. On the contrary, all other components allow a significant attenuation of the radiant heat flux acting on their inner surface (low |F|), with a rather high time lag φ_F.

Table 4.2 - Dynamic thermal properties for the room components defined in ISO 13792:2012 (in brackets, the test cases)

	|Y| [W m^{-2} K^{-1}]	|X| [W m^{-2} K^{-1}]	ϕ_X [h]	U [Wm^{-2} K^{-1}]	f [-]	|F| [-]	ϕ_F [h]
Wall (all cases)	3.28	0.053	-12.1	0.464	0.115	0.157	-2.6
Partition (all cases)	0.74	0.318	-1.5	0.327	0.972	0.928	-1.5
Ceiling (case 1)	0.59	0.005	-12.8	0.226	0.022	0.710	-1.2
Ceiling (case 2)	3.96	0.058	-10.9	0.631	0.092	0.053	-4.5
Roof (case 3)	3.95	0.060	-7.6	0.416	0.144	0.057	-3.3
Floor (case 1)	3.45	0.005	-12.8	0.226	0.022	0.172	-4.1
Floor (case 2 and 3)	3.45	0.058	-10.9	0.631	0.092	0.167	-4.4

As concerns the window, it is composed by a double pane glazing with an external shading device. The external, internal and cavity thermal resistances are assigned: as a results, the thermal transmittance U_w is 2.2 W m^{-2} K^{-1}. Furthermore,

the short-wave optical properties of both the glazing and the shade are assigned: this allows to easily calculate the rate of solar irradiance transmitted through the window, or absorbed by the glazing and re-emitted towards the indoor environment.

Finally, the ISO Standard also prescribes the time profile of the internal sources to be used in the simulations (people, appliances), and assigns an equal proportion to convection and radiation ($x_c = 0.5$).

Thus, all the input values needed for the simulations are assigned, and they can be easily implemented in the calculation procedure. The calculation is carried out by using $N_H = 6$ harmonics, since a preliminary analysis showed that no significant improvement of the results would be achieved by adding further harmonics.

As a result, the time profile of the indoor temperature $\theta_i$is obtained. This result can be also used to determine the mean radiant temperature θ_{mr}, according to equation (32):

$$\theta_{mr}(\tau) = \frac{\left(\sum_k A_k \cdot h_{ck} + A_w \cdot h_{cw}\right) \cdot \theta_i(\tau) + 0.34 \cdot n \cdot V \cdot \left(\theta_i(\tau) - \theta_o(\tau)\right) - x_c \cdot Q_{\text{int}}(\tau)}{\sum_k A_k \cdot h_{ck} + A_w \cdot h_{cw}} \quad (32)$$

This derives from the position that, if all the inner surfaces present the same temperature θ_{mr}, no reciprocal radiant heat exchange would occur, but only a convective heat transfer to the indoor air. Finally, the room operative temperature is provided by equation (33).

$$\theta_{op}(\tau) = \frac{\theta_{mr}(\tau) + \theta_i(\tau)}{2} \quad (33)$$

5 Validation of the proposed model

As described before, several test cases are considered in ISO Standard 13792. In particular, the test cases are aimed to check the reliability of the proposed model as follows:

- in relation to the size of the window and the climatic data (Case A or Case B);
- in relation to the features of the envelope components (Case 1, Case 2, Case 3);
- in relation to the rate of infiltration from outdoors (Case a or Case c).

The combination of these features produces a total of 12 different cases.

Now, Figure 5.1 shows the discrepancy Δ between the value of the room operative temperature calculated through the proposed methodology, and the reference values provided in the ISO Standard, for each test case considered in this study. The compliance of the calculation procedure to the Standard has to be assessed by looking at the minimum, the average and the maximum room operative temperature; thus, the diagram reports the discrepancy for each one of these parameters.

In Figure 5.1 there is also an indication of the threshold discrepancy in order for the calculation procedure to be rated in Class 1 (-1°C < Δ < 1°C). According to the displayed results, it is possible to state that the proposed methodology has a good reliability in the determination of the indoor operative temperature in free-running enclosures. Actually, not only the methodology can be classified in Class

I, but the discrepancy measured over the whole set of test cases is within ± 0.6°C. As a general rule, the best results pertain to the simulations characterized by high infiltration rates (n_a = 10 h^{-1}, cases c).

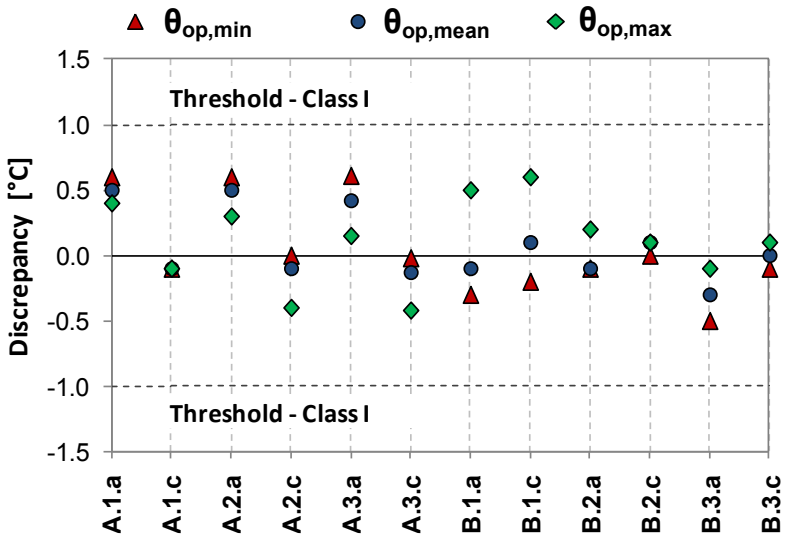

Figure 5.1 - Compliance of the proposed methodology with the ISO Standard

5.1 The effect of higher order harmonics

In the previousparagraph, it is shown that the analytical methodology presented proves sufficiently reliable with N_H = 6 harmonics. However, one must remark that both in the scientific literature and in the international Standards the dynamic thermal properties are normally used by looking only at the fundamental harmonic (n = 1).

Now, with reference to the cases A.2.a and B.2.a, Figure 5.2 shows that the room operative temperature calculated with N_H = 1 is not very different from that obtained with N_H = 6. Indeed, the difference between the two profiles does not

exceed 1°C in the worst case, i.e. in case B.2.a. Similar results can be found in all other cases.

If the validation procedure were carried out by using N_H = 1, the discrepancy shown in Figure 5.3 would be measured in all the test cases highlighted. Actually, the proposed methodology would still be classified in Class I, even if the precision would be lower than what observed in Figure 5.3 with N_H = 6. Indeed, in that case the highest discrepancy was as high as 0.6°C, whereas in Figure 5.3 the absolute value of the discrepancy measured either on the maximum or on the minimum indoor operative temperature frequently exceeds 0.8°C.

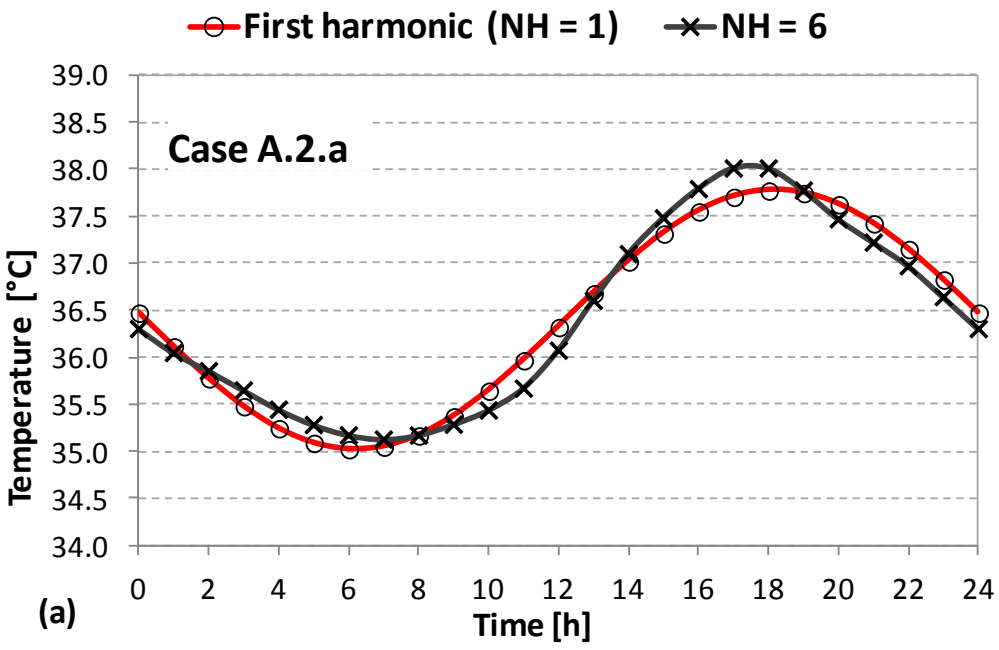

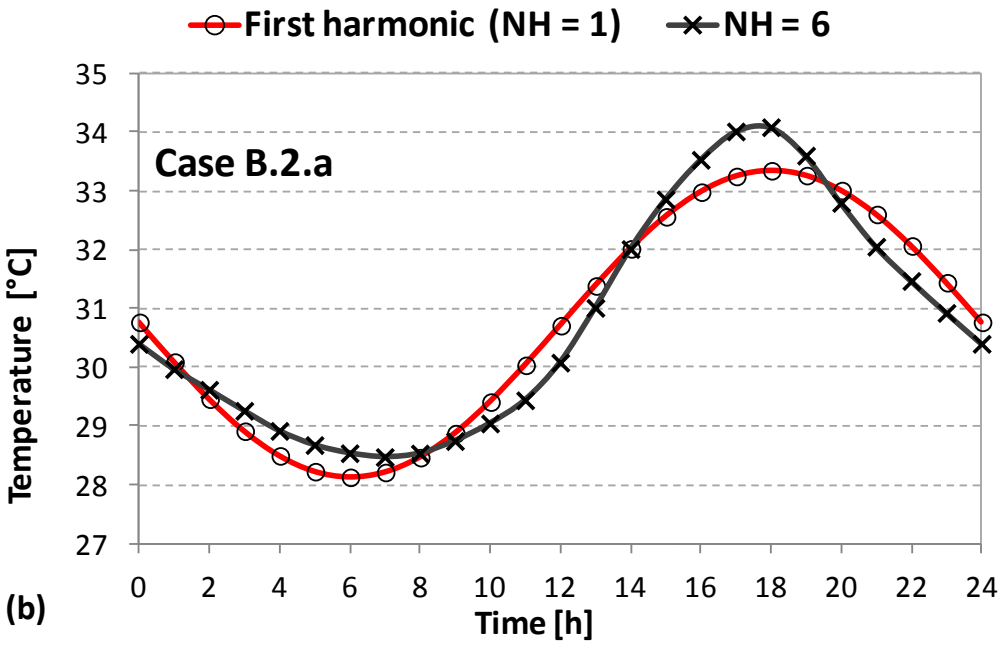

Figure 5.3 - Effect of the number of harmonics N_H on the solution. (a) case A.2.a, (b) case B.2.a

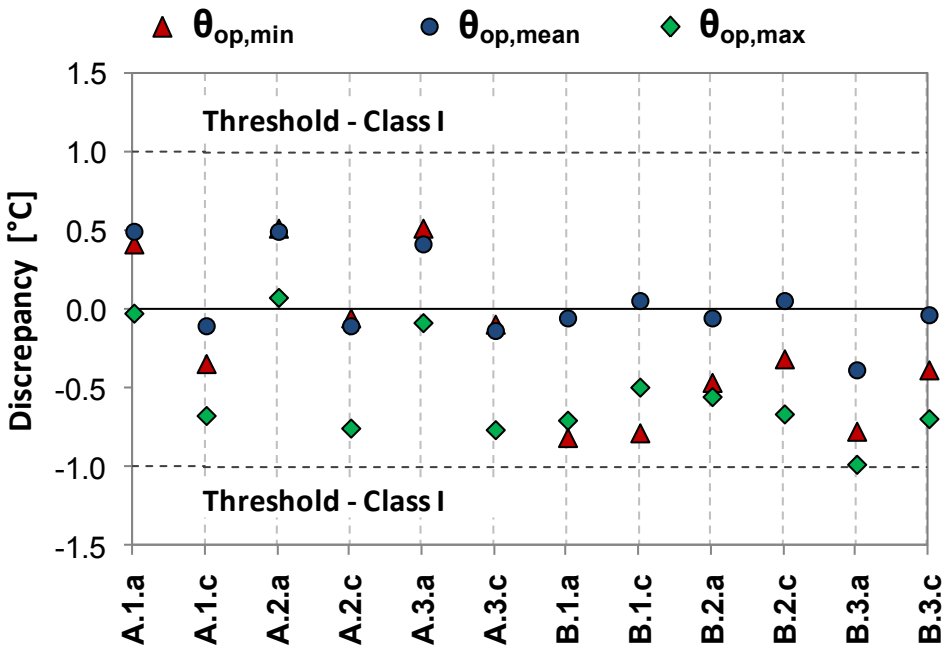

Figure 5.4 - Compliance of the proposed methodology with the ISO Standard, if N_H=1

6 The heat flux released by each envelope surface

The methodology presented and validated allows a sufficiently precise evaluation of the indoor air temperature profile through a purely analytical approach.

Furthermore, the use of the dynamic thermal properties allows the assessment of the convective heat fluxes released by each inner surface of the opaque envelope to the indoor air. In this case, what is more interesting is the possibility to assess the contribution due to every single forcing condition; this can facilitate the comprehension of the thermophysical processes, and can help to identify appropriate measures aimed to improve the thermal performance of the enclosure.

In particular, in relation to each envelope component, one can define the heat flux due to the outdoor temperature swing, see equation (34), and the convective heat flux released as a response to the radiant energy absorbed on the inner surface, see equation (35):

$$q_{i,XY} = U \cdot \left(\bar{\theta}_o - \bar{\theta}_i \right) + \sum_{n=1}^{N_H} (X_n \cdot \tilde{\iota}_{o,n} \quad {}_n \quad \tilde{}_{\iota,n}, \tag{34}$$

$$q_{i,F} = h_c \cdot R_{si} \cdot \alpha \cdot (\bar{F} \cdot \bar{\phi} + \sum_{n=1}^{N_H} F_n \cdot \tilde{\iota}_{n}, \tag{35}$$

Again, keep in mind that $\tilde{\theta}_i \quad \tilde{\theta}_o$ and $\bar{\theta}_i = \bar{\theta}_o$ when dealing with a partition or a ceiling separating two spaces with identical thermal conditions.

As an example, Figure 6.1 shows the time profile of the total convective heat flux released in case B.2.a both by the external wall and by a partition wall, together with the single contributions calculated through equation (34) and (35).

One can observe the high thermal inertia of the external wall ($|F|$ = 0.157, as reported in Table 4.2) allows a significant attenuation of the effects of the radiant heat flux absorbed on its inner surface, which is released at a slower rate and distributed through the day (see the curve q_F in Figure 6.2).

On the contrary, the partition walls (Figure 6.2), despite being not exposed to the outdoor environment, release a remarkable heat flux in the afternoon, with a peak value around 17:00, i.e. immediately after the peak of the solar radiation. This behaviour is almost entirely due to the very low thermal inertia of the partition, witnessed by the high surface factor ($|F|$ = 0.928) and the low time shift (φ_F = -1.5 h)

On the other hand, Figure 6.2 proposes the same type of analysis in relation to the ceiling. This time, two different test cases are compared, namely case B.1.a and case B.2.a. In case B.1.a the ceiling contains an additional insulating layer on the inner side, which is able to hide the thermal mass of the ceiling. This yields a fast reflection of the heat wave, witnessed by a high surface factor ($|F|$ = 0.71) and a low time shift (φ_F = -1.2 h), whereas in case B.2.a we have $|F|$ = 0.053 and φ_F = -4.5 h.

As a consequence, the heat flux q_F released in response to the radiant energy incident on the inner surface is far more important in case B.1.a than in case B.2.a.

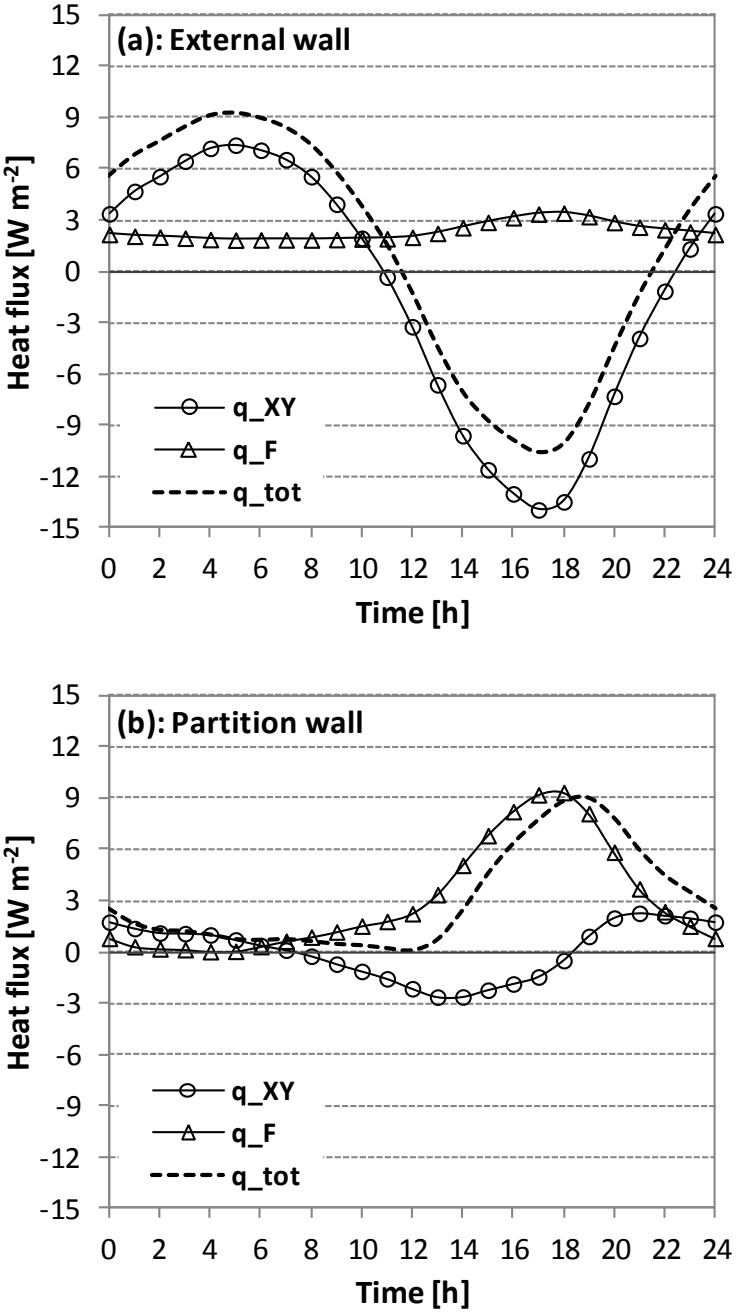

Figure 6.1 - Heat flux released in case B.2.a. (a) External wall, (b) Partition wall

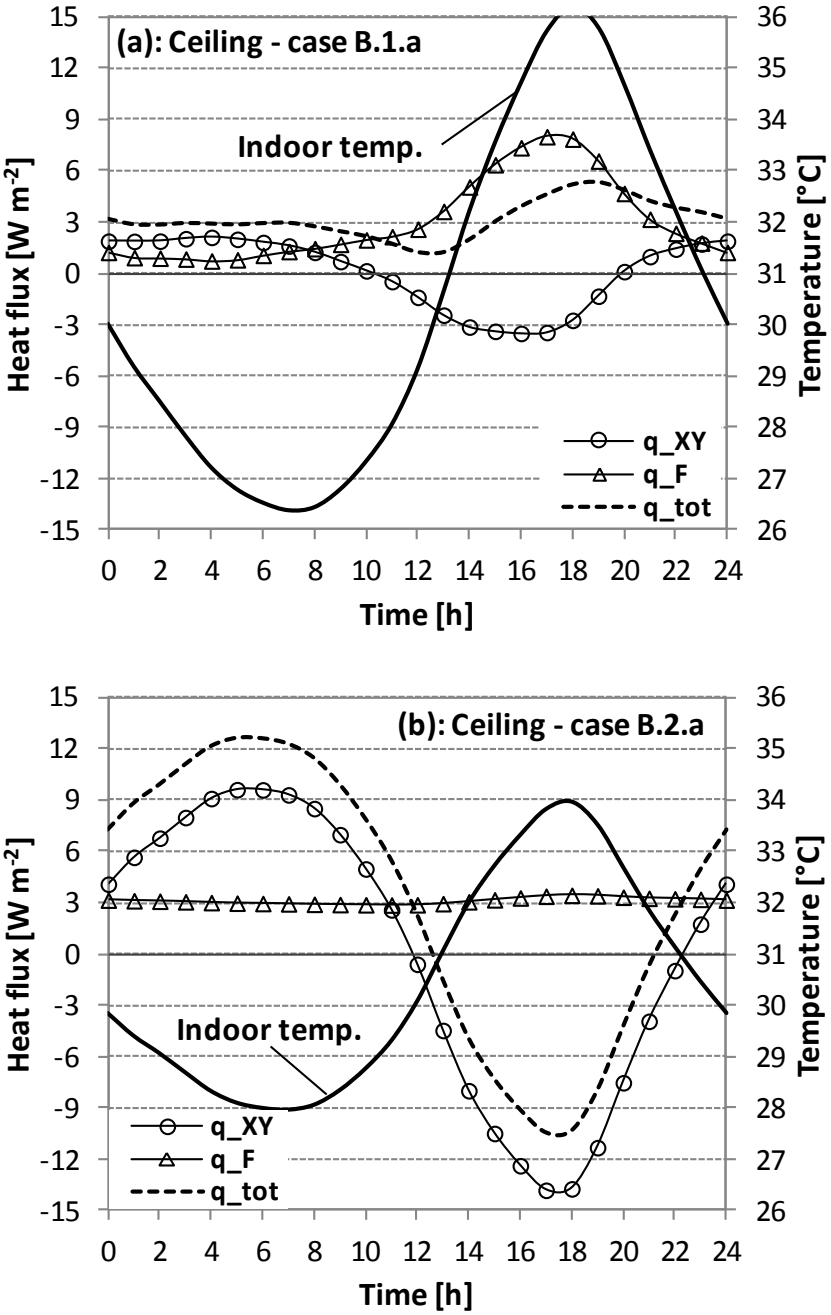

Figure 6.2 - Heat flux released by the ceiling. (a) Case B.1.a (b) Case B.2.a

Another interesting information emerging from this analysis regards the thermal admittance, and its relationship with the position of the thermal insulation. Indeed,

in Table 4.2 (page 49) one can remark that the amplitude $|Y|$ for the ceiling is almost seven times higher in case 2 than in case 1 (respectively, $|Y| = 3.96$ and $|Y| = 0.59$). This means that, because of the additional insulation layer adopted in case 1, the ceiling has a lower capacity of absorbing heat in its structure in response to an air temperature increase inside the room.

As a consequence, from Figure 4.2 one can observe that the ceiling absorbs a great amount of heat in case B.2.a during the daytime, i.e. when the indoor temperature tends to increase, thus avoiding excessive overheating. On the other hand, the ceiling tends to release part of this absorbed heat at night. The behaviour of the ceiling in case B.1.a is profoundly different (see Figure 6.2.a): due to its low thermal admittance, it is not able to store energy in response to an indoor temperature fluctuation, and this implies a remarkable overheating during the daytime. However, at night the ceiling releases a limited amount of heat, and this contributes to keep a lower indoor temperature.

7 Solar ResponseFactor

The parameter Ω (*Solar Response Factor*) is defined as the thermal power globally re-emitted to the environment from the internal walls of a room(A_p), per unit of incident solar radiation on the glass surface[3](A_v):

$$\Omega = \frac{\sum_{p} \left(\tilde{} \right)}{\sum_{v} \left(\tilde{} \right)} \qquad (19)$$

Solar radiation is considered as the global sum of the direct component and the diffuse component.

It should be noted here that the thermal energy within the room as a result of the action of solar radiation on the glass surface is composed of two aliquots:

1. <u>energy transmitted directly through the glass</u>: this component is the one falling in the field of low wavelengths (λ< 3 μm), and is proportional to the transparency of the glass τ_v;
2. <u>energy absorbed by the glass and re-emitted, infrared, towards the interior</u>; called g_s,the *g-value* of the window, we can assume that the aliquot is proportional to the term:

$$r_v = g_s - \tau_v \qquad (20)$$

The equation (19) can thus be rewritten as[4]:

[3] The variables marked with ~ are periodic variables of period Pn = 24 / n hours. Ω is thus a complex number, and as such describable in magnitude and phase, which in turn depend on the index of n-th harmonic.

$$\Omega = \frac{\sum_{p}\left(\tilde{\quad}\right)\big|_{t}\ \sum_{p}\left(\tilde{\quad}\right)\big|_{r}}{\sum_{v}\left(\tilde{\quad}\right)} = \frac{\sum_{p}\left(\tilde{\quad}\right)\big|_{t}}{\tilde{\quad}}\cdot\frac{\tilde{\quad}}{\sum_{v}\left(\tilde{\quad}\right)} + \frac{\sum_{p}\left(\tilde{\quad}\right)\big|_{r}}{\tilde{\quad}}\cdot\frac{\tilde{\quad}}{\sum_{v}\left(\tilde{\quad}\right)} \tag{21}$$

In cui:

$$\tilde{\quad}_{t} \quad \sum_{v}\left(\tilde{\quad}\right)_{v}\cdot\tilde{I}_{v}\ A_{v}\ F_{R}, \tag{22}$$

$$\tilde{\quad}_{r} \quad \sum_{v}\left(r_{v}\cdot\tilde{I}_{v}\ A_{v}\ F_{R}\right), \tag{23}$$

The terms above represent the thermal power entering through the transparent surfaces in the form of solar radiation transmitted ($\tilde{\quad}_{t}$) or re-emitted ($\tilde{\quad}_{r}$). The coefficient F_R summarizes all the factors of reduction to be applied to the incident solar radiation (the frame factor, external shadingfactor, internalshadingfactor). In the event that there is only one glass surface, or if it can be assumed that all glass surfaces have the same value of τ_v, r_v and F_R, equation (21) can be written as:

$$\Omega = F_R\cdot\left(\Omega_t\cdot\tau_v + \Omega_r\cdot r_v\right) \tag{24}$$

Here the coefficients Ω_t and $\Omega_r$can be interpreted as *Response Factors* of theinterior environment in respect to the radiation released, respectively, for transmission or for infrared reemission, by the glass. Whereas Ω is defined in relation to the total incident solar radiation.

[4] The subscript "t" denotes the rate of solar radiation transmitted, while the subscript "r" that re-emitted from the infrared glass (IR).

In equation (24), strictly speaking, τ_v and r_v depend on the angle of effect of the radiation on the glass, and thus ultimately on time. In this context, it is preferable to maintain the two coefficients constant, equal to the value assumed by them in relation to the diffuse radiation.

7.1 The Ulbricht sphere model and its limits.

Before proceeding to the calculation of the response factors, it is necessary to make assumptions about the distribution of solar and infrared radiation in the surroundings. Below, we will make use of the Ulbricht model, which enables us to calculate the circulating flow within a cavity hosting a source of radiant energy considered punctiform.

For the purpose, we can consider a hollow sphere, with an internal coating of diffusing material, equipped with a small opening from which a light beam penetrates (Figure 7.1).

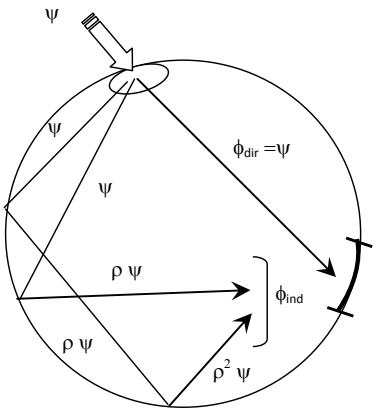

Figure 7.1 – Representation of the circulating flow conforming to the model Ulbricht

Under the assumption of perfect diffusion inside the sphere, the q_i incident energy per unit area for the receiver A_i is:

$$q_i = \frac{\phi_i}{A_i} = \frac{\phi_{tot}}{A_{tot}} = \text{cost} \tag{25}$$

Given that the total incident flux is composed of direct and indirect flow, we have:

$$\phi_{tot} = \phi_{dir} + \phi_{ind} \tag{26}$$

But:
$$\begin{cases} \phi_{dir} = \Psi \\ \phi_{ind} = \psi\rho + \psi\rho^2 + \psi\rho^3 + \ldots = \psi\rho \cdot \underbrace{(1 + \rho + \rho^2 + \ldots)}_{\text{serie geometrica}} \end{cases} \tag{27}$$

Noting now that for the geometric series with ratio ρ highlighted above is valid:

$$1 + \rho + \rho^2 + \ldots = \sum_{n=1}^{\infty} 1 + \rho^n = \frac{1}{1-\rho} \tag{28}$$

results: $$\phi_{tot} = \psi + \frac{\psi\rho}{1-\rho} = \frac{\psi}{1-\rho} \tag{29}$$

For non-spherical cavities (eg. of prismatic shape spaces), it is possible to replace the average $\rho_m$reflectivity with ρ. The flux effect on the wall is therefore (Ulbricht Formula)[5]:

$$q_i = \frac{\psi}{(1-\rho_m) \cdot A_{tot}} \tag{30}$$

[5]The same conclusion can be reached considering that, for the energy balance in the room, the flux absorbed by the walls ($a_m\phi_{tot}$) must equal the incoming fluxψ So, if the walls are opaque (τ = 0 and $a_m = 1 - \rho_m$) we have: $\psi = a_m\phi_{tot} = (1-\rho_m) \cdot q_i \cdot A_{tot}$ from which the (30).

In the case of "opaque" cavity walls to the circulating radiation, we can assume1-$\rho_m=a_m$. This is always true for walls as they are opaque by nature, whereas for glass such a formula is only valid in relation to infrared radiation.

On the contrary, the solar radiation that is not absorbed by the walls, and then re-circulates inside the cavity, is of small wavelength and as such, when incident on the glass, due to its transparency $\lambda< 3\mu m$, ends up escaping from the cavity. This effect is obviously felt much more the wider the glass surface, such as in solarized surroundings, and the more reflective the opaque walls are.

Since there is both walls and glass in the room, it is necessary to elicit a sufficiently general model to take both of the different compositions of the radiation field into account, and hence distinguish between the solar radiation (S) and infrared (IR), and between the different behaviour of the materials (walls and glass) in respect to both radiation fields.

7.1.1 Calculationof Ω_r

Assuming that hypothesis of validity of the Ulbricht model are met in the room, ie perfect diffusion for glass and walls, the thermal flux re-emitted from a wall, due to the rate of infrared radiation absorbed $a_{p,IR}$, can be written as:

$$\tilde{\varphi}_{IR} = \frac{\tilde{\Gamma}}{\left(1-\bar{\rho}_{IR}\right)\cdot A_{tot}}\cdot \angle_p \qquad (31)$$

Whereby:

$$\sum_p \left(\tilde{q}_p \cdot A_p \right)_r \cdot \sum_p \left(a_{p,IR} \cdot \frac{\tau_{IR}}{(1-\bar{\rho}_{IR}) \cdot A_{tot}} \cdot Z_p \cdot A_p \right) = \frac{\tau_{IR}}{(1-\bar{\rho}_{IR}) \cdot A_{tot}} \cdot \sum_p \left(a_{p,IR} \cdot Z_p \cdot A_p \right) \quad (32)$$

As, in relation to the infrared radiation, the building materials - including glass - are completely opaque (1 - ρ_{IR} = a_{IR} e τ_{IR} = 0), and behave like "almost black" bodies ($a_{IR} \approx 1$), the (32) becomes:

$$\sum_p \left(\tilde{q}_p \cdot A_p \right)_r \cdot \tau_{IR} \cdot \frac{\sum \left(Z_p \cdot A_p \right)}{A_{tot}} \quad (33)$$

and therefore:

$$\Omega_r = \frac{\sum_p \left(\tilde{q}_p \cdot A_p \right)_r}{\tau_{IR} \cdot q_r} = \frac{\sum_p \left(Z_p \cdot A_p \right)}{A_{tot}} \quad (34)$$

We note that $A_{tot}$is the total inner surface of the building envelope including the glass surface.

7.1.2 Calculationof Ω_t

Disregarding the directionality of the radiation transmitted directly through the glass, a uniform distribution within the room (Ulbricht hypothesis)is also assumed in this case. This hypothesis is also used by Oliveti et al. (2011) and accepted, under suitable hypothesis[6] by the UNI EN ISO 13791: 2005. We can then replicate the equation (31), indicating, however, with the symbol “s”, the value of

[6] That is, if the average reflectivity of the indoor environment to the solar radiation is greater than or equal to 0.7

the optical properties of the materials in relation to solar radiation - low wavelength - transmitted through the glass.

$$\frac{\tilde{\tau}}{(1-\bar{\rho}_s)\cdot A_{tot}}\cdot \angle_p \qquad (35)$$

It follows then:

$$\sum_p \frac{\tilde{\tau}}{(1-\bar{\rho}_s)\cdot A_{tot}}\cdot \sum_p \left(a_{p,s}\cdot Z_p\cdot A_p\right) \qquad (36)$$

In order to derive, from (36), an expression of operationalΩ_t, at this point it is worth introducing the quantity "*effective absorption coefficient of the indoor environment"*, indicated by the symbol$a_{cav}$and defined by Oliveti et al. as the ratio of the solar energy absorbed within the environment and solar energy penetrated by transmission through the window. Under this definition we can write, still using the Ulbricht hypothesis:

$$a_{cav} = \sum_p \left(a_{p,s}\cdot A_p \cdot \frac{\tilde{\tau}}{(1-\bar{\rho}_s)\cdot A_{tot}} \right) \cdot \frac{1}{\tilde{\tau}} = \frac{\sum_p \left(a_{p,s}\cdot A_p\right)}{\bar{\rho}_s)\cdot A_{tot}} \qquad (7)$$

Combining (36) and (37) results:

$$\sum_p \left(\tilde{q}_p \; A_p \right) \; \tilde{\tau} \; a_{cav} \; \frac{\sum_p \left(a_{p,s}\cdot Z_p\cdot A_p\right)}{\sum_p \left(a_{p,s}\cdot A_p\right)} \qquad (36.1)$$

In conclusion:

$$\Omega_t = \frac{\sum_p \left(\tilde{q}_p \; A_{p,} \right)_t}{\tilde{r}_t} = a_{cav} \cdot \frac{\sum_p \left(a_{p,s} \cdot Z_p \cdot A_p \right)}{\sum_p \left(a_{p,s} \cdot A_p \right)} \tag{38}$$

Ultimately, the *Solar Response Factor*can be calculated as:

$$\Omega = F_R \cdot \left(\underbrace{a_{cav} \cdot \frac{\sum_p \left(a_{p,s} \cdot Z_p \cdot A_p \right)}{\sum_p \left(a_{p,s} \cdot A_p \right)}}_{\Omega_t} \cdot \tau_v + \underbrace{\frac{\sum_p \left(Z_p \cdot A_p \right)}{A_{tot}}}_{\Omega_r} \cdot r_v \right) \tag{39}$$

7.2 Evaluation of the terma_{cav}

It should be noted at the outset that, not wanting to assume that for glass, reflectivity is nothing in comparison to radiationλ, the average reflectivity of the room can be written as:

$$\bar{\rho}_s = \frac{\sum_p A_p \cdot \bar{\rho}_{p,s} + A_v \cdot \rho_{v,s}}{A_{tot}} \qquad \text{co} \quad \text{with} \qquad \bar{\rho}_{p,s} = \left(1 - \bar{a}_{p,s} \right) \tag{40}$$

It is therefore easy to derive the relation:

$$\left(1 - \bar{\rho}_s \right) = f \cdot \left(1 - \rho_{v,s} \right) + \left(1 - f \right) \cdot \bar{a}_{p,s} \tag{41}$$

Where*f*is the fraction of window area compared to the total area of the building envelope:

$$f = \frac{A_v}{A_{tot}}$$

Using Eq. (41),the *effective absorption coefficient*a_{cav}, defined by Eq. (37), can be conveyed in the form:

$$a_{cav}(f) = \frac{\sum_{p}\left(a_{p,s} \cdot A_p\right)}{A_{tot} \cdot \left[f \cdot \left(1-\rho_{v,s}\right) + \left(1-f\right) \cdot \bar{a}_{p,s}\right]} \tag{37.1}$$

This parameter, in addition to being a function of the geometry of the room and of the optical properties of the materials, depends explicitly on the fraction f of the glass area.

It is important to observe that the above expression was derived by pure logical-mathematical deduction, starting from the assumptions of uniform spatial distribution of the circulating flow. Whereas Oliveti et al. propose a semi-experimental relation for the calculation ofa_{cav}, obtained by interpolation from the results of simulations performed with the TRNSYS software:

$$a'_{cav}(f) = 1 - a \cdot e^{\left[-b \cdot \left(\frac{\bar{a}_s}{f}\right)^c\right]} \tag{42}$$

In equation (42) we have the average absorption coefficient of the room $\bar{a}_s$and three coefficients calculated in function of the solar transmission factor τ_v of the glass relating to diffuse radiation:

$$a(\tau_v) = 3.500 - 5.453 \cdot \tau_v + 4.516 \cdot \tau_v^{\,2} \tag{43.1}$$

$$b(\tau_v) = 3.700 - 5.388 \cdot \tau_v + 3.462 \cdot \tau_v^{\,2} \tag{43.2}$$

$$c(\tau_v) = 0.124 + 0.545 \cdot \tau_v - 0.355 \cdot \tau_v^{\,2} \tag{43.3}$$

Finally, from the equations given in section 4.5.3 of the standard UNI EN ISO 13791: 2005 we can obtain a third operational definition of the *effective absorption coefficient*. The norm in question in fact indicates calculating the heat flow linked to the solar radiation absorbed by the internal surface of a wall as:

$$\tilde{\quad} \quad -f_{sa}\right)\cdot\left(1-f_{sl}\right)\cdot f_d\cdot\tilde{\quad} \tag{44}$$

In equation (44) wehave:

- f_{sa}:fraction of solar radiation transferred directly to the air in the room by convection; in the absence of furniture, we assume $f_{sa} = 0$.
- f_{sl}: fraction of solar energy lost through the glass towards the outside, to be calculated according to the equation[7]:

$$f_{sl} = \frac{\tau_v \cdot \sum_v A_v}{\left(1-\overline{\rho}_s\right)\cdot A_{tot}} = \frac{\tau_v \cdot f}{1-\overline{\rho}_s} \tag{45}$$

- f_d: fattore di distribuzione della radiazione solare; nell'ipotesi di cui alla nota 2, la norma in questione suggerisce di assumere $f_d = 1/A_{tot}$.

According to this approach, the *effective absorption coefficient* a_{cav}can be therefore written as:

$$a''_{cav}(f) = \frac{\sum_p\left(\tilde{\quad}\right)}{\tilde{\quad}} = \frac{\left(1-\frac{\tau_v\cdot f}{1-\overline{\rho}_s}\right)\cdot\frac{1}{A_{tot}}\cdot\sum_p\left(A_p\right)\cdot\tilde{\quad}}{\tilde{\quad}} = \left(1-\frac{\tau_v\cdot f}{1-\overline{\rho}_s}\right)\cdot\left(1-f\right) \tag{46}$$

[7] In this approach, the UNI norm requires the use of the value of τ_v with reference to normal radiation. For double glazing assume $\tau_v = 0.693$.

Figure 7.2 shows the values of a_{cav} according to the three methods described before, the variation of the fraction of window area f and for three values of the absorption coefficient average $\bar{a}_{ps}$ of opaque surfaces. The window has been projected with double glazing, with τ_v = 0.59 and ρ_{vs} = 0.23 for the scattered radiation.

In reading the diagrams in Figure 7.2, it is necessary to remember that all the proposed approaches are based on the Ulbricht hypothesis, and therefore become much less correct, from the physical point of view, the higher the average $\bar{a}_{ps}$ absorption coefficient of the walls and the size of the opening is.

The figures also show that the proposed method, which is labeled "Ulbricht", is in an intermediate position between that of Oliveti and that of the UNI-EN-ISO 13791: 2005.

Below, for the calculation of the *Solar Response Factor* Ω, it was decided to evaluate a_{cav} using the equation (36.1).

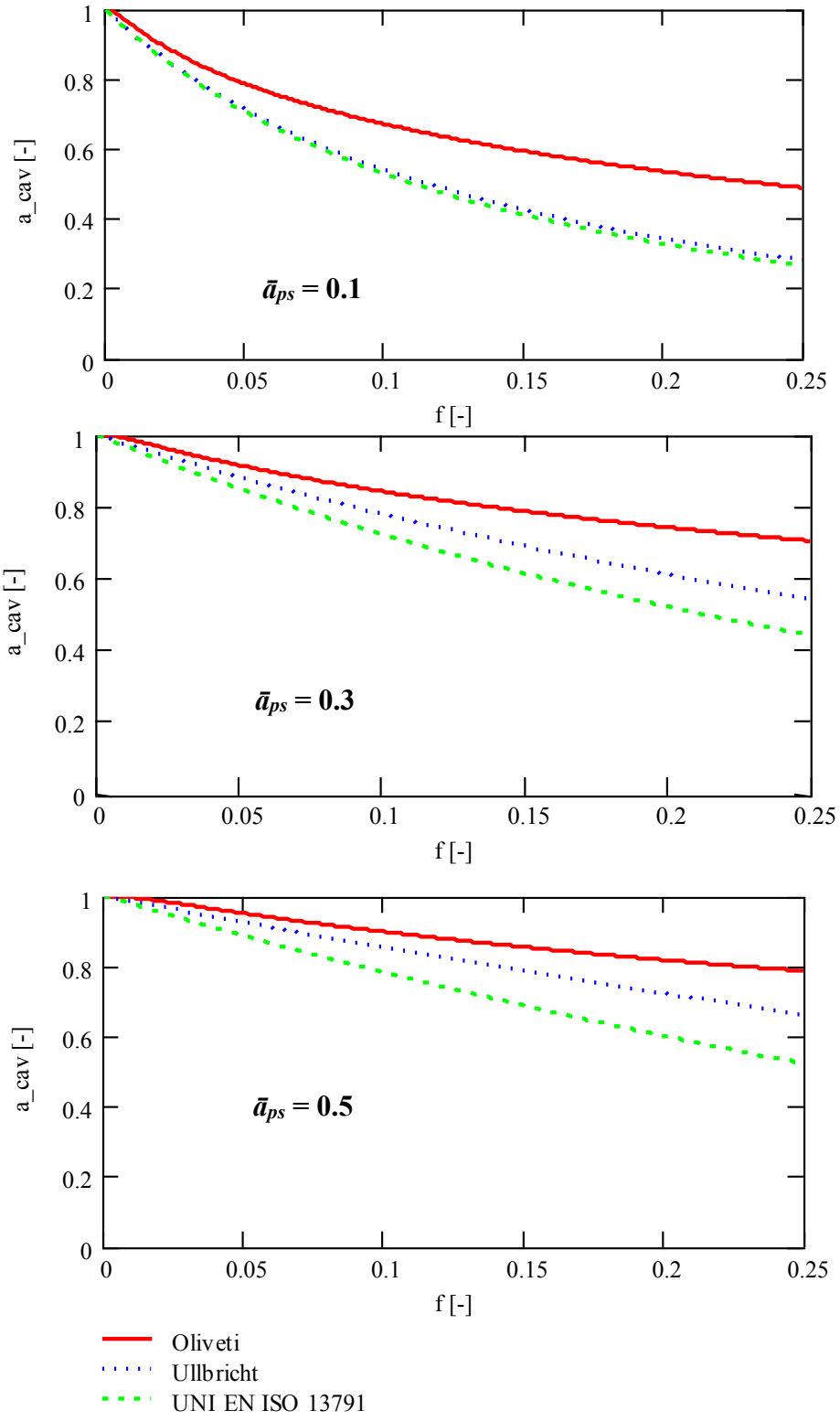

Figure7.2 – Calculation of $a_{cav}$with the variation of the average absorption coefficient $\bar{a}_{ps}$.

7.3 The Solar Response Factor for certain types of environment

Described below is the response of the building envelope to the incoming solar radiation through the glass surfaces, for a standard size room (5 x 5 x 3 m^3), through the module and the phase of the *Solar Response Factor* Ω with the variation of the percentage of glass surface *f* with respect to the total area of the room.

The calculation was done for four different types of buildings:

- Type A: historic buildings with massive masonry walls (stone walls);
- Type B: modern buildings with hollow clay bricks;
- Type C: : highly-insulated lightweight envelope
- Type D: ultralightprefab housing (site huts).

As regards type B, three different sub-cases were analyzed, in distinct function of the external parameter:

- Type B.1:Double-leaf cavity walls with the insulation placed in the cavity gap;
- Type B.2 : Double-leaf cavity walls with the insulation placed on the inner side of the wall
- Type B.3 :single leaf walls with distributed insulation (light-weight insulating bricks)

The details concerning the composition of walls, floors and ceilings are reported in the Appendix, where the values of the corresponding surface factors *F* are also provided. In the calculation, two walls are structured as *external walls*, whereas the others look like *internal walls.*Infact, of the four vertical parameters that surround the room, two simulate dividers, and as such separate the room in question from another room with similar characteristics; the remaining two parameters are exterior walls which include the window areas of variable size with parameter *f*. Details of the stratigraphy of the outer walls, dividers and floors for each type are given in the Appendix. The calculated value for the absorption $a_s$coefficient of the walls, ceiling and floor is kept even at 0.3.

Table 3 shows the optical properties chosen for the glass surfaces (the same as in Oliveti); in this first phase, the calculations were carried out assuming the presence of double pane windows. In calculating the solar response factor Ω no reduction factor was taken into account (chassis factor, external shielding factor, internal shield factor), assuming FR=1.

Table7.1 -Optical properties of glass surfaces (for diffuse radiation).

	τ	ρ	g-value
Single glass	0.749	0.14	0.857
Double glass	0.590	0.23	0.761

Looking at the diagram in Figure 7.3, pertinent to the Ω_t it is immediately obvious that the curves all have a decreasing trend with *f:* the higher the fraction f of the glass surface the higher the amount of radiation that emerges from the environment through the glass surface, per unit of solar energy allowed in.

Moreover, the 4 types of building envelope previously introduced maintain distinct behaviours, with the exception of a couple of them, for which there is a virtually total overlap of the curves B.1 (room with wallwith hollow bricks and insulation in the gap) and B.3 (single leaf walls with distributed insulation). The behaviour of type C (houses made of wood) and type D (lightweight prefabricated buildings) is very similar, especially for high values of *f*.

The curve associated with type A (historical masonry buildings) has by far the lowest values of Ω_t, testifying how the inertia of massive masonry envelope maximizes the attenuation of solar radiation permeated by transmission through the glass surface, whereas rooms with thin walls and / or insolated on the inner face (type C or D) behave in the opposite way, characterized by high solar radiation resubmissions.

A similar conclusion can be reached by analyzing the diagram in Figure 7.5, pertinent to the module of Ω_r, and then the response of the walls to the infrared radiation reemitted by the glass. However, this parameter is found to have a weaker dependence on the fraction*f*of the glass surface.

Finally, the distinction between the various types of building envelope remains valid even when you look at the module of the solar response factor Ω, as shown in Figure 7.5.As can be surmised from the definition of Eq. (39), the contribution related to the term $\Omega_t$is more significant, as it is multiplied by the coefficient τv, which is usually much higher than the term $r_v = g_s - \tau_v$.

From the reading of these results, it is therefore evident that the magnitude of the *Solar Response Factor*Ωis strongly influenced by the nature of the materials constituting the building envelope. In the case where the building envelope is

made from lightweight materials, with extensive use of insulation in a position close to the internal environment (type C and D), it returns a quantity of thermal energy to the environment which varies between 30% and 60 % of incident solar radiation, and in any case in proportion to the fraction f of the glass area. That rate goes down instead of up to values of 15-25% for massive envelopes (type A), reaching between 20% and 40% in the case of brick envelopes (category B types in general).

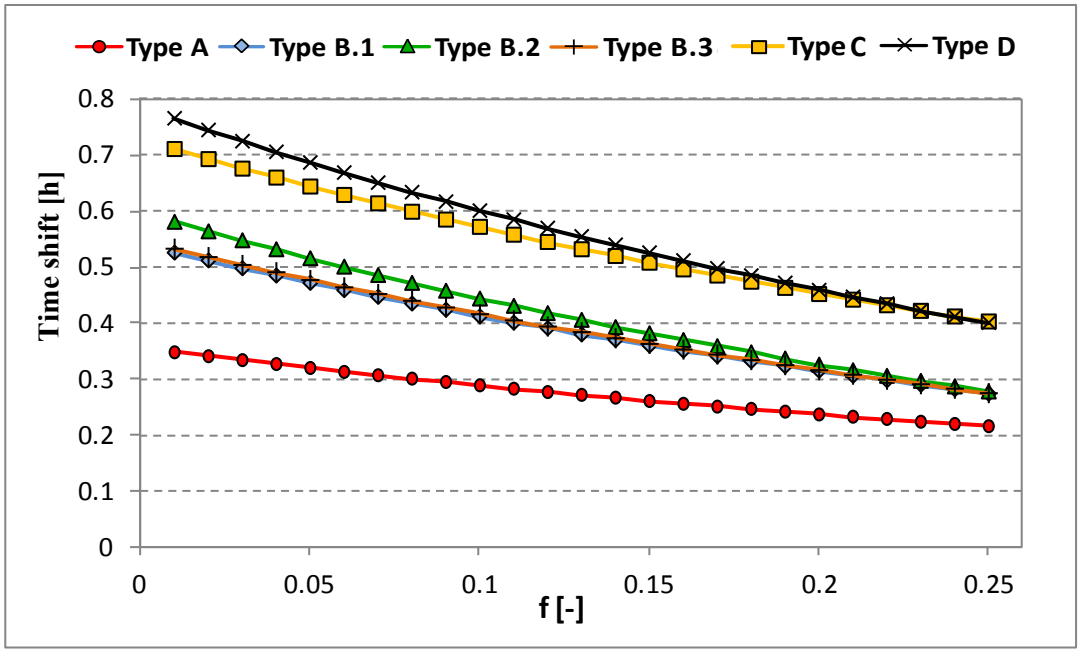

Figure7.3–Amplitude of Ω_t as a function of the glazing surface *f*

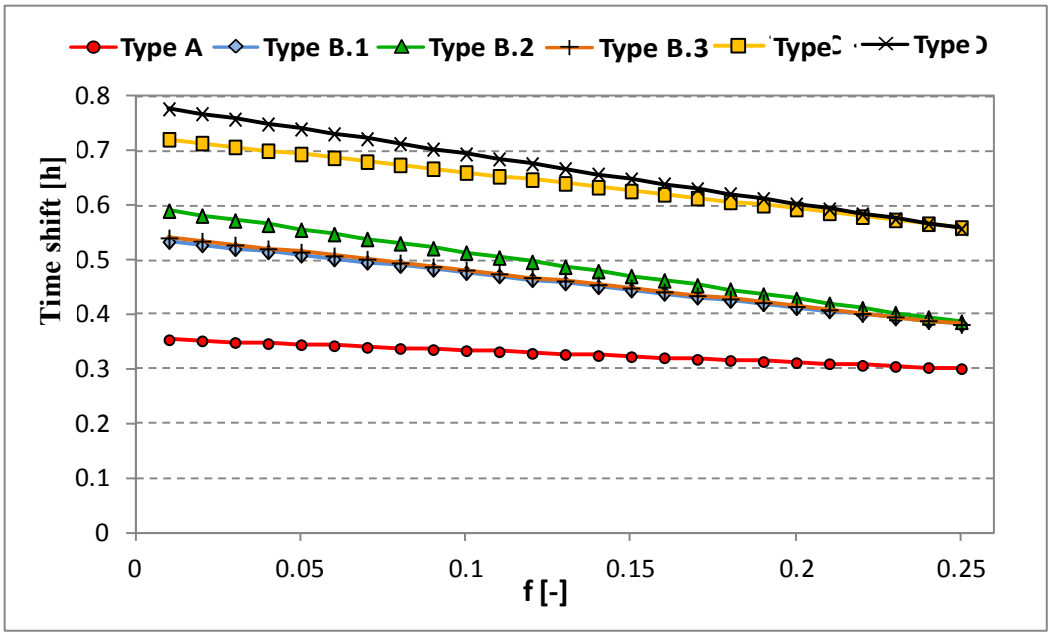

Figure7.44–Amplitude of Ω_r as a function of the glazing surface *f*

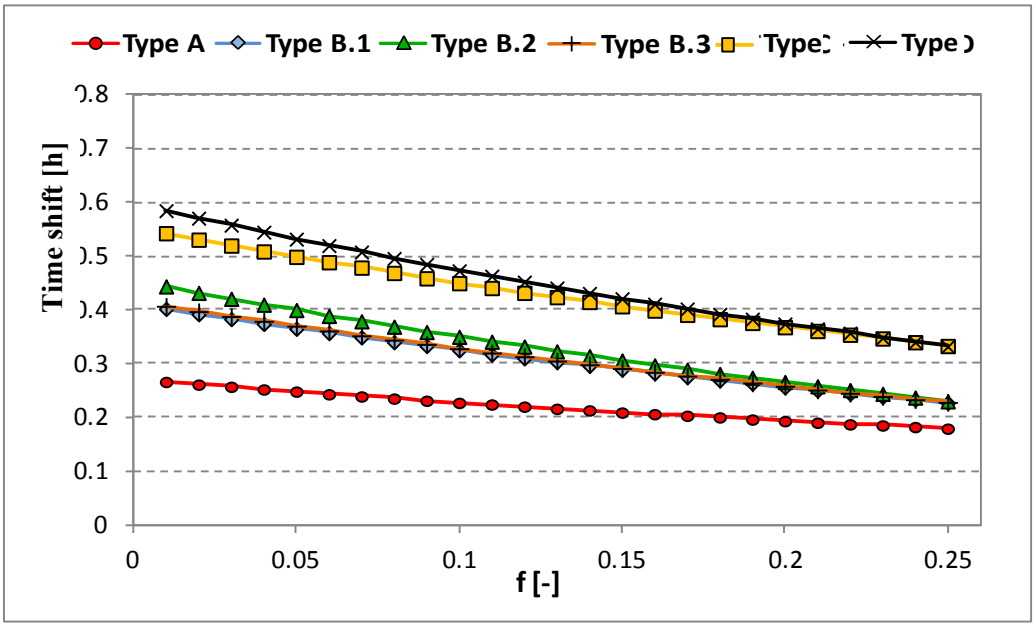

Figure 55–Amplitude of Ω as a function of the glazing surface f

The delay of Ω, for the various building types analyzed, is shown in Figure 7.6. In general the curves are now more distinct and almost all reveal a relative insensitivity to the glass fraction f.

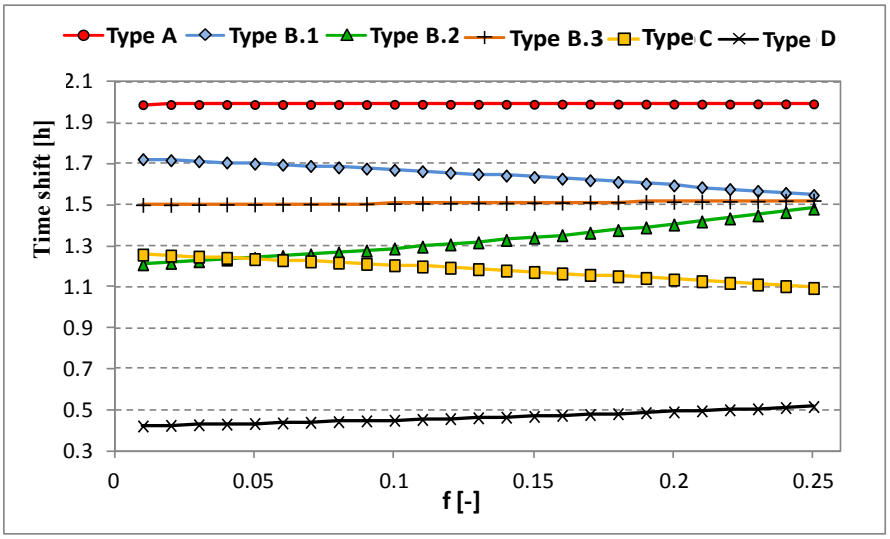

Figure7.6–Phase of Ω as a function of the glazing surface *f*

7.4 The response factor for the classification of solar buildings

The *Solar Response Factor* Ω can be used to classify the rooms (and eventually buildings) in relation to their behaviour towards solar radiation, in order to derive the necessary information to enhance or limit the gains in favour of the room.

Figure has been put forward as an example, showing a mapping of the values of the module and delay (calculated for the first harmonic) for the building types stated above. The values plotted refer to environments of 5 x 5 x 3 m^3 dimensions, with a glass surface equal to 10% of the total area of the inner (f = 0.1) and the absorption coefficient in the solar a_s=0.3 for the opaque surfaces.

Figure 7.7 shows the presence of distinct building envelope solutions even more clearly, and also suggests the possibility of classifying the buildings on 4 quadrants according to the response of the building envelope to the incident solar radiation:

- 1st quadrant: low attenuation, moderate delay;
- 2nd quadrant: low attenuation, long delay;
- 3rd quadrant: strong attenuation, moderate delay;
- 4th quadrant: strong attenuation, long delay.

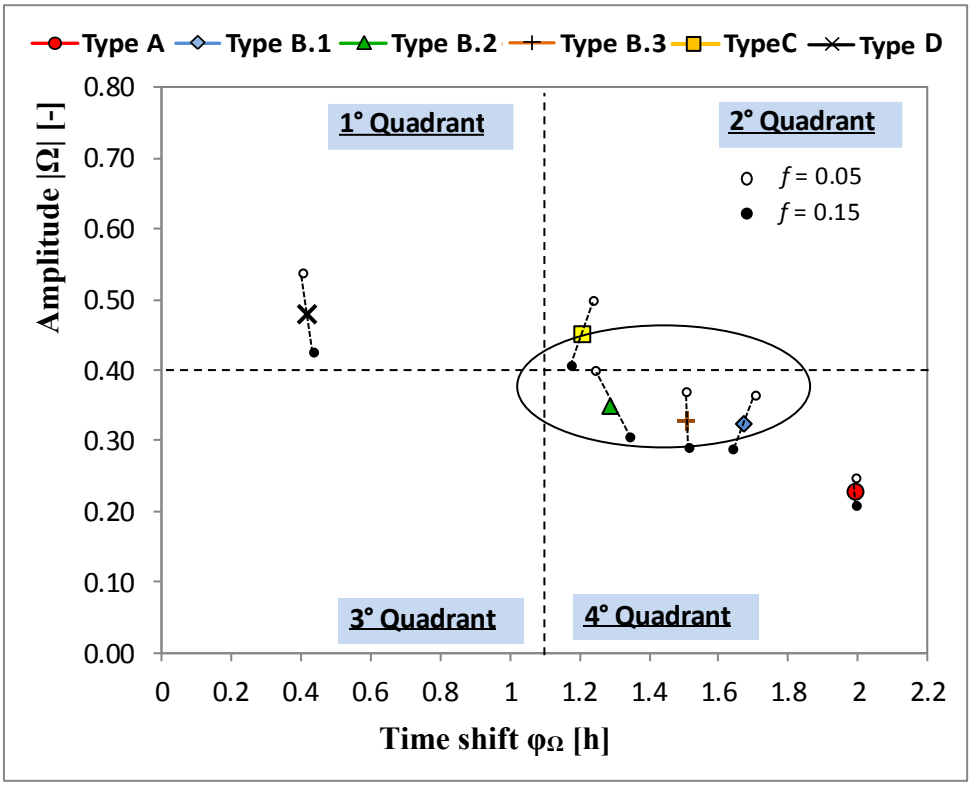

Figure7.76 - Mapping of the Solar Response Factor Ω for n = 1 e a_s = 0.3
(For each typology the position of the symbols corrisponde to f=0.1. the excursion of the symbolcorresponds to the f=0.05÷0.15)

In the figure, for each type considered, the position of the symbols corresponds to*f* = 0.1.

The range of the symbol corresponds to the interval *f* = 0.05 ÷ 0.15. So the area drawn around each direction suggests the scope of the possible values of magnitude and phase for each given typology category.

The elliptical area plotted in the figure, for example, would identify the sector of brick buildings (category B).

Obviously, the lines of demarcation between the four quadrants are arbitrary and their more precise identification would require more case studies than what has been examined here.

In any case, the opportunity has been outlined 1) to proceed in this way to a mapping of existing buildings, or 2) to adopt the normative classification of merit for new constructions in relation to the use of solar radiation within inhabited spaces.

7.5 Results

Among the indices designed to characterize the energy efficiency of buildings, the concept introduced here of the *Solar Response Factor*Ωseems appropriate and useful. This parameter is formulated on a purely logical-deductive and semi-empirical basis and concerns the heat returned by the environment, not that absorbed as a result of solar radiation, refers to incident radiation and not to that transmitted by glass, and as such implies and highlights - but surpasses by generality and rigor - the concept of the effective absorption coefficient. Furthermore, since it involves all the thermophysical and optical characteristics of the environment (from the stratigraphy of the walls to the optical properties of the glass) and it joins with simple analytical forms to surface factor Z, synthesizes - in two values: module and phase - also the dynamic behaviour of the structure.

The solar response factor Ω can therefore rightly be considered the transfer function of the complete physical system, constituted by the environment and by the glass. This is particularly useful in the case of solarized buildings, since it allows just with the calculation of amplitude and phase (ie without the aid of simulations) to characterize dynamic regime in the cavity as a whole. As such, it could also be used for the classification of existing buildings, in relation to the characteristics of response to solar gains.

8 Conclusions

In this study, the validation of an original calculation methodology for the evaluation of the dynamic thermal response of buildings is addressed. This methodology is based on the dynamic thermal properties and - amongst these - on the surface factor, a concept not always sufficiently exploited in the literature, that allows the explicit consideration of the radiant heat gains acting on the surfaces of the enclosure.

Actually, some simplified procedures are available in the literature to this aim, such as the Carrier method; here the inertial capacity of the opaque components is treated through *thermal storage factors* determined by interpolating over a high number of simulated results, and reported in appropriate tables. However, such simplified methods introduce a certain inaccuracy, and are not suitable for being implemented in automatic calculation codes.

On the contrary, the methodology proposed is based on a rigorous analytical approach, can be easily implemented in any calculation tool and proves to be very reliable, as it largely deserves Class I according to the validation procedure of the ISO standard 13792.

In this work it is also shown that, since the proposed methodology is based on the harmonic analysis, the adoption of the only fundamental harmonic may introduce a certain approximation in the evaluation of the building thermal response. However, that proved not to be critical for the rating of the proposed model, that would in any case remain in Class I.

Finally, another relevant quality of the proposed methodology is the possibility to single out the heat fluxes released by each inner envelope surface in response to every single forcing wave. This can help the user to adopt appropriate measures to improve the dynamic thermal performance of the building envelope.

Then it was introduced the *Solar Response Factor*, that is an appropriate and very useful parameter to characterize the energy performance of buildings. Indeed, by using this parameter, it makes possible to quantify the heat flow transferred by convection from the inner surface of the envelope to the indoor air in response to the solar radiation acting on the glazing, thus allowing the determination of the thermal loads. The formulation of this parameter is derived analytically, and involves all of the thermophysical properties of the envelope.

The main quality of the Solar Response Factor is that it represents a transfer function of the whole enclosure, and allows to qualify the response of the building to solar excitations through a single complex number, i.e. through a couple of real numbers (amplitude and time shift). In this sense, it can be used to make comparisons between different building solutions in the design stage, or to classify existing buildings in relation to their capacity to attenuate the effects of solar radiation, without the need of complex dynamic simulations. If compared to the thermal storage factor defined in the Carrier method (Carrier, 1962), or to the effective absorption coefficient proposed by (Oliveti et al., 2011), the Solar Response Factor shows solid theoretical bases and is more general and rigorous.

Furthermore, the Solar Response Factor can be integrated, in the framework of the Admittance Method, with other dynamic transfer properties such as the thermal admittance and the decrement factor, thus allowing a complete analytical solution

of the thermal balance on the indoor air. This approach can be implemented in whatever user-defined software, and requires a very limited computational effort.

APPENDIX A

The calculation method described above was validated, not only with the technical regulations, but also using Energy Plus which allows building simulations in dynamic regime on the basis of the Heat Balance Method. It has an enormous potential for combination of building and system components, user profiles and environmental conditions. For these reasons, it is one of the most credited simulation tools for researchers in the world.

However, its complexity makes it not very practical for use by professionals, who prefer to interface with software which is easier to use.

Any error found to occur when using the algorithm developed from the Admittance method in place of Energy Plus is always less than 10% (relative to the various types implemented by us), as can be seen from Figure A.

The subsequent figures outline the performance of a room under various operating conditions, as detailed in the captions:

- The influence of the room exposure to thermal load and indoor temperature is shown in figures A.1 to A.9
- The influence of windows area to thermal load and indoor temperature is shown in figures A.12
- The influence of ventilation rate to thermal load and indoor temperature is shown in figures A.14 and A.15
- The influence of the transmittance of the glass is shown in figures A.16 and A.17

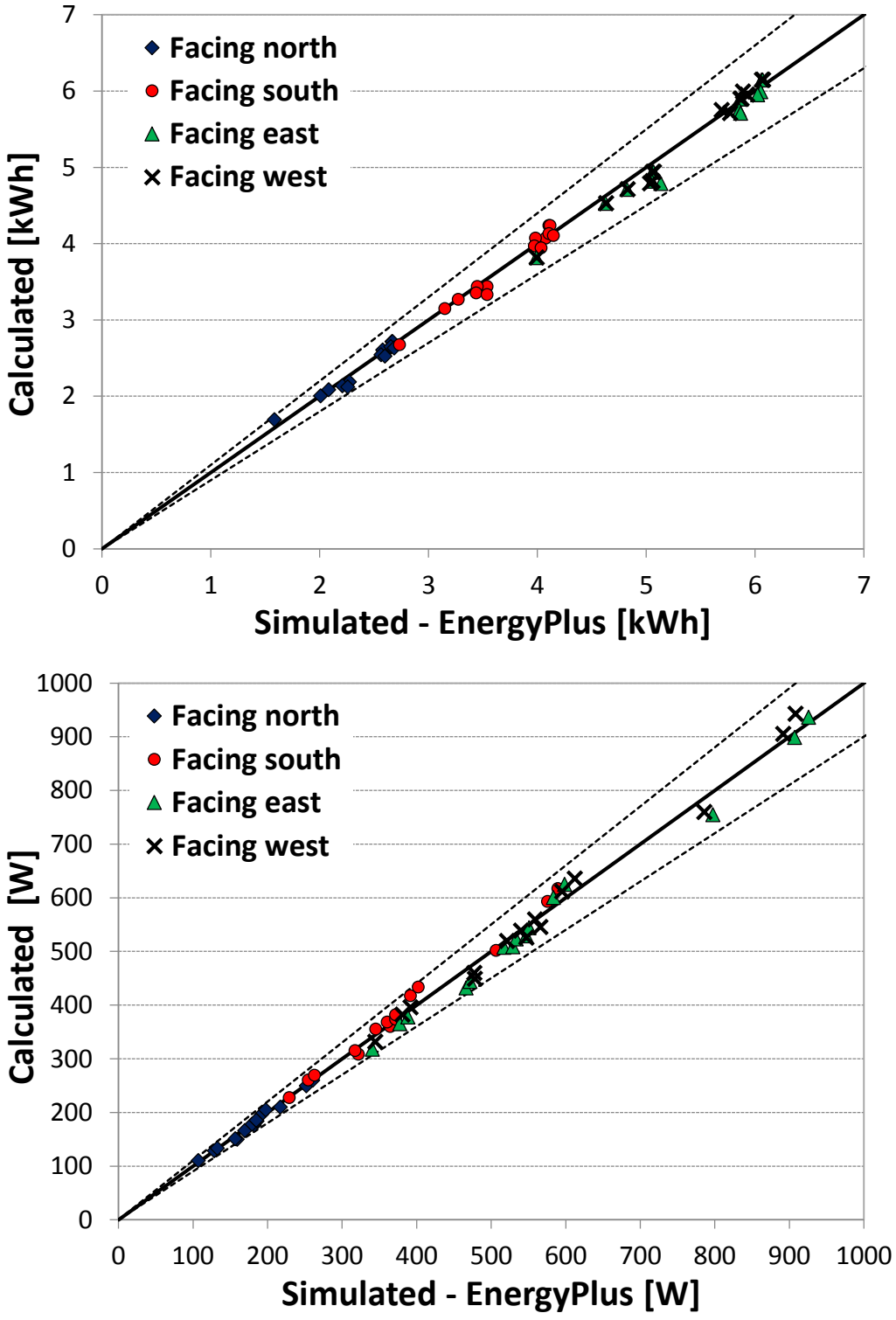
Facing north
Facing south
Facing east
Facing west
Calculated [kWh]
Simulated - EnergyPlus [kWh]
0
1
2
3
4
5
6
7
Facing north
Facing south
Facing east
Facing west
Calculated [W]
Simulated - EnergyPlus [W]
0
100
200
300
400
500
600
700
800
900
1000

Figure A

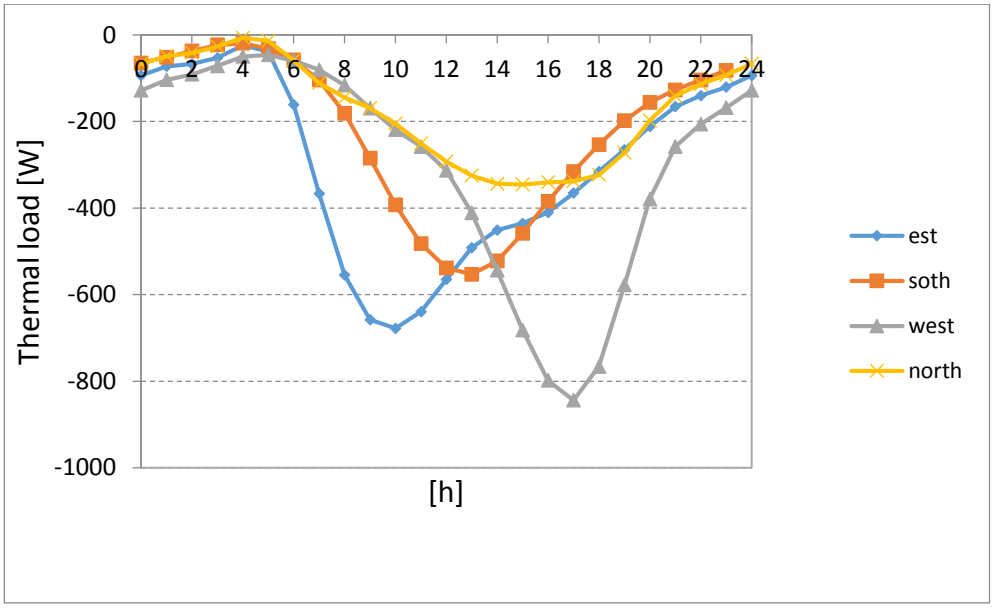

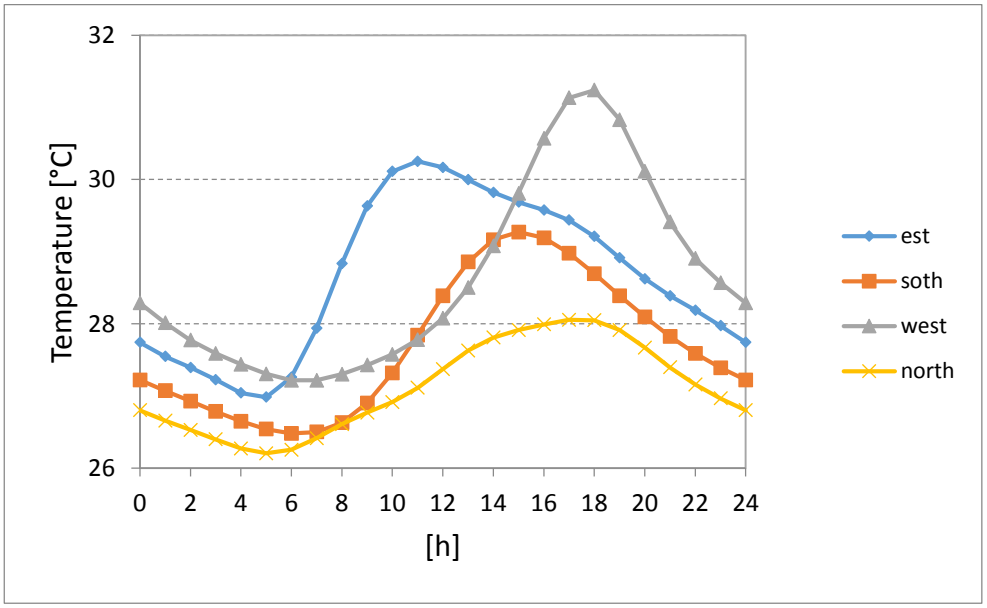

Figure A.1: Thermal load and indoor air temperature for room with light wall insulated from inside (ventilation rate 0.5 v/h; window surface 2 m^2; transmittance 5 W/m^{2}K; internal loads 0; variable exposure of the external wall).

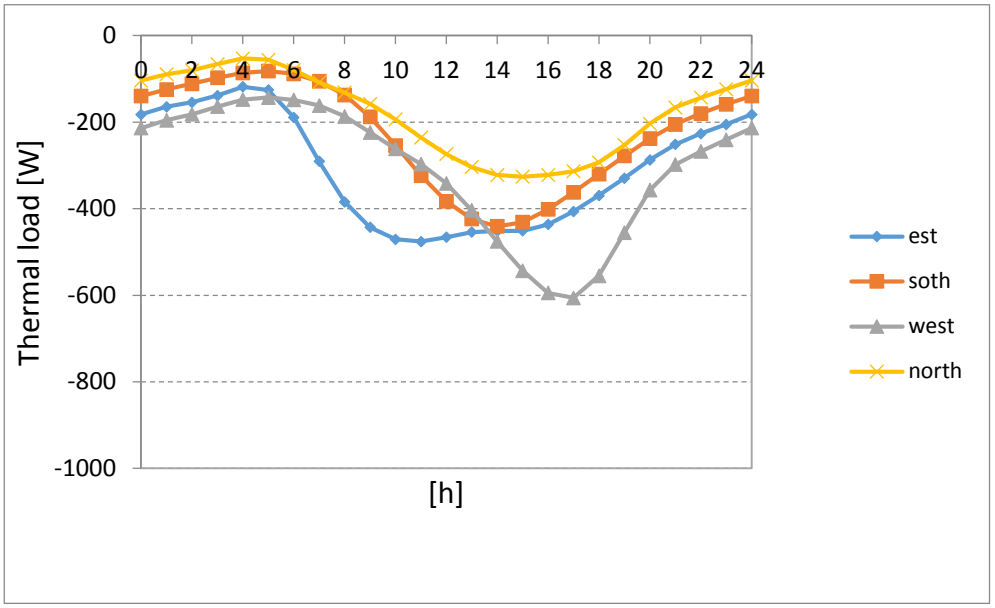

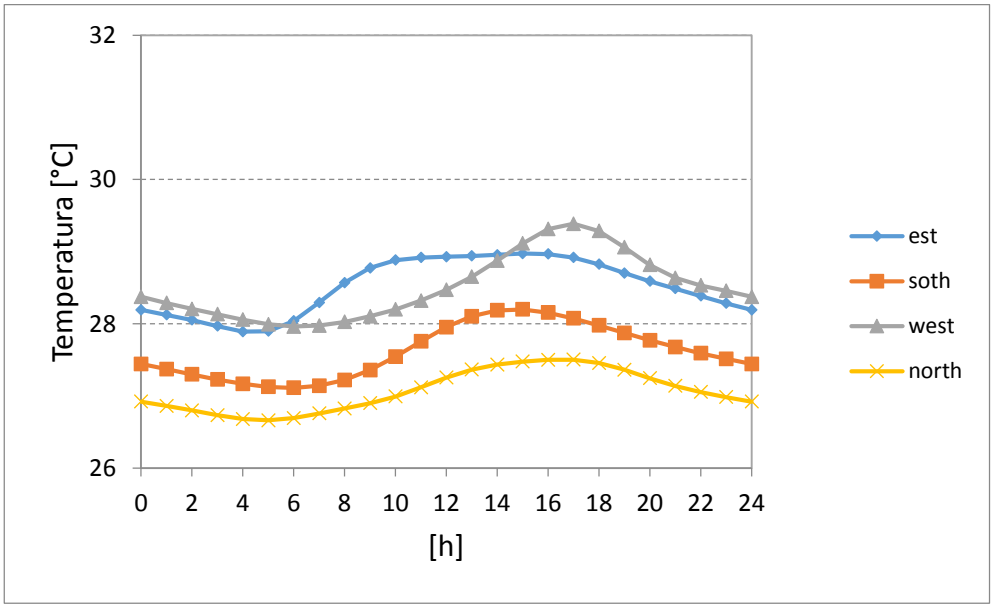

Figure A.2: Thermal load and indoor air temperature for room with heavy wall insulated from outside (ventilation rate 0.5 v/h; window surface 2 m^2; transmittance 5 W/m^2K; internal loads 0; variable exposure of the external wall).

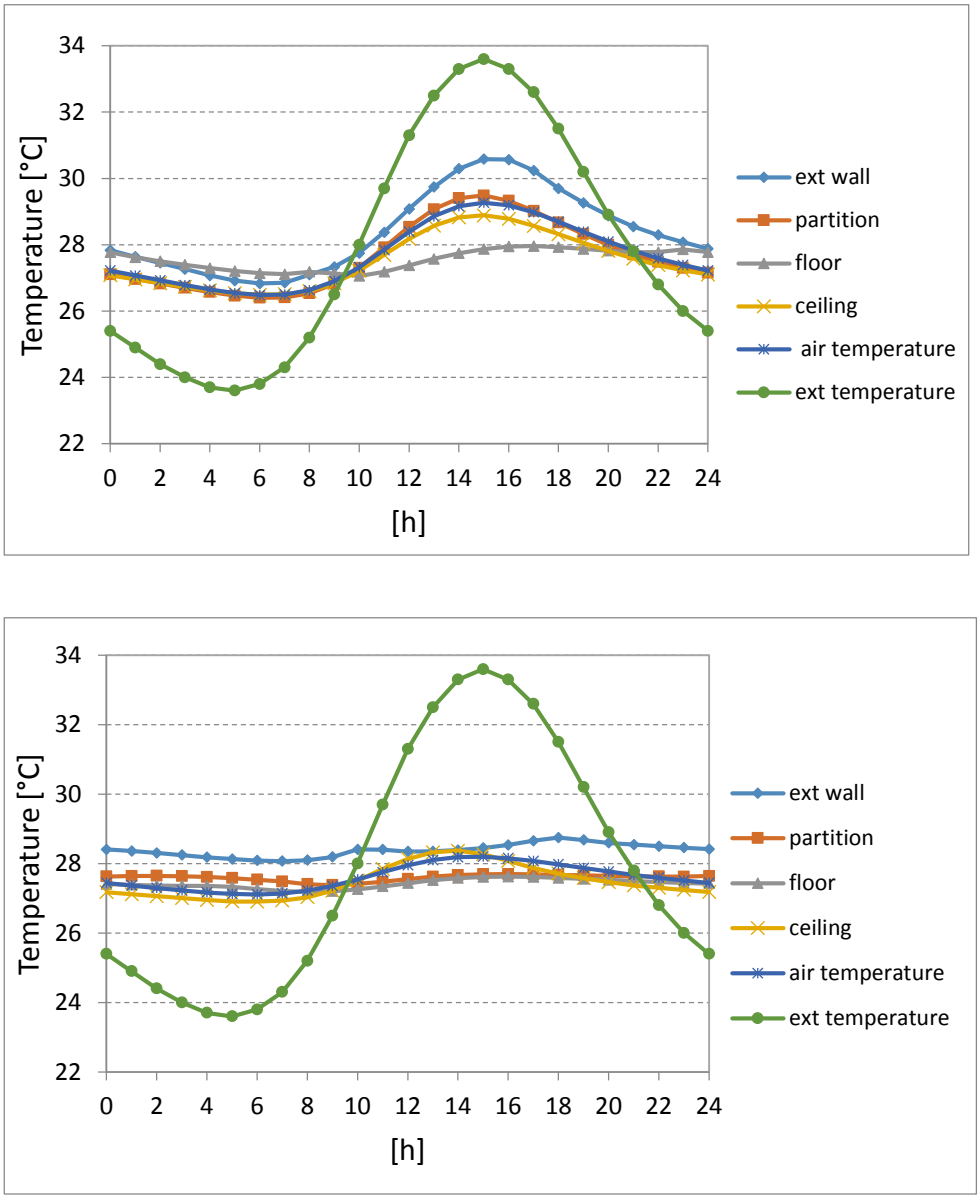

Figure A.3: Wall surface temperature in southern exposed room (ventilation rate 0.5 v/h; window surface 2 m^2; transmittance 5 W/m^2K; internal loads 0; southern exposure). Up: light wall. Bottom: heavy wall.

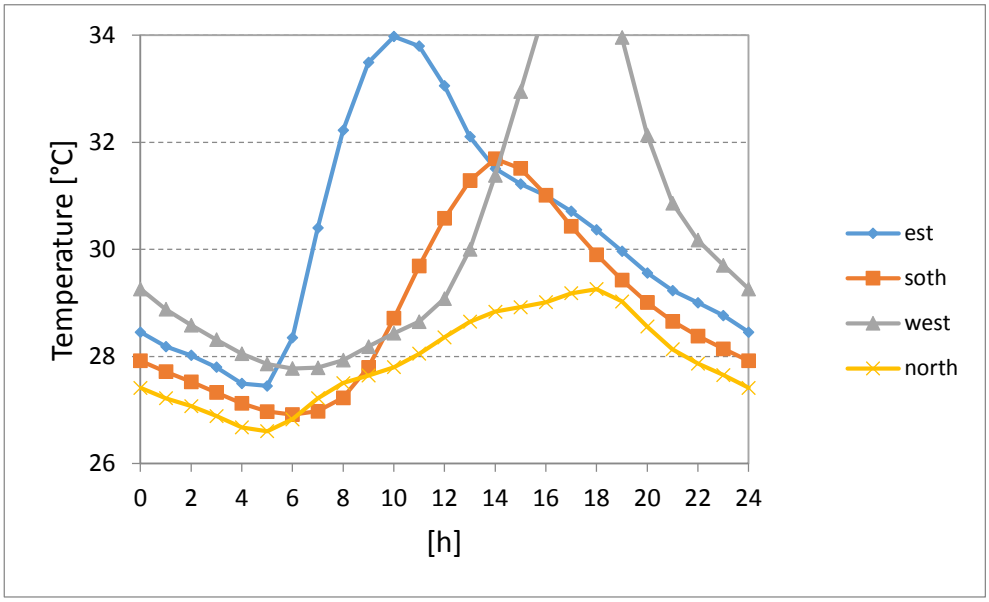

Figure A.4.a.1: Surface indoor temperature of external wall with variable exposition of external wall (light wall; indoor insulation; free running room; ventilation rate 0.5 v/h; window surface 2 m^2; transmittance 5 W/m^2K; internal loads 0; southern exposure).

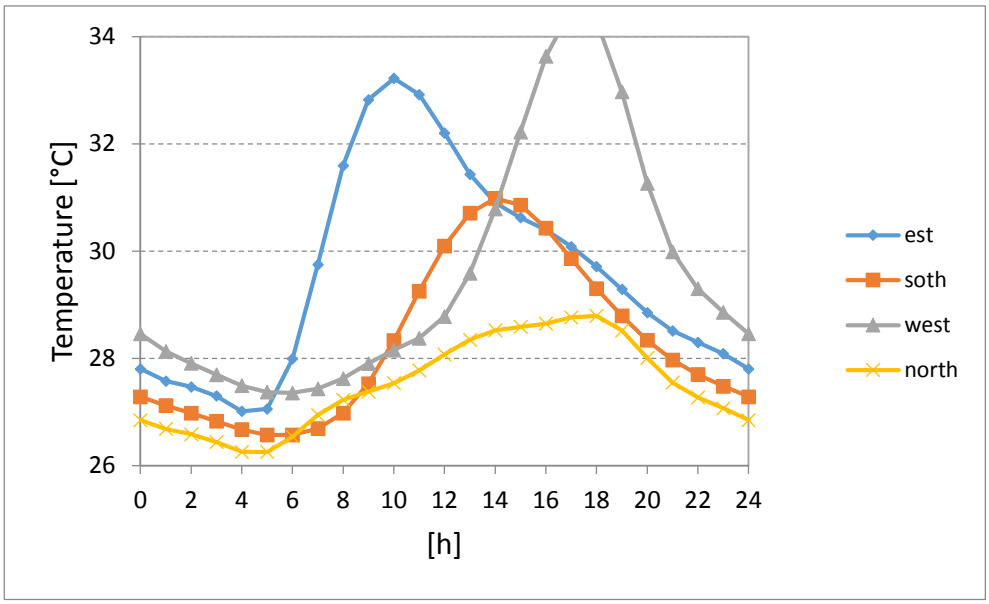

Figure A.4.a.2: Surface temperature of internal wall in a room with variable exposition of external wall (light wall; indoor insulation; free running room; ventilation rate 0.5 v/h; window surface 2 m^2; transmittance 5 W/m^2K; internal loads 0; southern exposure).

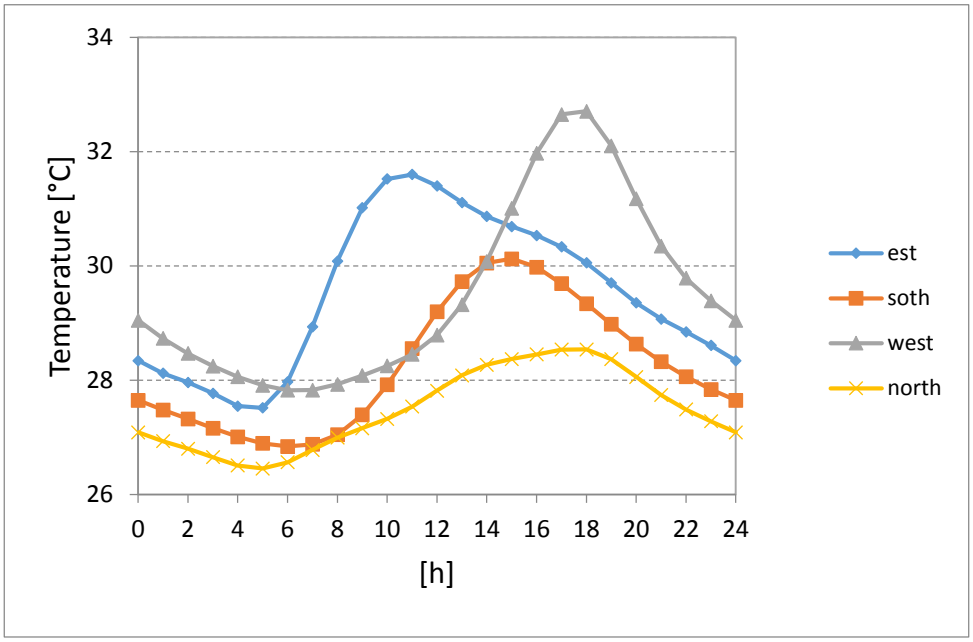

Figure A.4.a.3: Surface temperature of floor in a room with variable exposition of external wall (light wall; indoor insulation; free running room; ventilation rate 0.5 v/h; window surface 2 m²; transmittance 5 W/m²K; internal loads 0; southern exposure).

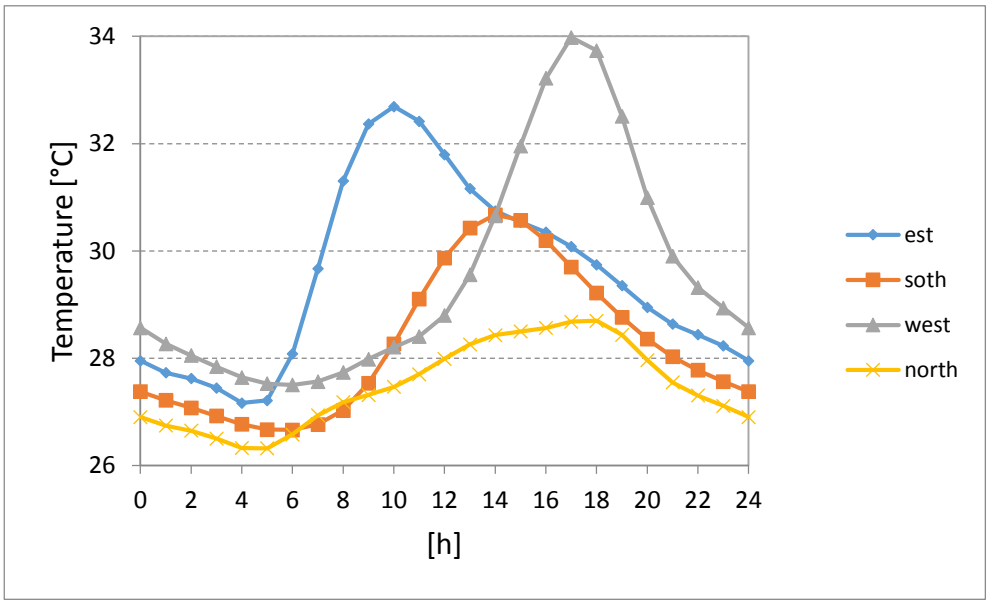

Figure A.4.a.4: Surface temperature of ceiling in a room with variable exposition of external wall (light wall; indoor insulation; free running room; ventilation rate 0.5 v/h; window surface 2 m²; transmittance 5 W/m²K; internal loads 0; southern exposure).

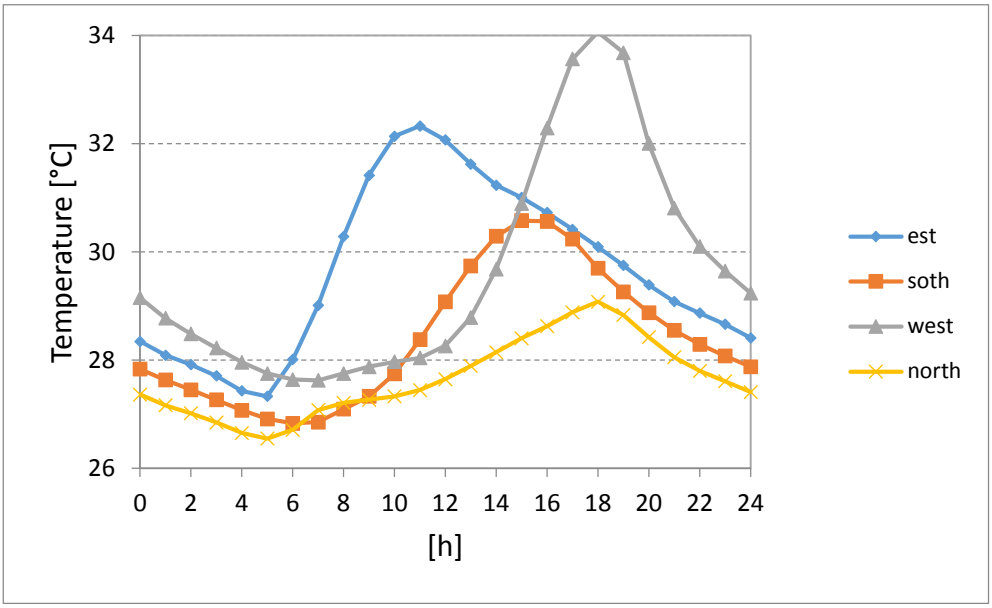

Figure A.4.b.1: Surface indoor temperature of external wall with variable exposition of external wall (light wall; indoor insulation; setted temperature; ventilation rate 0.5 v/h; window surface 2 m^2; transmittance 5 W/m^2K; internal loads 0; southern exposure).

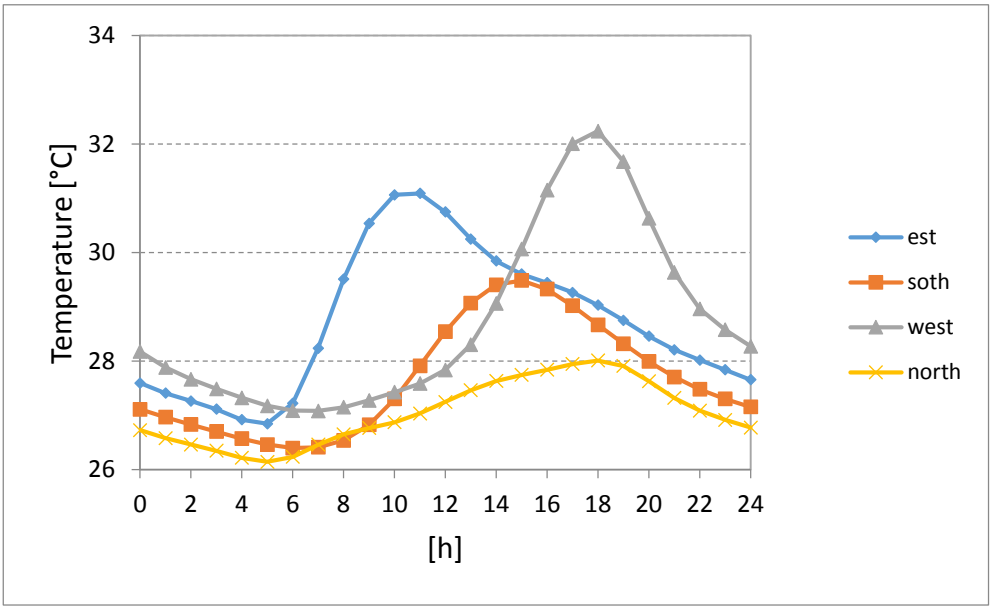

Figure A.4.b.2: Surface temperature of internal wall in a room with variable exposition of external wall (light wall; indoor insulation; setted temperature; ventilation rate 0.5 v/h; window surface 2 m^2; transmittance 5 W/m^2K; internal loads 0; southern exposure).

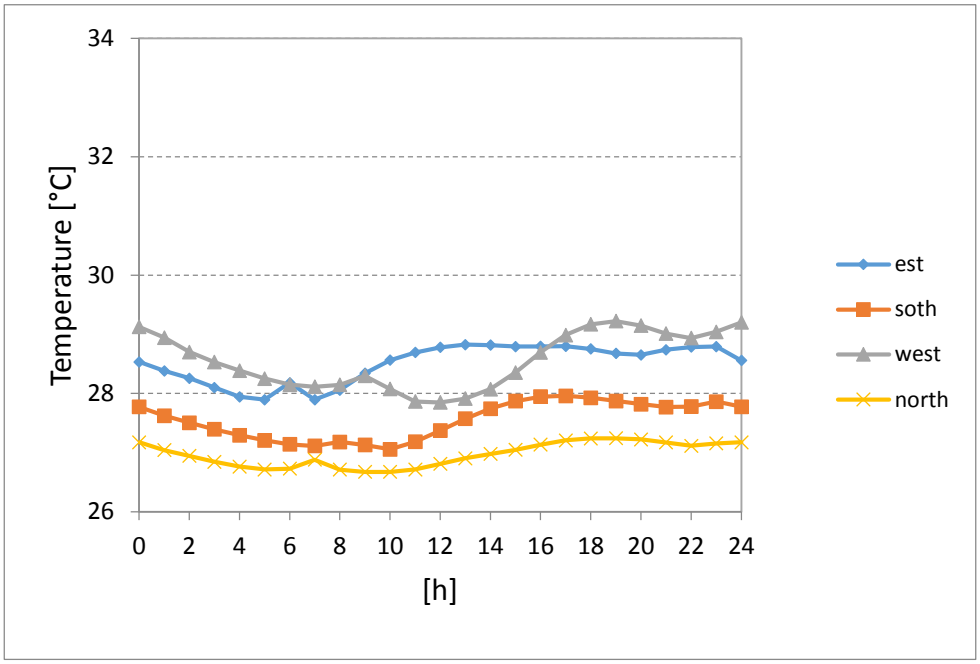

Figure A.4.b.3: Surface temperature of floor in a room with variable exposition of external wall (light wall; indoor insulation; setted temperature; ventilation rate 0.5 v/h; window surface 2 m^2; transmittance 5 W/m^{2}K; internal loads 0; southern exposure).

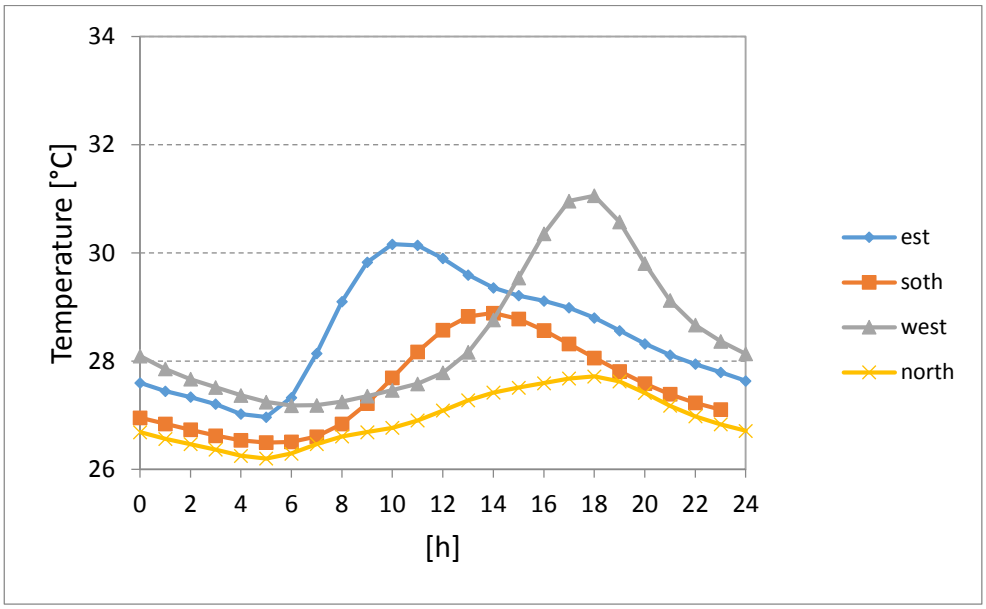

Figure A.4.b.4: Surface temperature of ceiling in a room with variable exposition of external wall (light wall; indoor insulation; setted temperature; ventilation rate 0.5 v/h; window surface 2 m^2; transmittance 5 W/m^{2}K; internal loads 0; southern exposure).

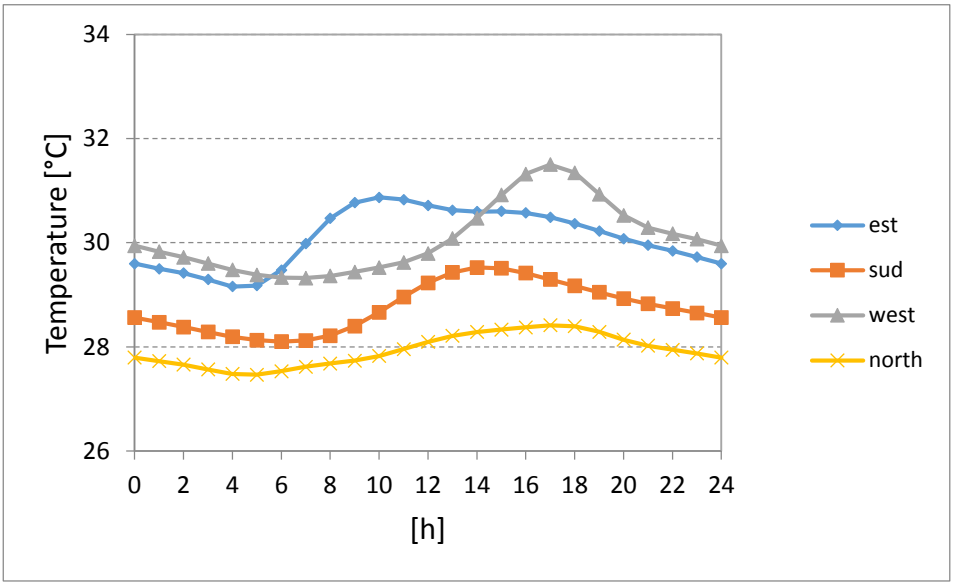

Figure A.5.a.1: Surface indoor temperature of external wall variably exposed (heavy wall; outdoor insulation; free running room; ventilation rate 0.5 v/h; window surface 2 m^2; transmittance 5 W/m^{2}K; internal loads 0; southern exposure).

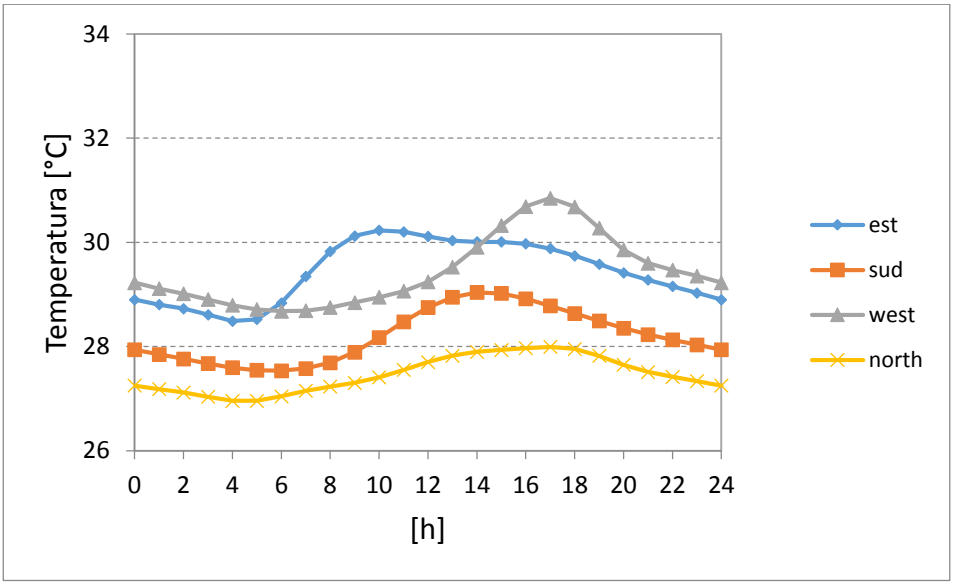

Figure A.5.a.2: Surface temperature of internal wall in a room with variable exposition of external wall (heavy wall; outdoor insulation; free running room; ventilation rate 0.5 v/h; window surface 2 m^2; transmittance 5 W/m^{2}K; internal loads 0; southern exposure).

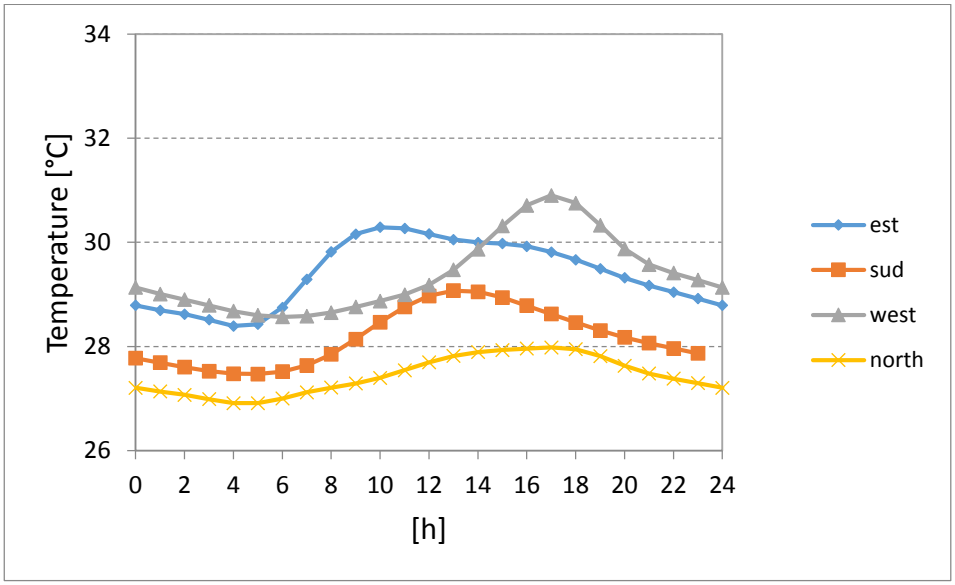

Figure A.5.a.3: Surface temperature of floor in a room with variable exposition of external wall (heavy wall; outdoor insulation; free running room; ventilation rate 0.5 v/h; window surface 2 m^2; transmittance 5 W/m^{2}K; internal loads 0; southern exposure).

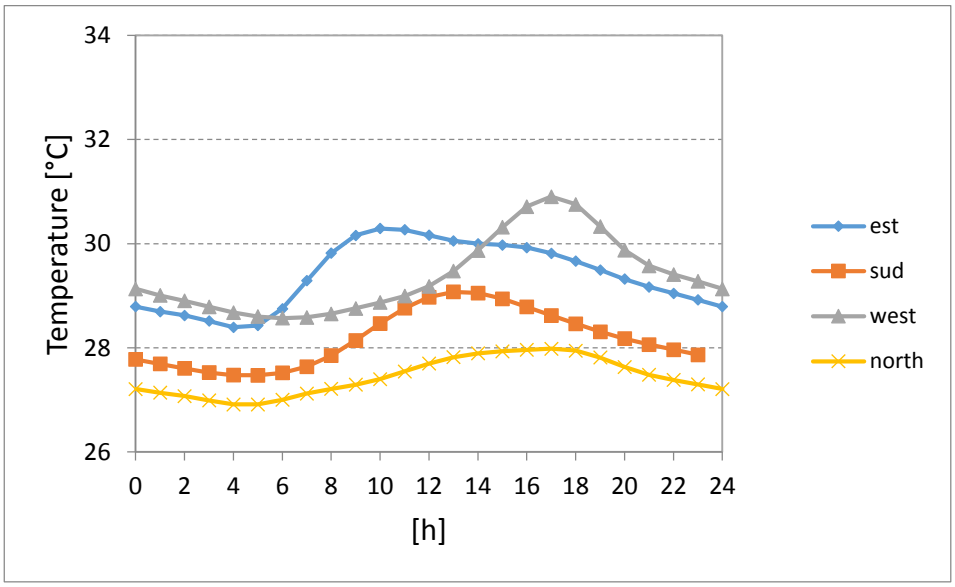

Figure A.5.a.4: Surface temperature of ceiling in a room with variable exposition of external wall (heavy wall; outdoor insulation; free running room; ventilation rate 0.5 v/h; window surface 2 m^2; transmittance 5 W/m^{2}K; internal loads 0; southern exposure).

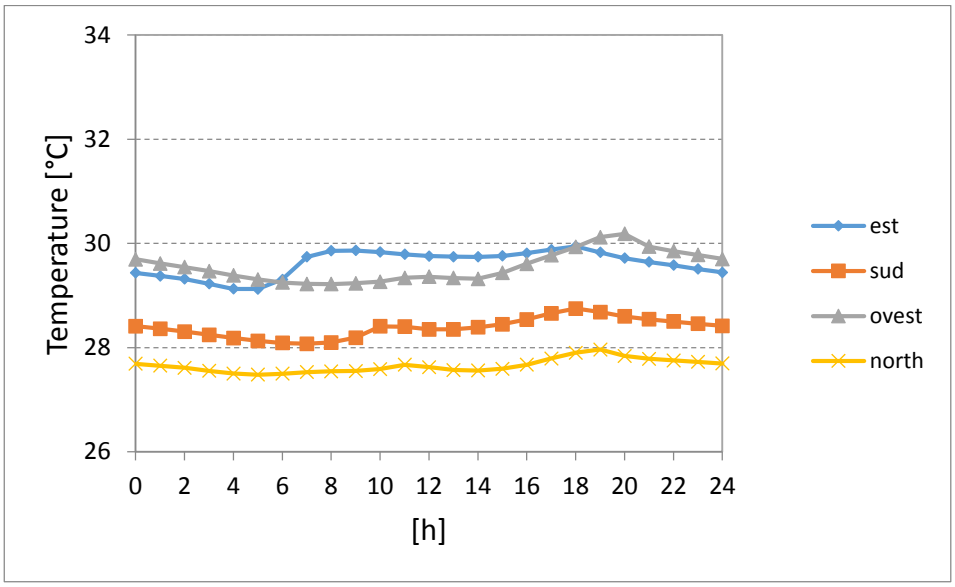

Figure A.5.b.1: Surface indoor temperature of external wall with variable exposition of external wall (heavy wall; outdoor insulation; setted temperature; ventilation rate 0.5 v/h; window surface 2 m^2; transmittance 5 W/m^{2}K; internal loads 0; southern exposure).

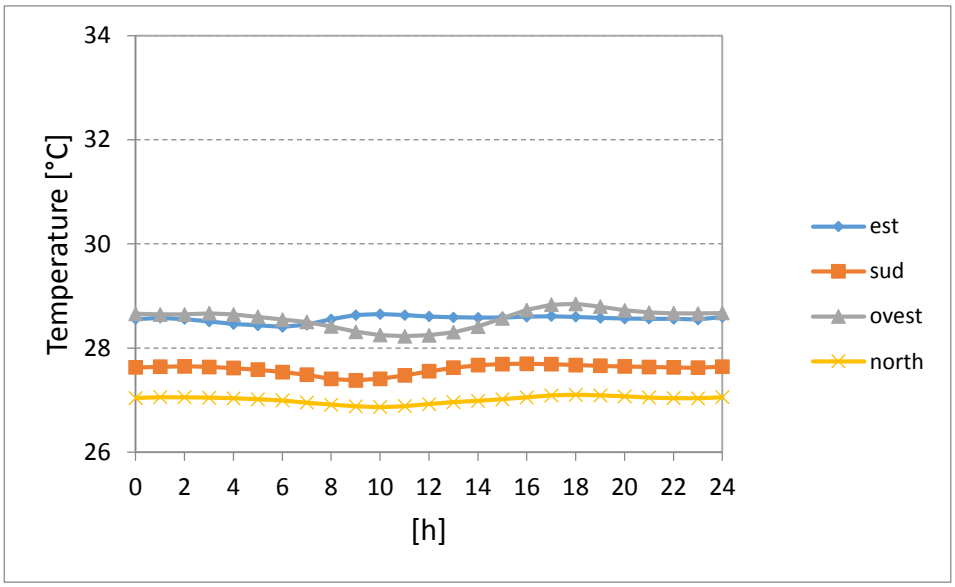

Figure A.5.b.2: Surface temperature of internal wall in a room with variable exposition of external wall (heavy wall; outdoor insulation; setted temperature; ventilation rate 0.5 v/h; window surface 2 m^2; transmittance 5 W/m^{2}K; internal loads 0; southern exposure).

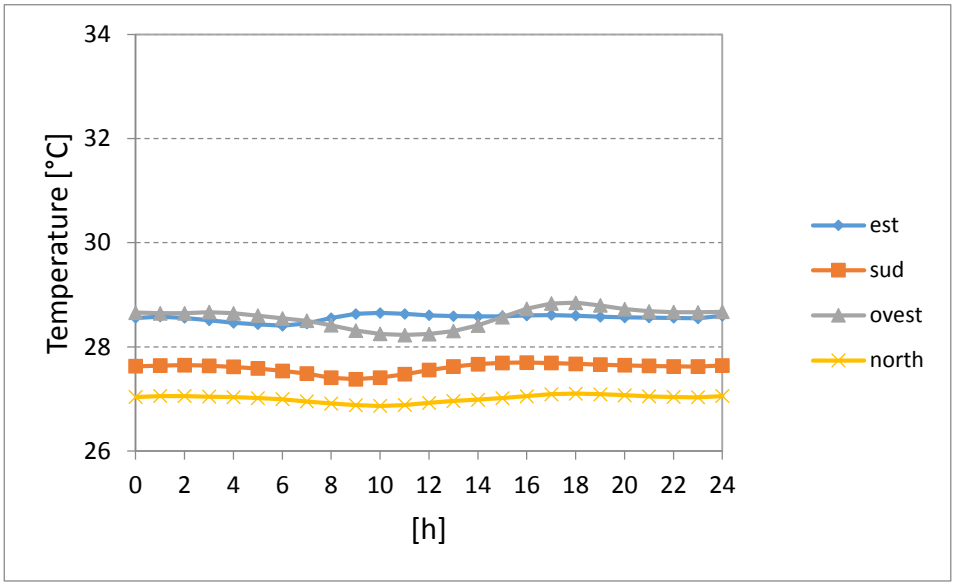

Figure A.5.b.3: Surface temperature of floor in a room with variable exposition of external wall (heavy wall; outdoor insulation; setted temperature; ventilation rate 0.5 v/h; window surface 2 m^2; transmittance 5 W/m^{2}K; internal loads 0; southern exposure).

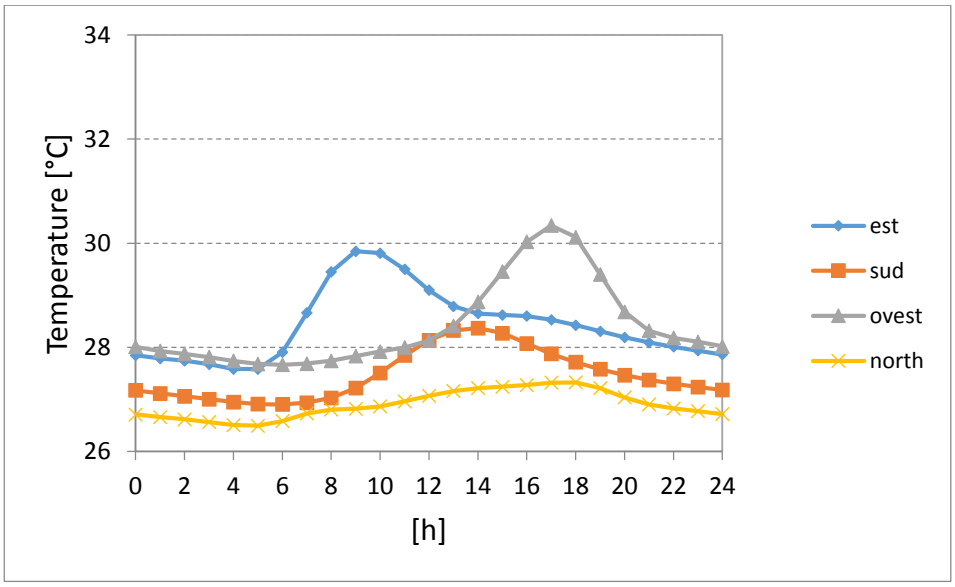

Figure A.5.b.4: Surface temperature of ceiling in a room with variable exposition of external wall (heavy wall; outdoor insulation; setted temperature; ventilation rate 0.5 v/h; window surface 2 m^2; transmittance 5 W/m^{2}K; internal loads 0; southern exposure).

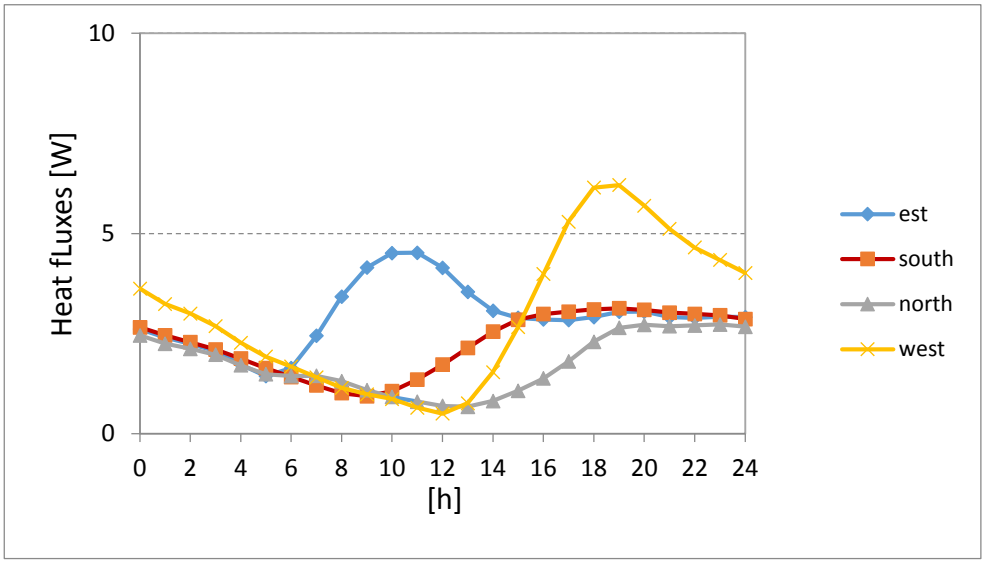

Figure A.6.a.1: Heat fluxe occurring on the external wall of a room with variable exposition (light wall; indoor insulation; free running room; ventilation rate 0.5 v/h; window surface 2 m^2; transmittance 5 W/m^2K; internal loads 0; southern exposure).

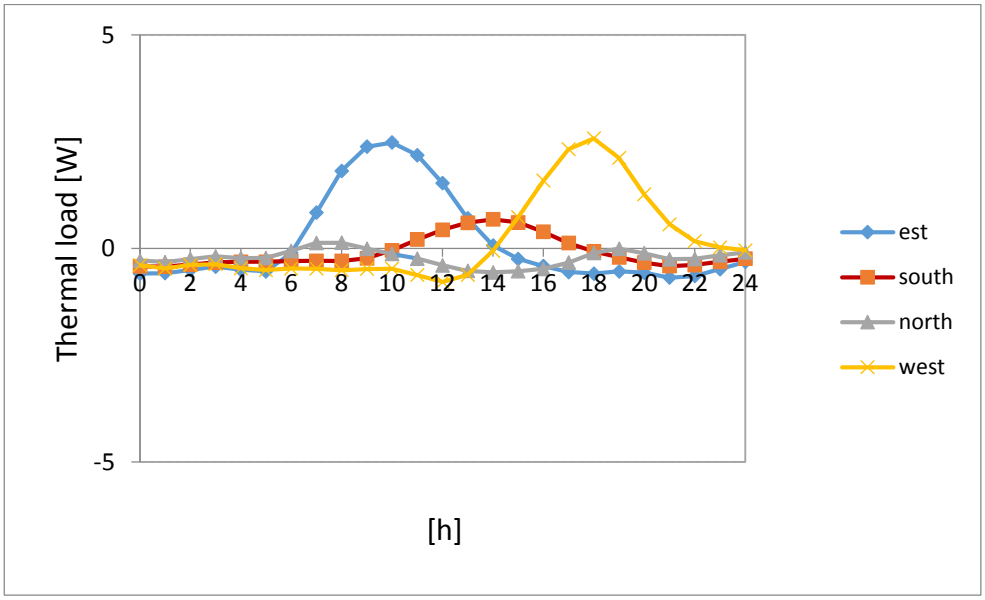

Figure A.6.a.2: Heat fluxe occurring on the internal wall of a room with variable exposition of the external wall (light wall; indoor insulation; free running room; ventilation rate 0.5 v/h; window surface 2 m^2; transmittance 5 W/m^2K; internal loads 0; southern exposure).

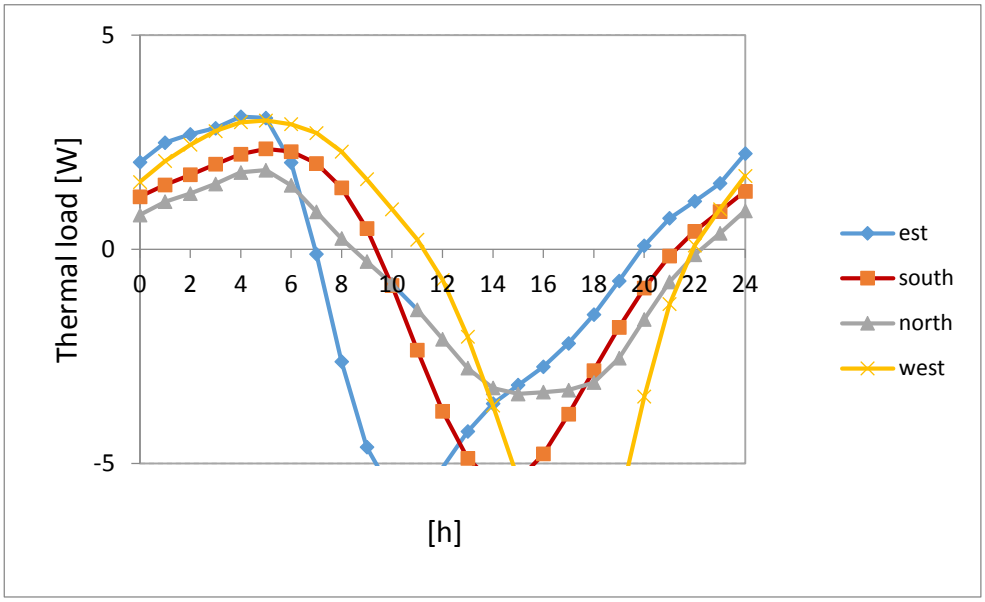

Figure A.6.a.3: Heat fluxe occurring on the floor of a room with variable exposition of the external wall (light wall; indoor insulation; free running room; ventilation rate 0.5 v/h; window surface 2 m^2; transmittance 5 W/m^2K; internal loads 0; southern exposure).

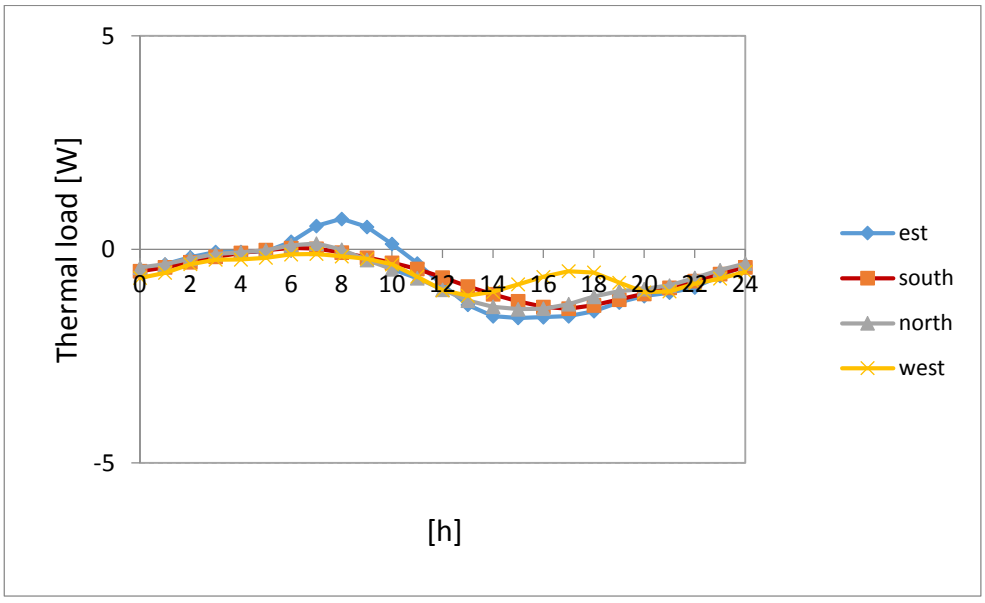

Figure A.6.a.4: Heat fluxe occurring on the ceiling of a room with variable exposition f the external wall (light wall; indoor insulation; free running room; ventilation rate 0.5 v/h; window surface 2 m^2; transmittance 5 W/m^2K; internal loads 0; southern exposure).

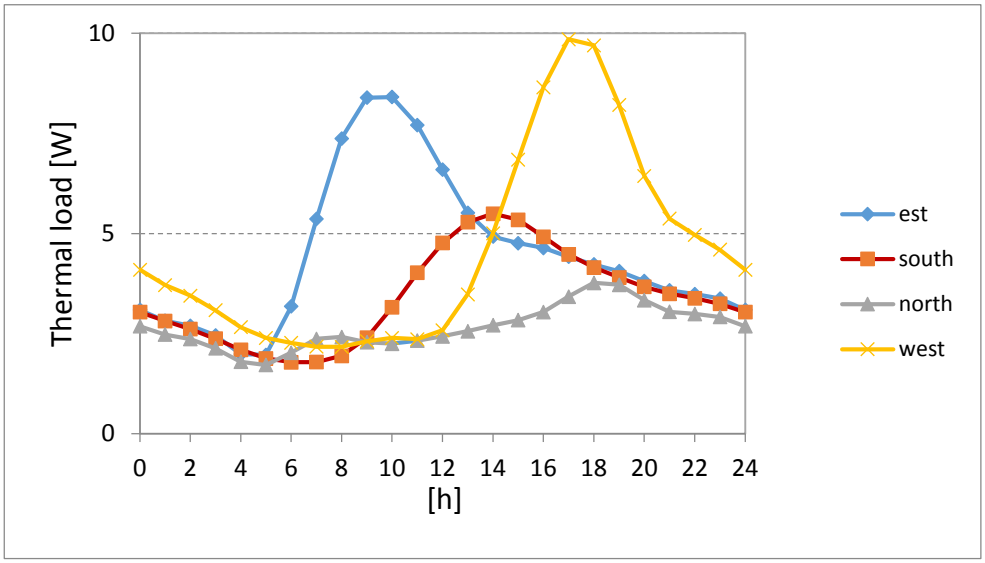

Figure A.6.b.1: Heat fluxe occurring on the external wall of a room with variable exposition (light wall; indoor insulation; setted temperature; ventilation rate 0.5 v/h; window surface 2 m^2; transmittance 5 W/m^2K; internal loads 0; southern exposure).

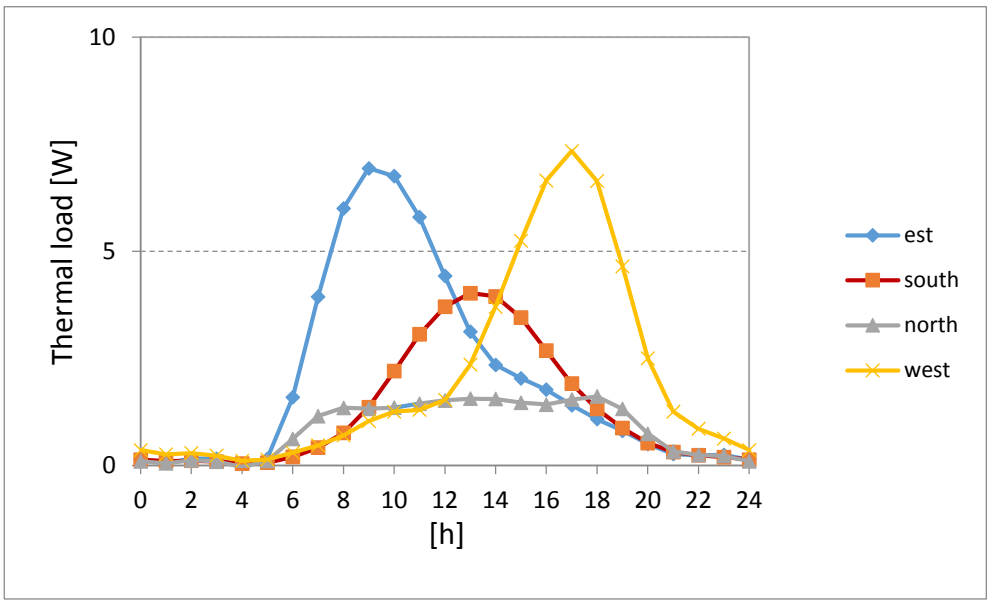

Figure A.6.b.2: Heat fluxe occurring on the internal wall of a room with variable exposition of the external wall (light wall; indoor insulation; setted temperature; ventilation rate 0.5 v/h; window surface 2 m^2; transmittance 5 W/m^2K; internal loads 0; southern exposure).

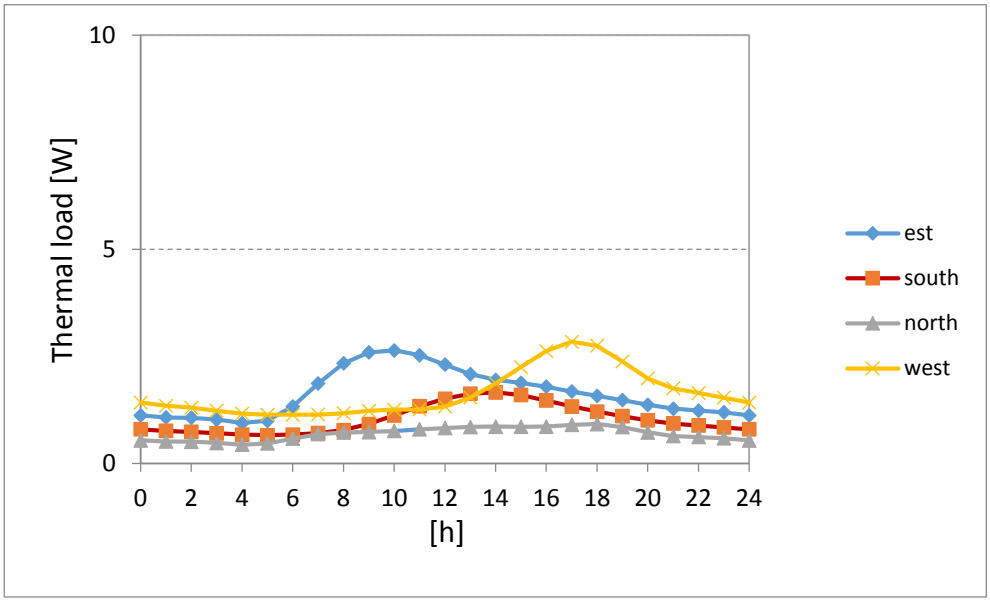

Figure A.6.b.3: Heat fluxe occurring on the floor of a room with variable exposition of the external wall (light wall; indoor insulation; setted temperature; ventilation rate 0.5 v/h; window surface 2 m^2; transmittance 5 W/m^2K; internal loads 0; southern exposure).

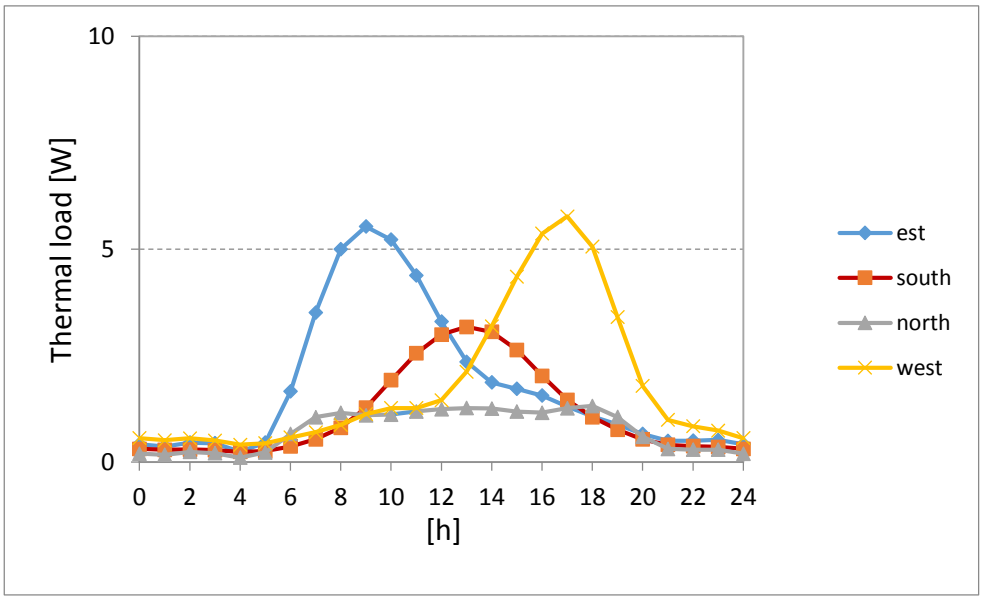

Figure A.6.b.4: Heat fluxe occurring on the ceiling of a room with variable exposition of the external wall (light wall; indoor insulation; setted temperature; ventilation rate 0.5 v/h; window surface 2 m^2; transmittance 5 W/m^2K; internal loads 0; southern exposure).

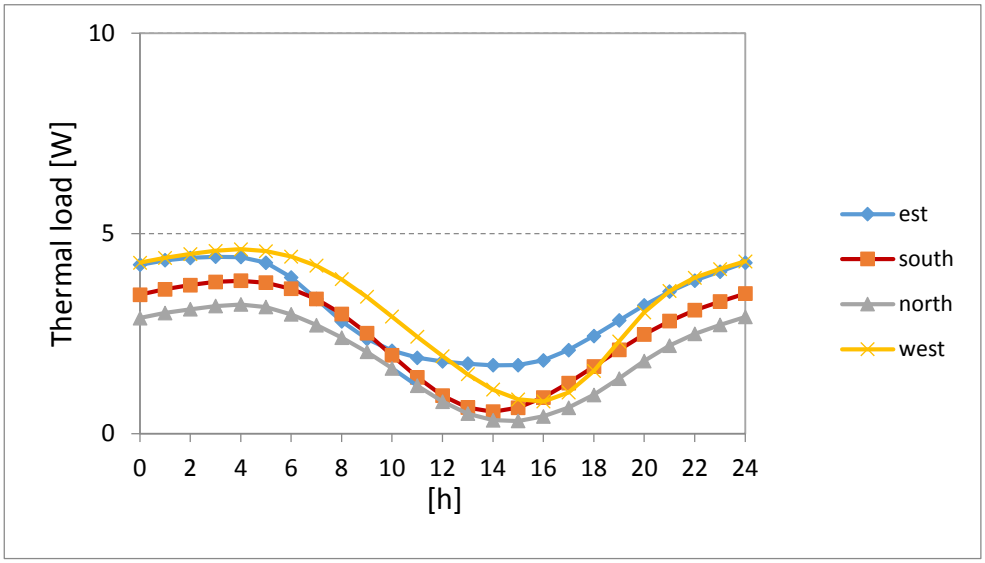

Figure A.7.a.1: Heat fluxe occurring on the external wall of a room with variable exposition (heavy wall; outdoor insulation; free running; ventilation rate 0.5 v/h; window surface 2 m^2; transmittance 5 W/m^2K; internal loads 0; southern exposure).

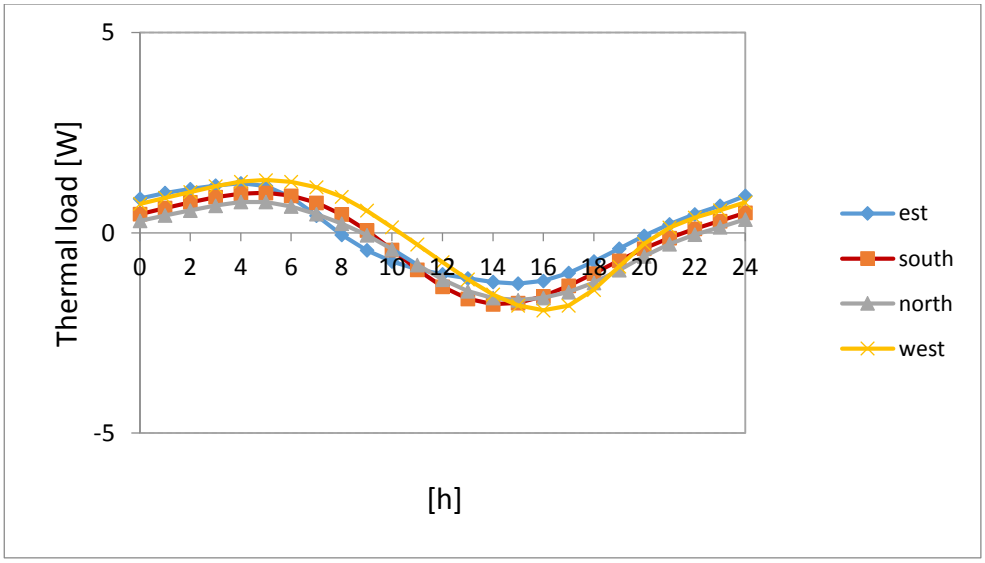

Figure A.7.a.2: Heat fluxe occurring on the internal wall of a room with variable exposition of the external wall (heavy wall; outdoor insulation; free running; ventilation rate 0.5 v/h; window surface 2 m^2; transmittance 5 W/m^2K; internal loads 0; southern exposure).

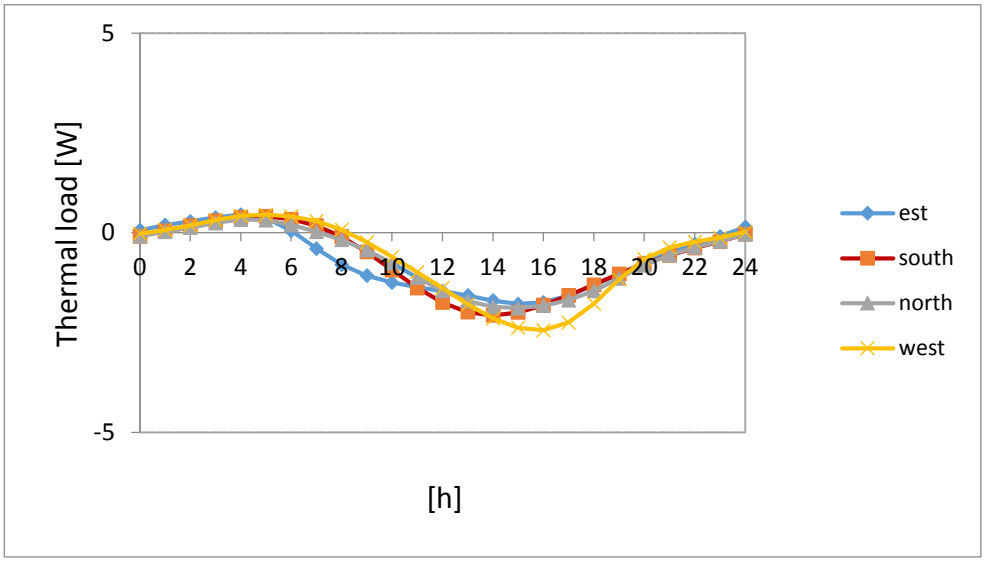

Figure A.7.a.3: Heat fluxe occurring on the floor of a room with variable exposition of the external wall (heavy wall; outdoor insulation; free running; ventilation rate 0.5 v/h; window surface 2 m^2; transmittance 5 W/m^2K; internal loads 0; southern exposure).

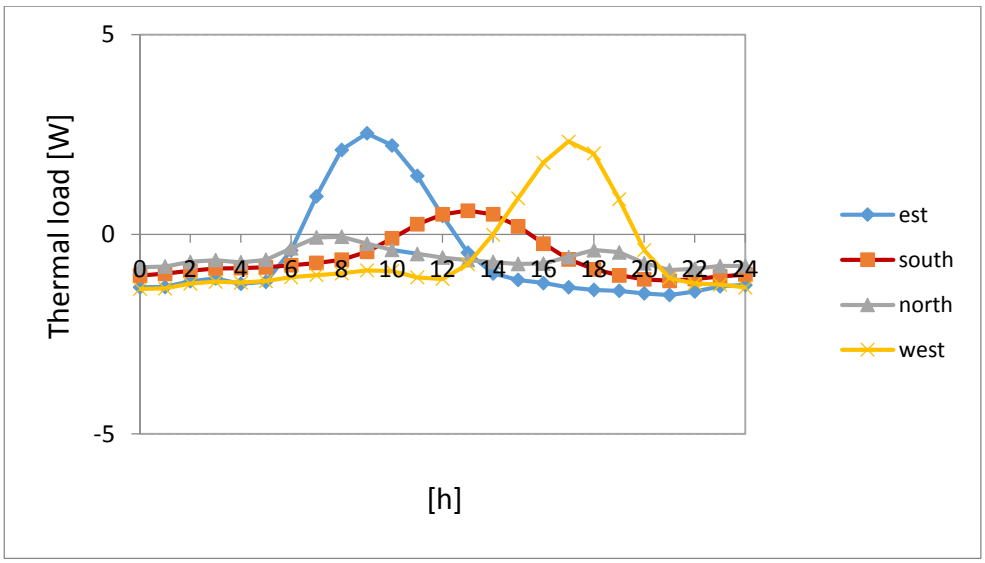

Figure A.7.a.4: Heat fluxe occurring on the floor of a room with variable exposition of the external wall (heavy wall; outdoor insulation; free running; ventilation rate 0.5 v/h; window surface 2 m^2; transmittance 5 W/m^2K; internal loads 0; southern exposure).

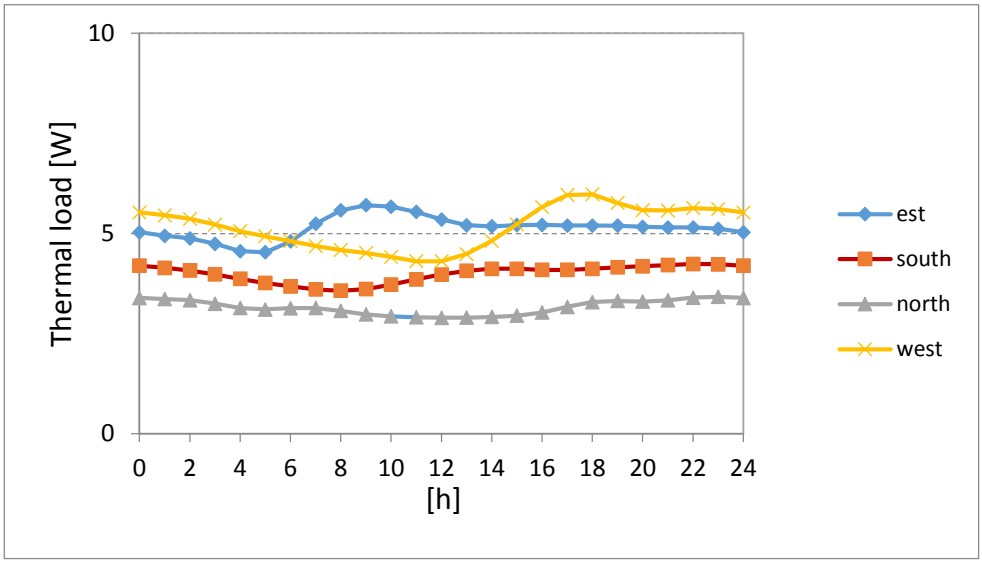

Figure A.7.b.1: Heat fluxe occurring on the external wall of a room with variable exposition (heavy wall; outdoor insulation; setted temperature; ventilation rate 0.5 v/h; window surface 2 m^2; transmittance 5 W/m^2K; internal loads 0; southern exposure).

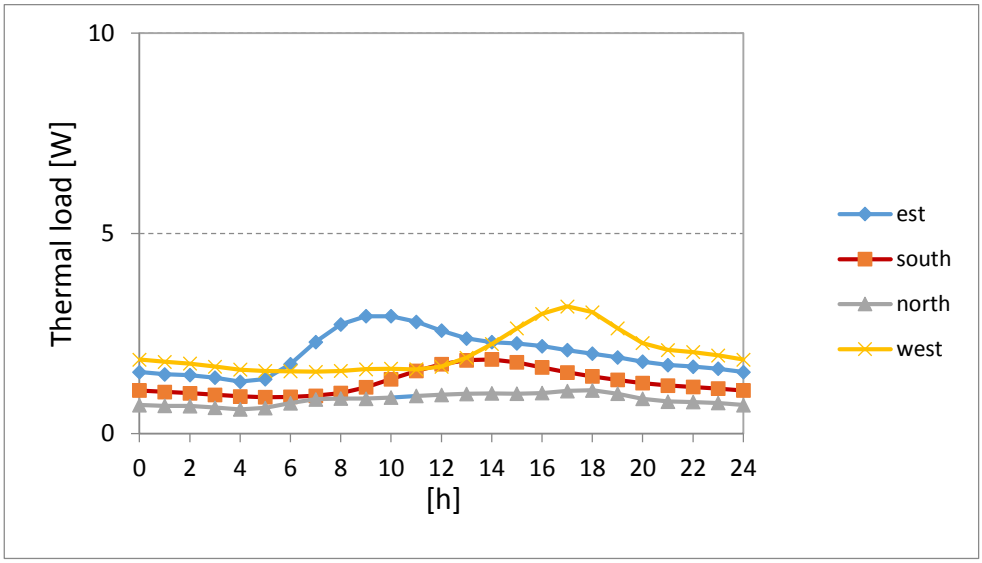

Figure A.7.b.2: Heat fluxe occurring on the internal wall of a room with variable exposition of the external wall (heavy wall; outdoor insulation; setted temperature; ventilation rate 0.5 v/h; window surface 2 m^2; transmittance 5 W/m^2K; internal loads 0; southern exposure).

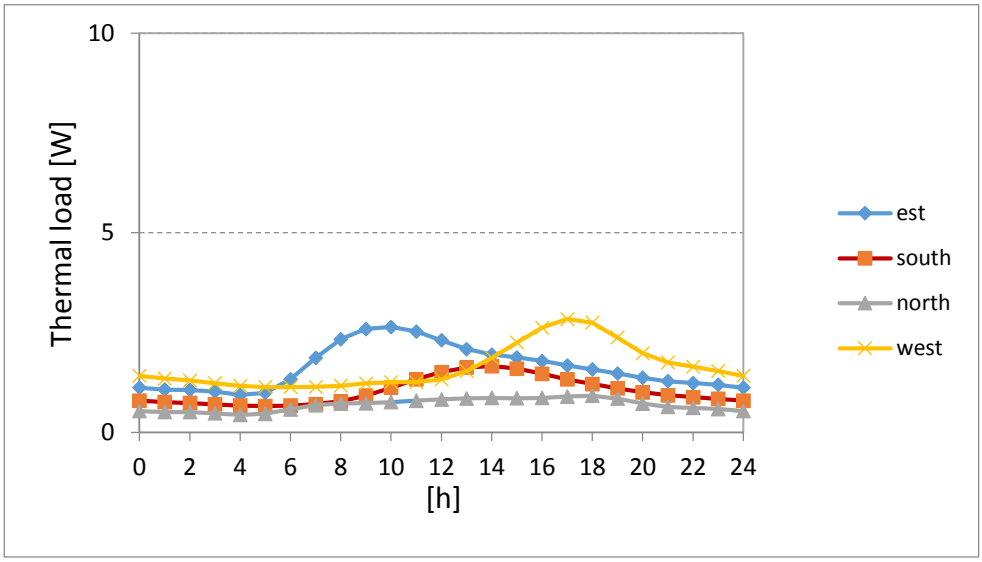

Figure A.7.b.3: Heat fluxe occurring on the floor of a room with variable exposition of the external wall (heavy wall; outdoor insulation; setted temperature; ventilation rate 0.5 v/h; window surface 2 m^2; transmittance 5 W/m^{2}K; internal loads 0; southern exposure).

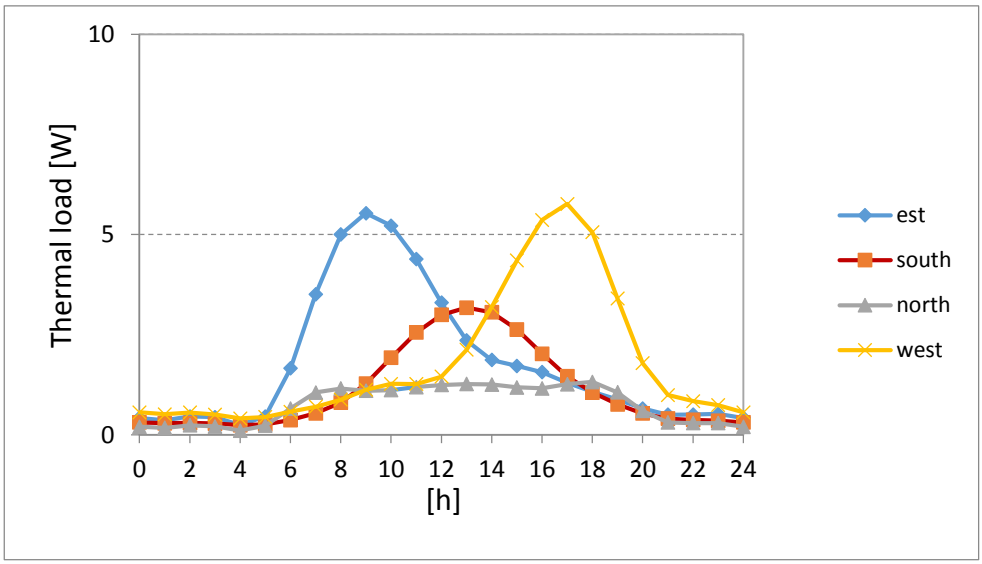

Figure A.7.b.4: Heat fluxe occurring on the ceiling of a room with variable exposition of the external wall (heavy wall; outdoor insulation; setted temperature; ventilation rate 0.5 v/h; window surface 2 m^2; transmittance 5 W/m^{2}K; internal loads 0; southern exposure).

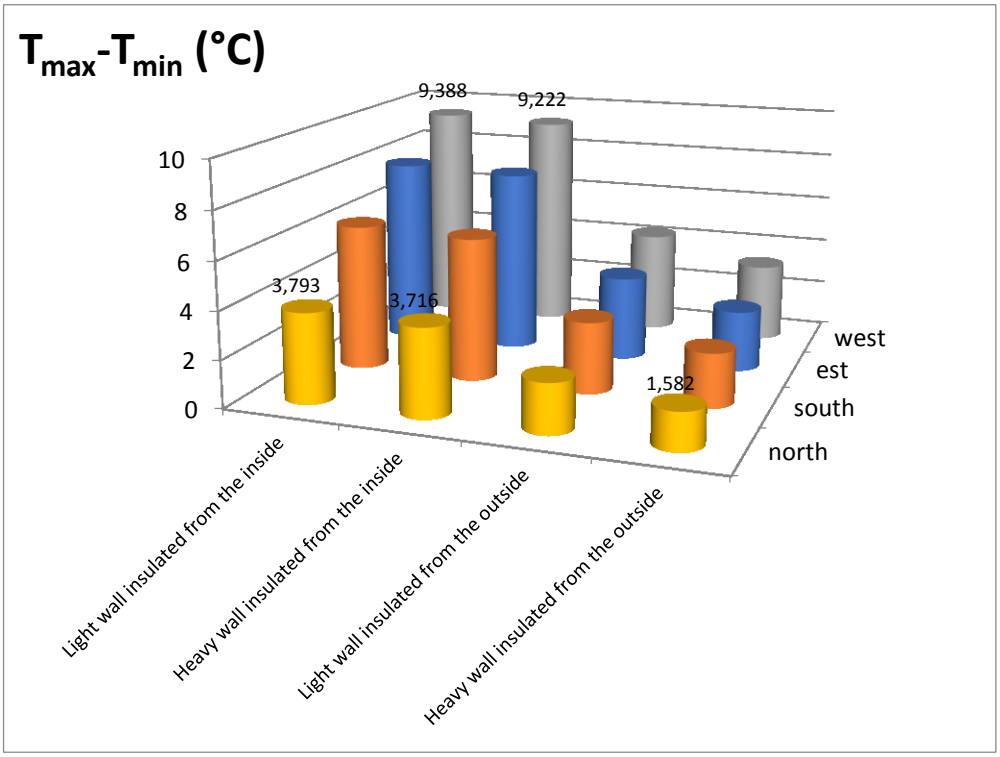

Figure A.8: difference between maximum and minimum temperature (boundary conditios: window surface 4 m^2, glass transmittance 5 W/m^2K; ventilation rate 5 v/h)

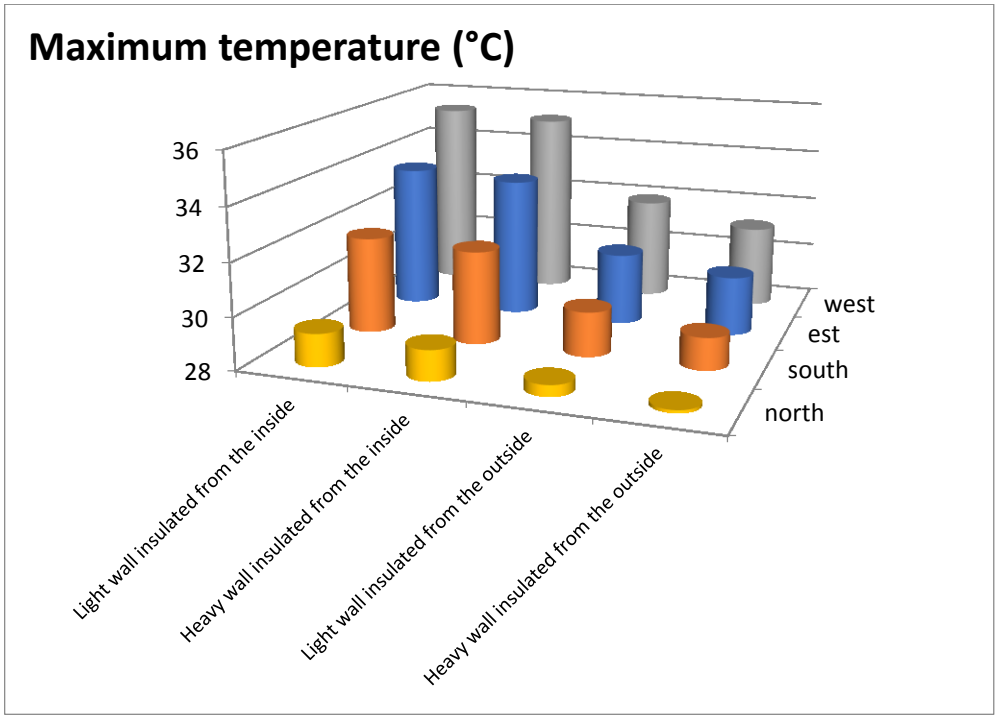

Figure A.9

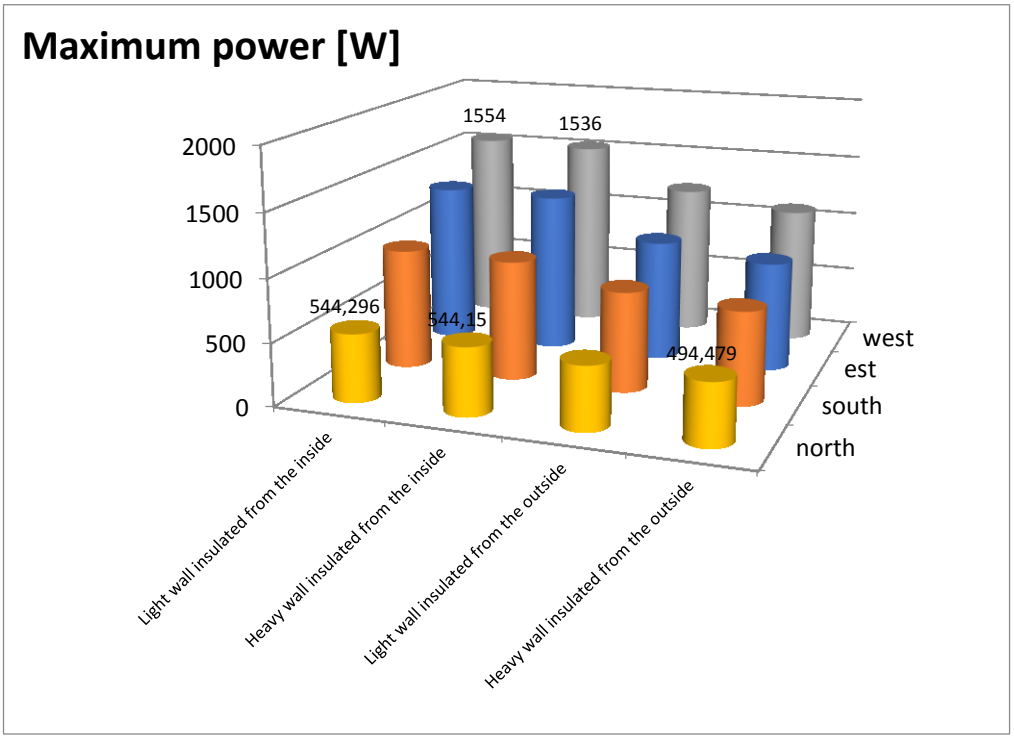

Figure A.10

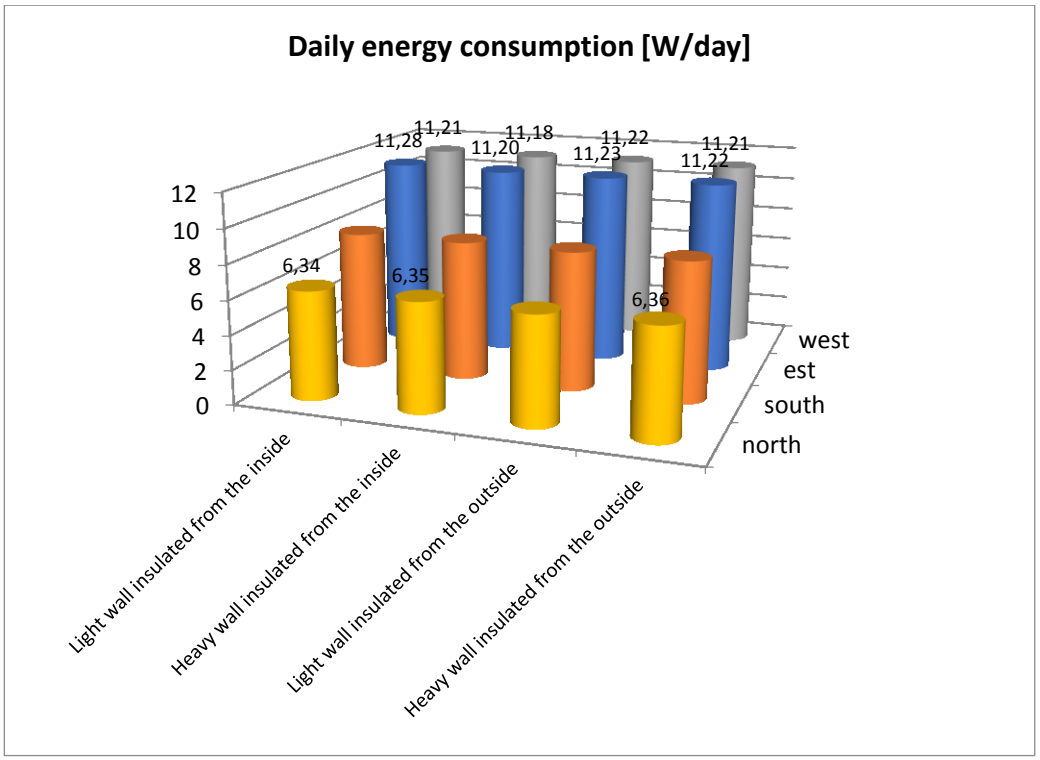

Figure A.11

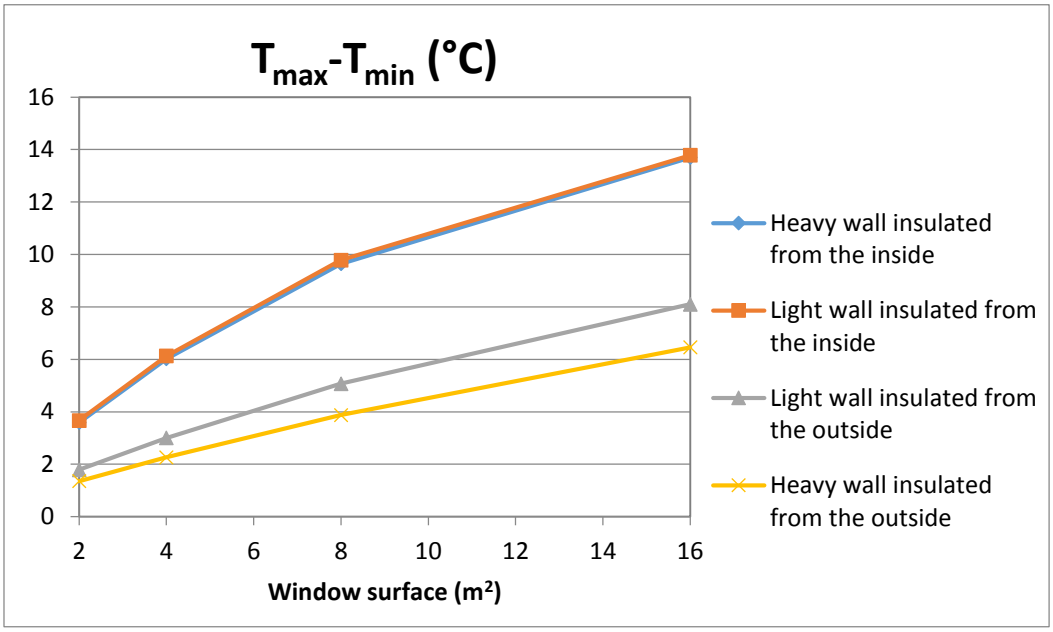

Figure A.12.a: Difference between maximum and minimum temperature in function of window suface for different types of wall (Ventilation rate 0v/h; indoor thermal loads 0)

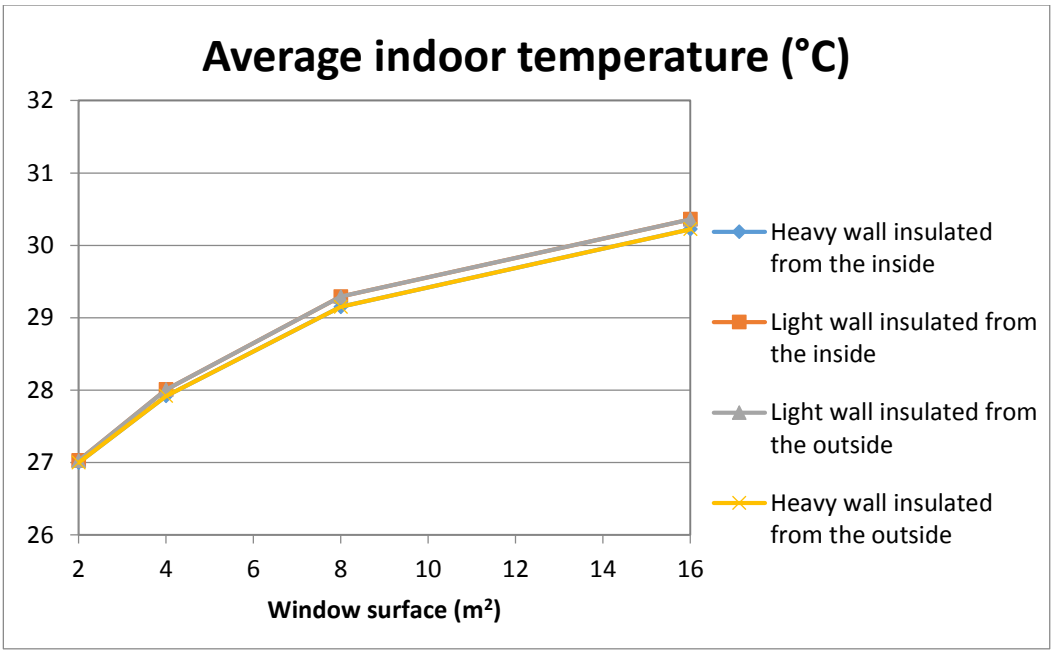

Figure A.12.b: Average air temperature for room with different types of wall in function of window suface for different types of wall (Ventilation rate 0v/h; indoor thermal loads 0)

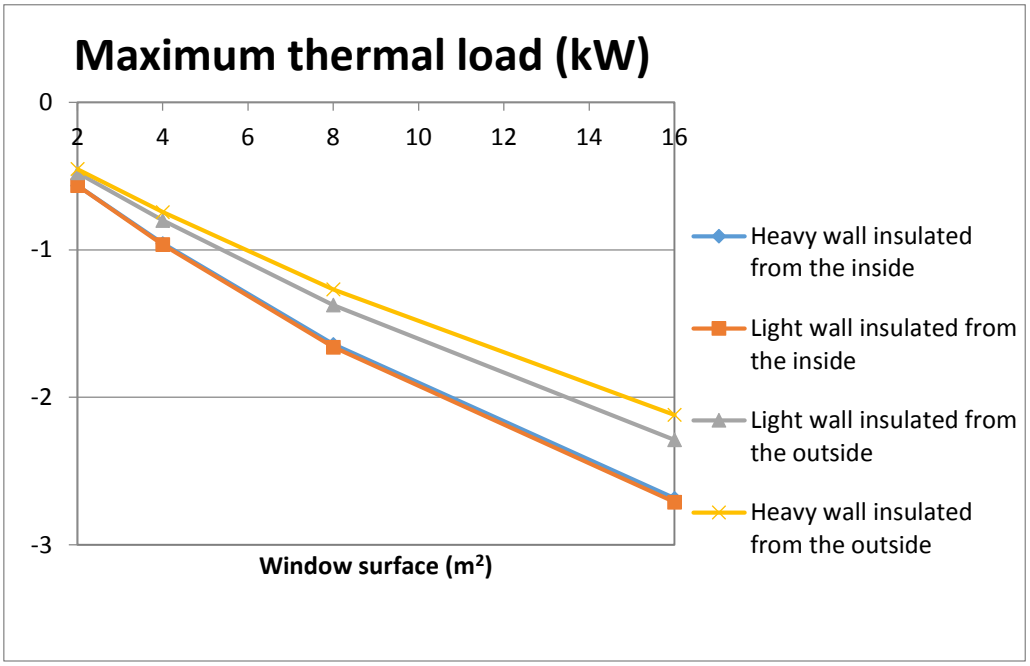

Figure A12.c: Maximum thermal load for room with different types of wall in function of window suface for different types of wall (Ventilation rate 0v/h; indoor thermal loads 0)

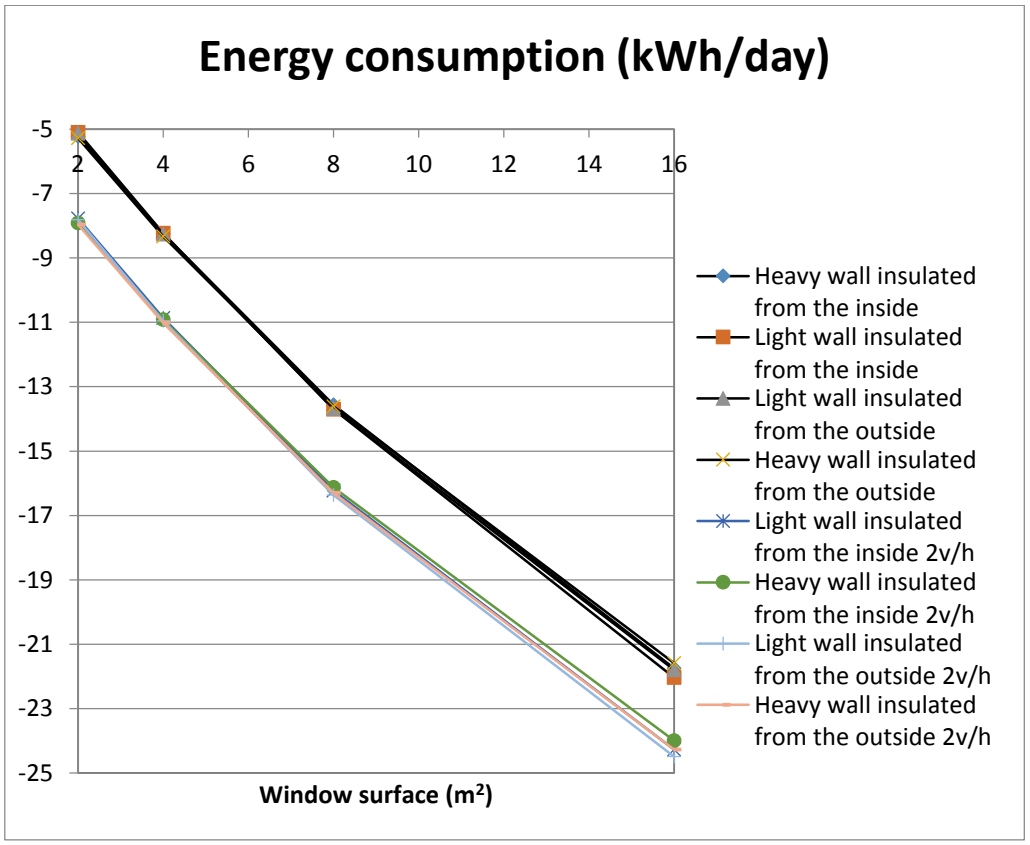

Figure A.12.d: Energy consumption for room with different types of wall and different ventilation rate printed in function of window suface for different types of wall

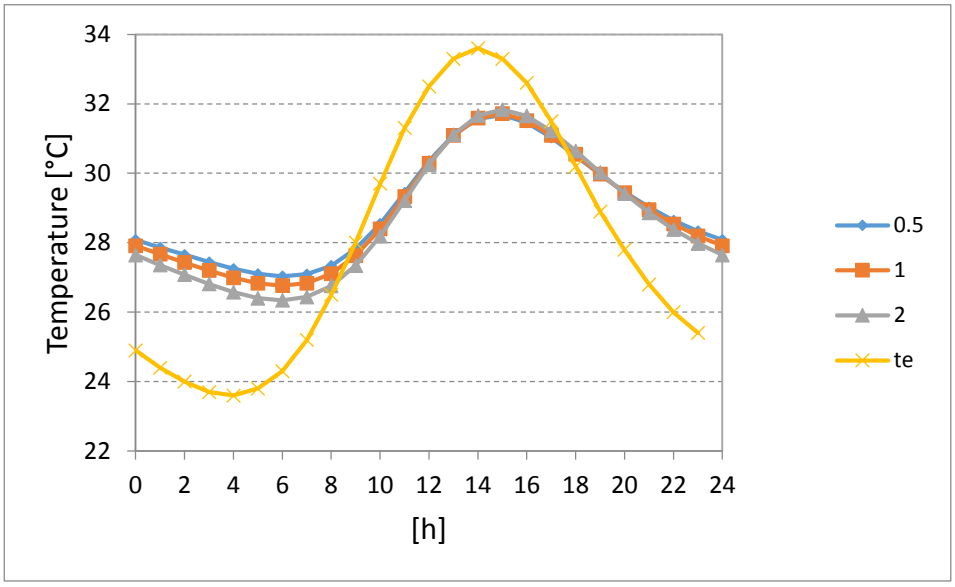

Figure A.14.a: Air temperature in a southern exposed room, with differnt ventilation rate (boundary conditions: window surface 4 m^2; window trasmittance 5 W/m^{2}K; light wall; indoor insulation; indoor thermal load=0)

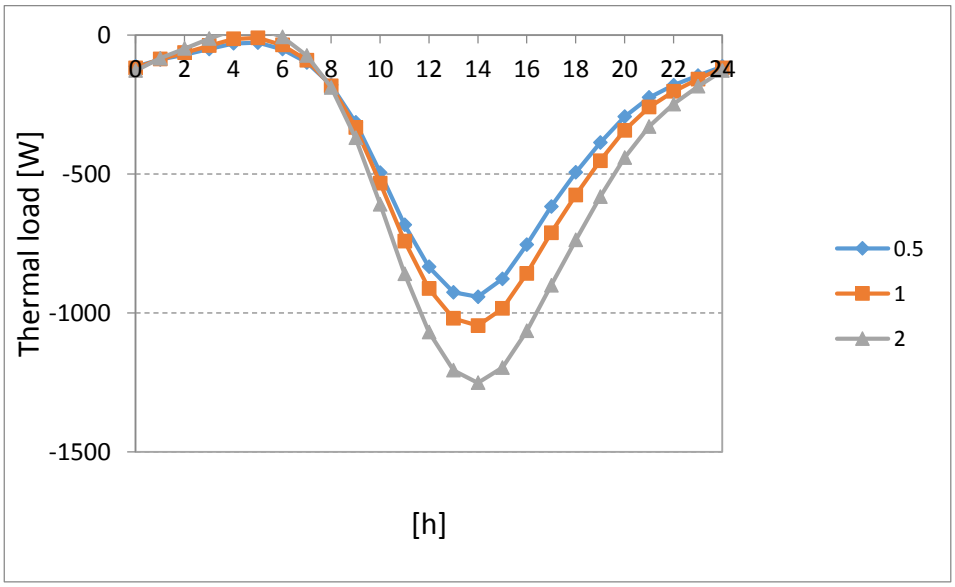

Figure A.14.b: Thermal load in a southern exposed room, with differnt ventilation rate (boundary conditions: window surface 4 m^2; light wall; indoor insulation; indoor thermal load=0)

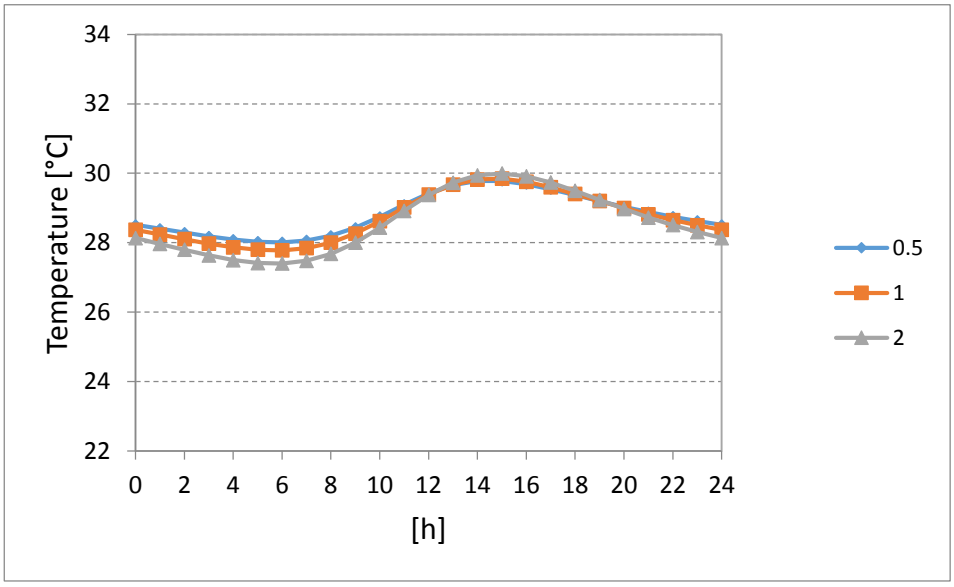

Figure A.15.a: Air temperature in a southern exposed room, with differnt ventilation rate (boundary conditions: window surface 4 m^2; window trasmittance 5 W/m^{2}K; heavy wall; outdoor insulation; indoor thermal load=0)

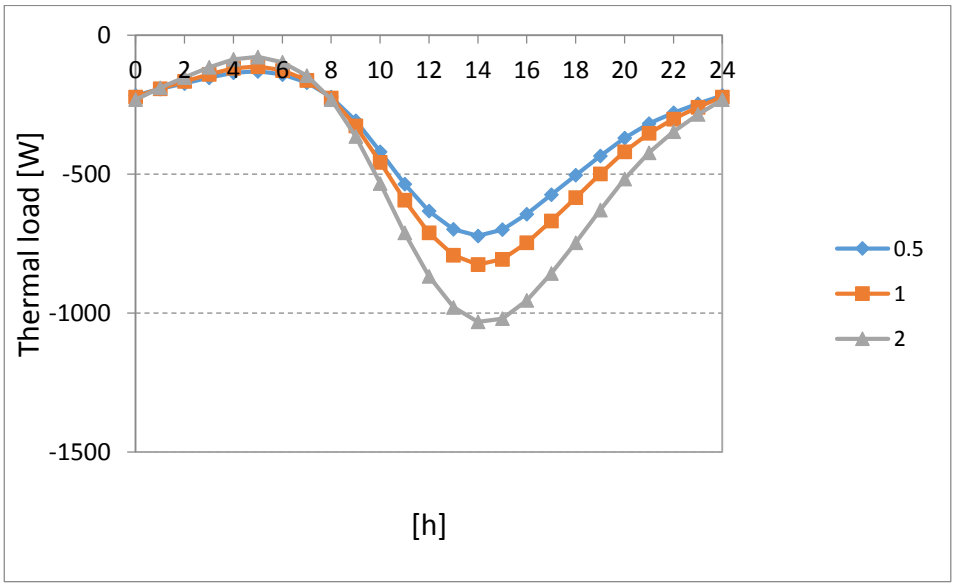

Figure A.15.b: Thermal load in a southern exposed room, with differnt ventilation rate (boundary conditions: window surface 4 m^2; heavy wall; outdoor insulation; indoor thermal load=0)

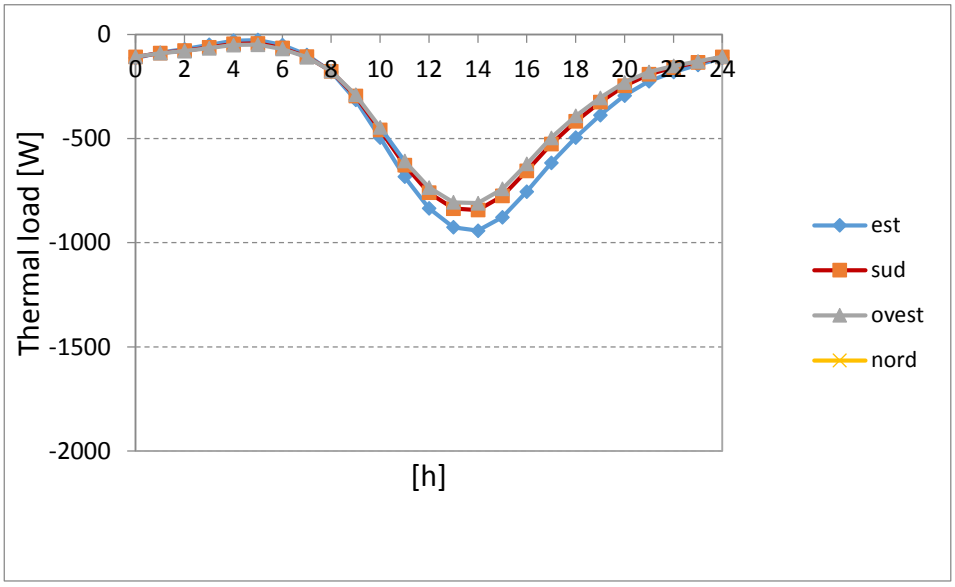

Figure A.16.a: Thermal load in a southern exposed room, with differnt values of glass trasmittance (boundary conditions: window surface 4 m^2; light wall; indoor insulation; indoor thermal load=0)

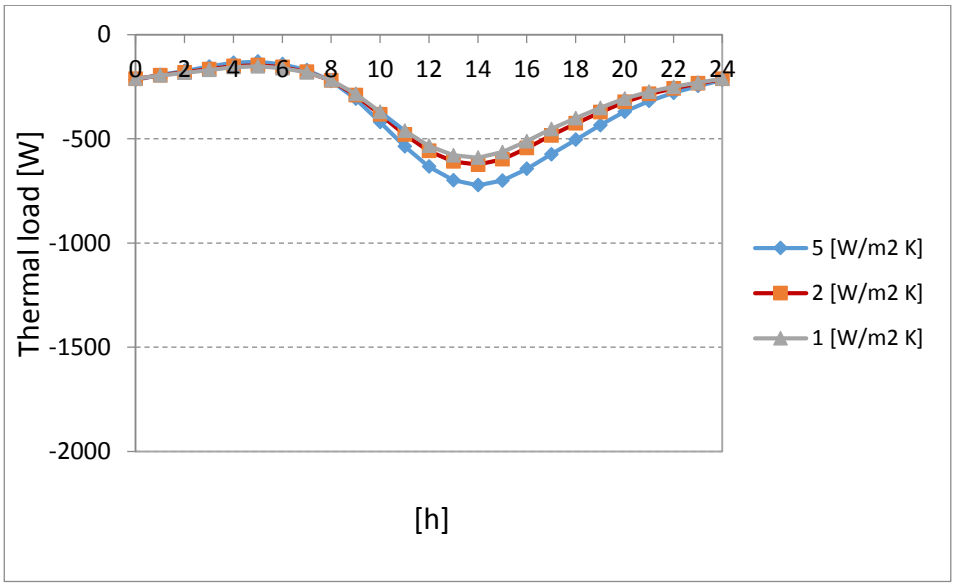

Figure A.16.b: Thermal load in a southern exposed room, with differnt values of glass trasmittance (boundary conditions: window surface 4 m^2; heavy wall; outdoor insulation; indoor thermal load=0)

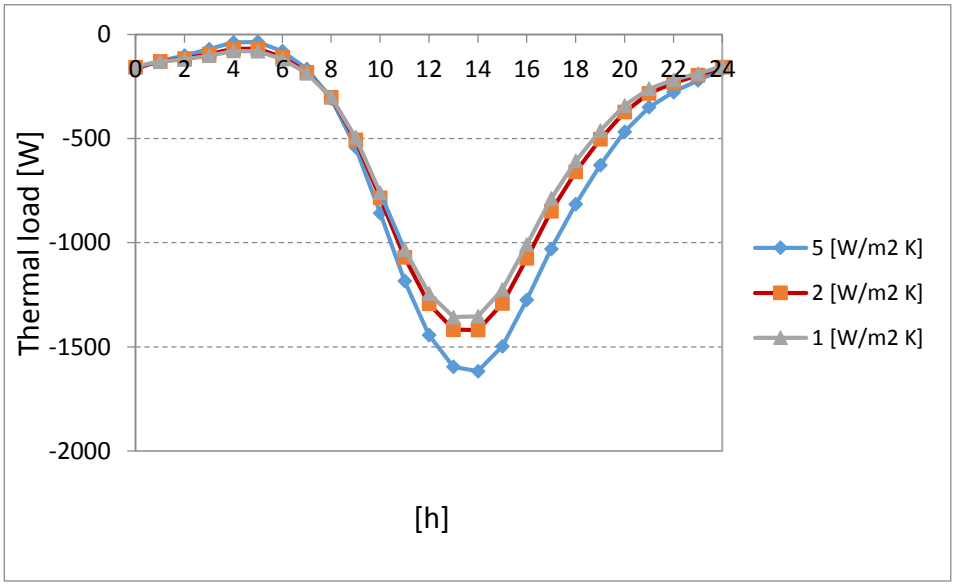

Figure A.16.c: Thermal load in a southern exposed room, with differnt values of glass trasmittance (boundary conditions: window surface 8 m^2; light wall; indoor insulation; indoor thermal load=0)

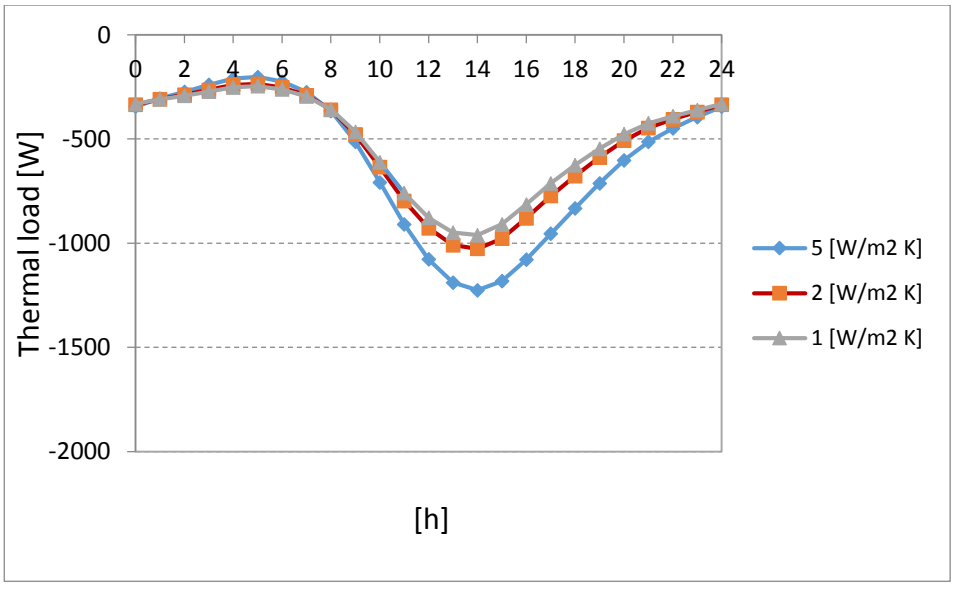

Figure A.16.d: Thermal load in a southern exposed room, with differnt values of glass trasmittance (boundary conditions: window surface 8 m^2; heavy wall; outdoor insulation; indoor thermal load=0)

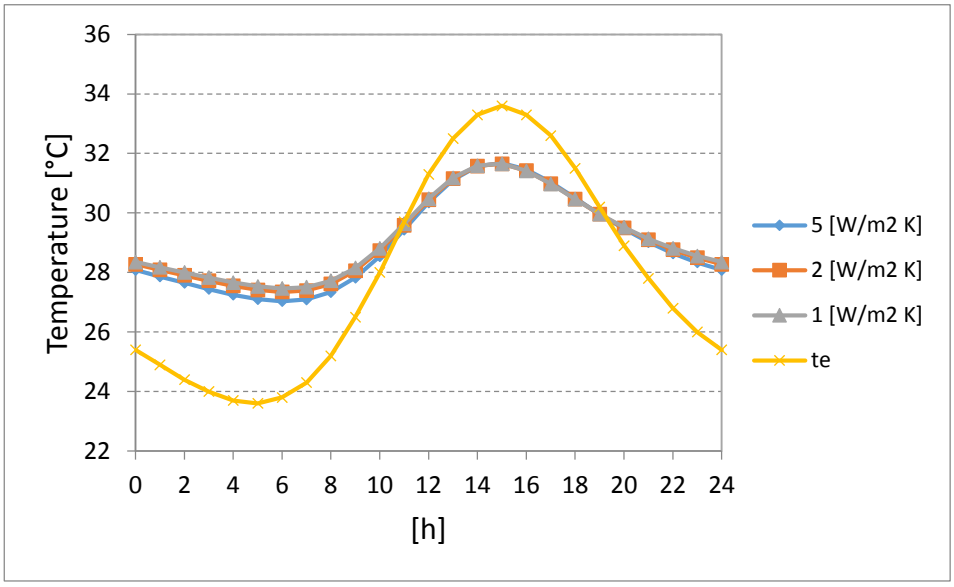

Figure A.17.a: Air temperature in a southern exposed room, with differnt values of glass trasmittance (boundary conditions: window surface 4 m^2; light wall; indoor insulation; indoor thermal load 0)

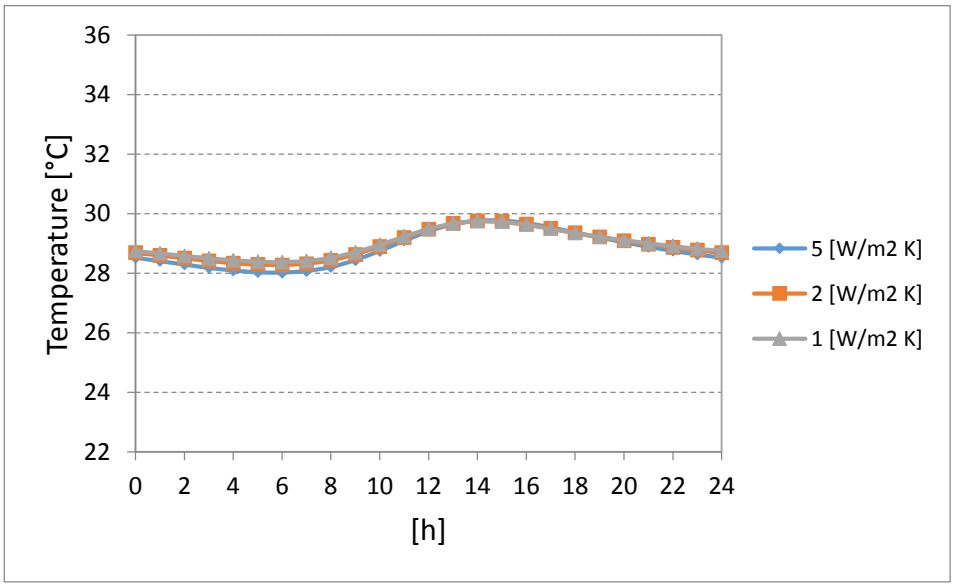

Figure A.17.b: Air temperature in a southern exposed room, with differnt values of glass trasmittance (boundary conditions: window surface 4 m^2; heavy wall; outdoor insulation; indoor thermal load 0)

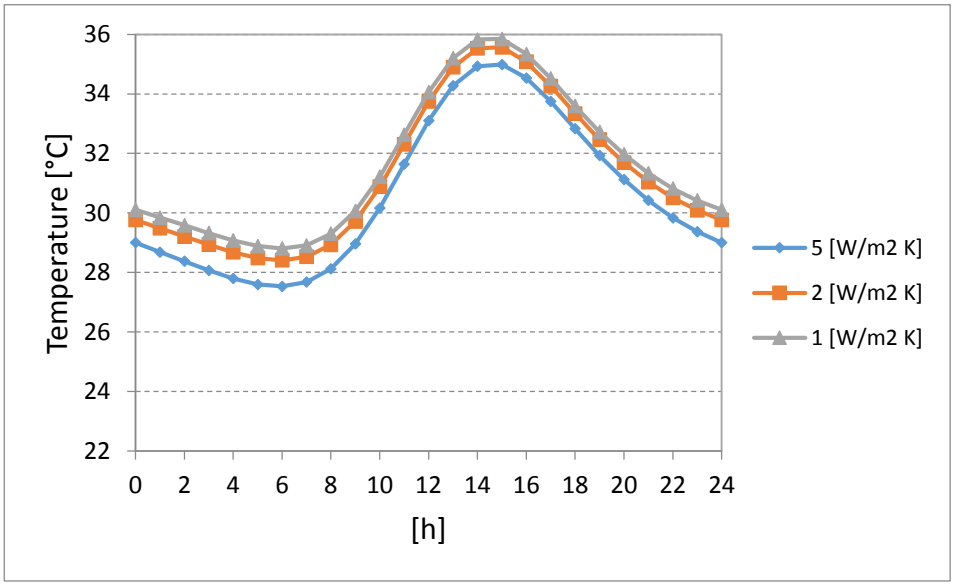

Figure A.17.c: Air temperature in a southern exposed room, with differnt values of glass trasmittance (boundary conditions: window surface 8 m^2; light wall; indoor insulation; indoor thermal load 0)

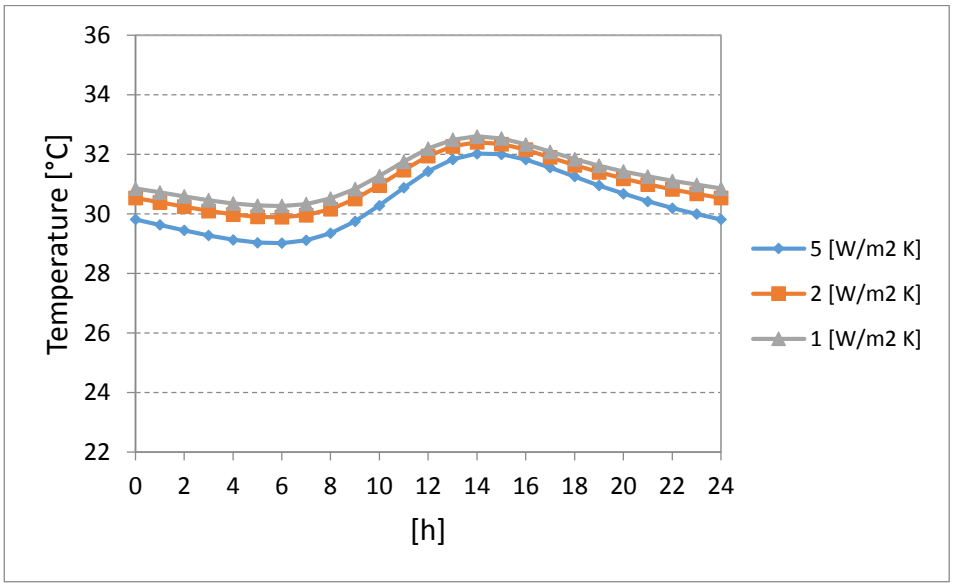

Figure A.17.d: Air temperature in a southern exposed room, with differnt values of glass trasmittance (boundary conditions: window surface 8 m^2; heavy wall; outdoor insulation; indoor thermal load 0)

APPENDIX B: INVENTORY

EXTERNAL WALL: Type A

Material	s [m]	F [-]	φ_F [h]
Inner plaster	0.01		
Lava stones	0.60	**0.096**	**-2.3**
Outer plaster	0.01		

EXTERNAL WALL: Type B.1

Material	s [m]	F [-]	φ_F [h]
Inner plaster	0.01		
Hollow clay bricks	0.08		
Air cavity	0.03	**0.352**	**-3.3**
Polystyrene	0.05		
Hollow clay bricks	0.25		
Outer plaster	0.01		

EXTERNAL WALL: Type B.2

Material	s [m]	F [-]	φ_F [h]
Inner plaster	0.01		
Polystyrene	0.05		
Hollow clay bricks	0.08	**0.678**	**-1.5**
Air cavity	0.03		
Hollow clay bricks	0.25		
Outer plaster	0.01		

EXTERNAL WALL: Type B.3

Material	s [m]	F [-]	φ_F [h]
Inner plaster	0.01		
Lightweight clay bricks	0.38	**0.398**	**-2.4**
Outer plaster	0.01		

EXTERNAL WALL: Type C

Material	s [m]	F [-]	φ_F [h]
Steel	$0.5\ 10^{-3}$		
Polyurethane	0.08	**0.812**	**-0.4**
Steel	$0.5\ 10^{-3}$		

INTERNAL WALL: Type A

Material	s [m]	F [-]	φ_F [h]
Inner plaster	0.01		
Lava stones	0.40	**0.095**	**-2.2**
Outer plaster	0.01		

INTERNAL WALL: Type B (all)

Material	s [m]	F [-]	φ_F [h]
Inner plaster	0.01		
Hollow clay bricks	0.08	**0.335**	**-2.3**
Outer plaster	0.01		

INTERNAL WALL: Type C

Material	s [m]	F [-]	φ_F [h]
Gypsum board	0.012		
Air cavity	0.06	**0.812**	**-0.4**
Gypsum board	0.012		

FLOOR: Type A

Material	s [m]	F [-]	φ_F [h]
Concrete tiles	0.01		
Lean concrete	0.06	**0.192**	**-3.6**
Pumice-gypsum flooring	0.12		
Inner plaster	0.01		

FLOOR: Type B (all)

Material	s [m]	F [-]	φ_F [h]
Concrete tiles	0.01		
Lightweight screed	0.05	**0.319**	**-2.0**
Concrete-slabs flooring	0.2		
Inner plaster	0.01		

FLOOR: Type C

Material	s [m]	F [-]	φ_F [h]
Linoleum	0.004	**0.43**	**-1.2**
Lightweight screed	0.05		

CEILING: Type A

Material	s [m]	F [-]	φ_F [h]
Inner plaster	0.01		
Pumice-gypsum flooring	0.12	**0.295**	**-2.7**
Lean concrete	0.06		
Concrete tiles	0.01		

CEILING: Type B (all)

Material	s [m]	F [-]	φ_F [h]
Inner plaster	0.01		
Concrete-slabs flooring	0.20		
Polystyrene	0.05	**0.124**	**-2.5**
Lightweight screed	0.05		
Concrete tiles	0.01		

CEILING: Type C

It has the same structure as the external wall. However, due to the different surface thermal resistance, the following values hold:

$|\mathbf{F}| = 0.75$ $\varphi_F = -0.5$ [h]

Bibliography

Asan, H. 2000. Investigation of wall's optimum insulation position from maximumtime lag and minimum decrement factor point of view.*Energy and Buildings*32: 197–203.

Asan, H. 2006. Numerical computation of time lags and decrement factorsfor different building materials.*Building and Environment* 41: 615–620.

Aste, N., A. Angelotti and M. Buzzetti. 2009. The influence of the external walls thermal inertia on the energy performance of well insulated buildings.*Energy and Buildings*41: 1181–1187.

Balcomb, J.D., 1983-a. Heat storage and distribution inside passive solar buildings, Los Alamos National Lab. Report LA-9694-MS.

Balcomb, J.D., 1983-b. Prediction of internal temperature swings in direct gain passive solar buildings, Proceed. Solar World Congr. Perth.

Beattie, K.H., Ward, I.C., 1999. The advantages of building simulation for building design engineers, Proceedings of IBPSA International Conference, Kyoto, Japan.

Bojic,M.L.,and D.L. Loveday.2007. The influence on building thermal behavior of theinsulation/masonry distribution in a three layered construction.*Energy and Buildings* 26: 153–157.

Carrier Air Conditioning Company, 1962. System Design Manual, Syracuse, New York.

Ciampi, M., F. Fantozzi, F. Leccese, and G. Tuoni. 2004. Multi-layered wall design to optimizebuilding plant interaction.*International Journal of Thermal Science* 43: 417–429

CIBSE. 2006. Guide A: Environmental Design. 7th ed. London: Chartered Institute of Building Services Engineers.

Davies, M.G. 1973. The thermal Admittance of layered walls.*Building Science*8: 207-220.

Davies, M.G. 1994. The thermal response of an enclosure to periodic excitation: the CIBSE approach.*Building and Environment* 29 (2): 217-235.

De Gracia, A., A. Castell, M. Medrano, and L.F. Cabeza. 2011. Dynamic thermal performanceof alveolar brick construction system.*Energy Conversion and Management* 52: 2495–2500.

Directive 2010/31/EU of the European Parliament and of the Council of 19 May 2010 on the energy performance of buildings (recast), Official Journal of the European Communities, Brussels (June) (2010).

Evola, G., and L.Marletta. 2013. A dynamic parameter to describe the thermal response of buildings to radiant heat gains. *Energy and Buildings* 68: 7-18.

Gasparella, A., G. Pernigotto,B. Barattieri,and P. Baggio. 2011. Thermal dynamic thermal properties of the opaque envelope: analytical and numerical tools for the assessment of the response to summer outdoor conditions.*Energy and Buildings*43: 2509-2517.

Hall M., and D. Allinson. 2008. Assessing the moisture-content-dependent parametersof stabilized earth materials using the cyclic-response admittance method. *Energy and Buildings* 40: 2044–2051.

ISO 6946:2007. Building components and building elements. *Thermal resistance and thermal transmittance*. Calculation method.

ISO 13786:2007. Thermal performance of building components - Dynamic thermal characteristics - Calculation methods. Geneva: International Organization for Standardization.

ISO 13791:2012. Thermal performance of buildings - Calculation of internal temperatures of a room in summer without mechanical cooling - General criteria and validation procedures. Geneva: International Organization for Standardization.

ISO 13792:2012. Thermal performance of buildings - Calculation of internal temperatures of a room in summer without mechanical cooling – Simplified methods. Geneva: International Organization for Standardization.

Loudon, A.G., 1968. Summertime temperatures in buildings without air conditioning, Journal of Heating and Vent. Eng., vol. 36, pp. 137-152.

Loudon, A.G. 1970. Summertime temperatures in buildings without air conditioning.*Journal of The Institution of Heating and Ventilation Engineers* 37: 280-292.

Marletta, L., Evola, G., Giuga, M. 2015. Using the dynamic thermal properties to assess the internal temperature swings in free running buildings. A general

model and its validation according to ISO 13792, *Energy and buildings* 87: 57-65

Millbank, N.O., and J. Harrington-Lynn. 1974. Thermal response and the admittance procedure.*Building Service Engineering* 42: 38-51.

Oliveti, G., Arcuri, N., Bruno, R., De Simone, M., 2011. An accurate calculation procedure of solar heat gain through glazed surfaces, Energy and Buildings, vol. 43, pp. 269-274.

Rees, S.J., Spitler, J.D., Davies M.G., Haves, P., 2000. Qualitative comparison of North American and U.K. cooling load calculation methods, International Journal of HVAC&R Research, vol. 6, no. 1, pp. 75-99.

UNI EN 410:2011. Glass in building. Determination of luminous and solar characteristics of glazing.

UNI EN 673:2011. Glass in building. Determination of thermal transmittance. Calculation method.

UNI EN ISO 6946:2008. Building components and building elements – Thermal resistance and thermal transmittance – Calculation method.

UNI 10375. Metodo di calcolo della temperatura interna estiva degli ambienti.